



Schneider, Eric Vaughn Captain (2023) *Fish aggregating devices (FADs) as conservation tools: understanding community dynamics at pelagic moored FADs*. PhD thesis.

<https://theses.gla.ac.uk/83926/>

Copyright and moral rights for this work are retained by the author

A copy can be downloaded for personal non-commercial research or study, without prior permission or charge

This work cannot be reproduced or quoted extensively from without first obtaining permission from the author

The content must not be changed in any way or sold commercially in any format or medium without the formal permission of the author

When referring to this work, full bibliographic details including the author, title, awarding institution and date of the thesis must be given

Enlighten: Theses

<https://theses.gla.ac.uk/>  
[research-enlighten@glasgow.ac.uk](mailto:research-enlighten@glasgow.ac.uk)

**Fish aggregating devices (FADs) as conservation tools:  
Understanding community dynamics at pelagic moored FADs**

Eric Vaughn Captain Schneider, MSc

Submitted in fulfilment of the requirements for the degree of Doctor of Philosophy (PhD)



School of Biodiversity, One Health & Veterinary Medicine  
College of Medical, Veterinary & Life Sciences  
University of Glasgow

November 2022

## **Abstract**

The pelagic ocean covers the majority of the planet and is the largest ecosystem by volume. It is estimated to harbor considerable biodiversity, and a few select species support some of the largest fisheries in existence. The expanse of the open ocean provides important resources and services to humans, and also poses challenges to understanding the biology and ecology of its resident species. Focusing effort, both fishing and research, on hotspots or other aggregation sites increases the feasibility of interacting with these often patchily-distributed animals. Fish aggregating devices (FADs) have become a widespread fishing tool in many of the world's oceans. Leveraging the natural behavior of many fish species to aggregate around floating or submerged structures, FADs are used to increase the capture efficiency in a range of marine fisheries and the scale of their use has raised concerns around potential effects these artificial structures have on the ecosystems in which they are used. Research efforts have focused on understanding these impacts by taking advantage of the fisheries-related opportunities and data made available by these fishing tools and the fleets that use them. However, this may potentially bias studies towards fishing hotspots and larger, commercially important species. Here, we discuss how subsurface FADs, purpose-built and discretely deployed, can act as useful research platforms to address important pelagic ecology questions and conservation topics. We describe the colonization of new FADs and the aggregation fluctuations through long-term video and visual surveys, provide evidence for invertebrate micronekton aggregation as a potential mechanism behind fish attraction to FADs, and detail a new acoustic telemetry array design that can provide previously unavailable position metrics of tagged fish in the open ocean, a notably challenging habitat to study. These new data and scientific tools will allow for the continued and enhanced study of the pelagic ecosystem and the diversity of species that inhabit it.

# Table of Contents

Abstract .....	ii
List of figures .....	vi
List of tables .....	xiii
Acknowledgements .....	xvii
Author's declaration .....	xviii
1. General Introduction .....	1
1.1. Pelagic Zone .....	1
1.2. Surveying Pelagic Fish Populations .....	1
1.3. Structure Affecting Animal Behavior .....	2
1.4. Animal Tracking in the Ocean .....	3
1.5. Fish Aggregating Devices .....	4
1.6. FADs in Research .....	5
1.7. Objectives .....	6
1.8. Methodological Outline .....	8
2. Design and deployment of an affordable and long-lasting deep-water subsurface fish aggregating device .....	10
2.1. Abstract .....	10
2.2. Introduction .....	10
2.3. Methods .....	13
2.3.1. FAD Design .....	13
2.3.2. Construction .....	15
2.3.3. Deployment .....	18
2.3.4. Removal Potential .....	22
2.4. Results and Discussion .....	23
2.4.1. Design Considerations .....	23
2.4.2. Research Applications and Conclusions .....	24
3. Colonization, diversity, and seasonality at pelagic fish aggregating devices (FADs) assessed using visual and video surveys .....	28
3.1. Abstract .....	28

3.2. Introduction .....	28
3.3. Methods .....	30
3.4. Results .....	33
3.5. Discussion .....	45
4. Invertebrate micronekton aggregation to a pelagic moored fish aggregating device (FAD)	50
4.1. Abstract .....	50
4.2. Introduction .....	50
4.3. Methods .....	52
4.3.1. Study Location .....	52
4.3.2. Light Trap Survey .....	52
4.3.3. Echosounder Survey .....	53
4.3.4. Echosounder Data Processing .....	54
4.3.5. Data Analysis .....	56
4.4. Results .....	57
4.5. Discussion .....	66
5. Fine-scale acoustic positioning of structure-associated pelagic fishes using a 3-D acoustic telemetry array .....	71
5.1. Abstract .....	71
5.2. Introduction .....	71
5.3. Methods .....	74
5.3.1. Vertical Component- Moored FAD .....	74
5.3.2. Vertical Component- Drifting Buoy .....	76
5.3.3. Horizontal Component- Drifting Buoy .....	77
5.3.4. Full Array .....	78
5.3.5. Data Analysis .....	78
5.4. Results .....	79
5.4.1. Detectability Analysis .....	79
5.4.2. Detection Time Difference .....	81
5.4.3. Barracuda positioning .....	86
5.5. Discussion .....	87
6. General Discussion .....	90

6.1. Ecological Insights .....	90
6.2. Methodological Insights .....	93
6.3. Conclusion .....	95
7. References .....	96
8. Appendix .....	114
8.1. Section 3 (Chapter 2) Supplementary Materials .....	114
8.2. Section 4 (Chapter 3) Supplementary Materials .....	121

## List of Figures

Figure 1.8-1. An illustration of each of the projects that are included in this thesis. The inset numbers refer to the corresponding chapter, along with a brief text description of that project. Chapter 2 (top left) details the design, construction, and deployment of the subsurface moored research FADs. A small boat is depicted towing the mooring anchor, which is suspended by a lift bag, with the trailing mooring line and buoys at the sea surface. Chapter 3 (top right) depicts the field of view of a video camera mounted on the FAD used during the visual and video survey project, after the FAD is in its subsurface placement. Chapter 4 (bottom left) depicts a small boat towing an echosounder mounted on a glider frame (with the area of ensonification shown as a downward facing cone). The vertical line depicts a series of small cylindrical light traps that sampled the micronekton throughout the water column around the FAD. Chapter 5 (bottom right) depicts a drifting FAD (grey oval at the sea surface) with six black acoustic receivers suspended beneath it using extendable poles and rope. A fish tagged with an acoustic transmitter (marked with a star) is depicted swimming near the array.....8

Figure 2.3.1-1. Schematic of the subsurface fish aggregating device (FAD) currently being used at The Cape Eleuthera Institute, The Bahamas. FAD design consists of a concrete anchor block, mooring line, and two steel buoys. Steel buoys are moored 10 m below the sea surface to prevent detection by fishers and to create tension and verticality in the mooring line for gear deployment. Diagram not to scale. .... 15

Figure 2.3.2-2. Stainless steel round stock bail that was incorporated into the top of the concrete anchor block to serve as the attachment point between the block and metal chain, which was the beginning of the mooring line. .... 17

Figure 2.3.2-3. Top end of the mooring line showing an eye splice to a rope connector, swivel, bolt through shackle, and 7/8” (22.2 mm) master link to which the buoys (and a safety line during deployment) were attached..... 18

Figure 2.3.3-4. Initial stage of the FAD deployment process. The concrete anchor block is suspended by lift bags and attached to the mooring line that has been deployed overboard onto the sea surface down current from the anchor. The anchor is positioned 1/3 the length of the mooring line up current of the targeted resting location. .... 21

Figure 2.3.3-5. Schematic showing the process of removing slack from the mooring line following deployment. A diver attaches a deflated lift bag to the slack mooring line using a Prusik hitch and slowly inflates the bag. This process is repeated until the desired tension on the mooring line has been reached and the steel buoys are then attached. .... 22

Figure 3.4-1. Water temperature (° C) measured at the two FAD locations taken at the beginning of each survey, from January 2018 to March 2020. Red dots indicate measurements taken at the North FAD and blue dots indicate measurements taken at the South FAD..... 36

Figure 3.4-2. Values of estimated species richness in relation to survey number are shown here using species accumulation curves that have been calculated based on video (black and red) and visual (green and blue) surveys at each FAD location, with bars representing 95% confidence intervals. The two survey locations are the North FAD (NFAD in legend) and the South FAD (SFAD in legend)..... 37

Figure 3.4-3. Stacked bar chart showing observation frequency of different taxonomic or functional groups during the two types of surveys (i.e., what type of survey was more effective at surveying a given group). On days when video and visual surveys both occurred at the same location, the bars represent the percentage of surveys that each listed taxonomic or functional group was seen in. For example, small forage fishes were seen in 96.9% of all surveys: they were seen *only* in visual surveys (and not on the video survey that occurred at the same time) 2.5% of the time, only in video surveys (and not on the visual survey that occurred at the same time) 8.6% of the time, and in both surveys (visual and video surveys that occurred at the same time) 85.8% of the time..... 38

Figure 3.4-4. Cubic spline generated plot of smoothed fit from the GAM showing the partial effect of time (FAD age) on shark abundance with partial residual points plotted. The hash marks above the x axis indicate the distribution of observed values, and the grey shaded columns highlight the warm/wet season (May 1 – Oct 31) of each year. The y axis represents the smooth term contribution to the GAM (edf = 3.22), which is the scaled partial effect of age on shark abundance and is centered around the model’s constant term. The shaded blue area represents 95% confidence intervals..... 39

Figure 3.4-5. Partial effects of survey method and season on the variation in shark abundance predicted by a GAM. Because survey method and season are categorical variables, the horizontal solid black lines above each factor show the predicted partial effect on shark abundance for that variable centered around the model’s constant term. The dashed lines above and below the solid black lines represent 95% confidence intervals. The carpet of black ticks above each variable on the X axis denotes each measurement and appears as a solid line..... 39

Figure 3.4-6. Cubic spline generated plot of the smoothed fit from the GAM showing the partial effect of time (FAD age) on total fish abundance with partial residual points plotted. The hash marks above the x axis indicate the distribution of observed values, and the grey shaded columns highlight the warm/wet season (May 1 – Oct 31) of each year. The y axis represents the smooth term contribution to the GAM (edf = 7.68) centered around the model’s constant term. The shaded blue area represents 95% confidence intervals..... 40

Figure 3.4-7. Partial effects of survey method and season on the variation in total fish abundance predicted by a GAM. Because survey method and season are categorical variables, the horizontal solid black lines above each factor show the predicted partial effect on fish abundance for that variable centered around the model’s constant term. The dashed lines above and below the solid black lines represent 95% confidence intervals. The carpet of black ticks above each variable on the X axis denotes each measurement and appears as a solid line..... 41

Figure 3.4-8. Cubic spline generated plot of the smoothed fit from the GAM showing the partial effect of time (FAD age) on Shannon diversity with partial residual points plotted. The hash marks above the x axis indicate the distribution of observed values, and the grey shaded columns highlight the warm/wet season (May 1 – Oct 31) of each year. The y axis represents the smooth term contribution to the GAM (edf = 8.44) centered around the model’s constant term. The shaded blue area represents 95% confidence intervals..... 41

Figure 3.4-9. Partial effects of survey method and season on the variation in Shannon diversity predicted by a GAM. Because survey method and season are categorical variables, the horizontal solid black lines above each factor show the predicted partial effect on Shannon diversity for that variable centered around the model’s constant term. The dashed lines above and below the solid black lines represent 95% confidence intervals. The carpet of black ticks above each variable on the X axis denotes each measurement and appears as a solid line..... 42

Figure 3.4-10. Linear regression showing the measured Shannon diversity observed using video surveys in relation to water temperature measured at the surveyed FAD. The shaded region represents 95% confidence intervals..... 43

Figure 3.4-11. Cubic spline generated plot of the smoothed fits from the GAMs showing the partial effect of time (FAD age) on abundance of individual fish species with partial residual points plotted. The hash marks above the x axes indicate the distribution of observed values, and the grey shaded columns highlight the warm/wet season (May 1 – Oct 31) of each year. The y axes represent the smooth term contribution to the GAMs centered around the model’s constant term, with edf indicated in the y axis labels. The shaded blue areas represent 95% confidence intervals. Figures are shown for all species with significant effects..... 44

Figure 4.3.3-1. Study location showing the island of Eleuthera, the Exuma Sound (deep water that is shaded darker blue in the bottom left of each map), and the approximate location of each surveyed FAD circled in red. The inset frame shows the radial star survey pattern with each point representing a geolocated data point collected by the echosounder..... 54

Figure 4.3.4-2. Dataflow, or series of processes followed using the echosounder data processing software Echoview, to prepare the raw acoustic data for analysis. The magenta pentagon labeled ‘Fileset 1: T1 (70 kHz)’ represents the echosounder towed behind the boat. The arrows leading away from the bottom left of the echosounder icon represent the order of the data processing operators used..... 55

Figure 4.4-3. Catch per unit effort (CPUE: total individuals of any species trapped per hour) in relation to distance away from the FAD for all of the light trapping stations (at the FAD = 0, 500 and 1000 m away). The intersection of the zeros on each axis in the top left of the figure represents the position of the FAD..... 59

Figure 4.4-4. Total length (mm) of all individuals trapped, with data points jittered around the three distances away from the FAD where traps were deployed. A linear regression (blue line) with 95% confidence intervals shaded around it has been added..... 60

Figure 4.4-5. Mean temperature during each echosounder survey over time (October 2018 to May 2019) measured by the Hobo logger attached to the echosounder glider frame at five meters

depth. Red dots represent temperatures during surveys at the North FAD and blue dots represent temperatures during surveys at the South FAD..... 61

Figure 4.4-6. Boxplot showing biomass (represented by logNASC [nautical area scattering coefficient] which is unitless) of strong scatterers ( $S_v > -50$  dB) measured during the towed echosounder surveys at both locations shown over varying distances from the FADs. Values were binned every 50 m for visual clarity due to the large number of raw points..... 62

Figure 4.4-7. Boxplot showing biomass (represented by logNASC [nautical area scattering coefficient] which is unitless) of weak scatterers ( $-50$  dB  $> S_v > -85$  dB) measured during the towed echosounder surveys at both locations shown over varying distances from the FADs. Values were binned every 50 m for visual clarity due to the large number of raw points..... 63

Figure 4.4-8. Boxplot showing biomass (represented by logNASC [nautical area scattering coefficient] which is unitless) of weak scatterers ( $-50$  dB  $> S_v > -85$  dB) measured during the towed echosounder surveys grouped by location- North (North FAD) and South (South FAD). 64

Figure 4.4-9. Boxplot showing biomass (represented by logNASC [nautical area scattering coefficient] which is unitless) of weak scatterers ( $-50$  dB  $> S_v > -85$  dB) measured during the towed echosounder surveys at both locations grouped by period- day and night..... 65

Figure 4.4-10. Biomass (represented by logNASC [nautical area scattering coefficient] which is unitless) of weak scatterers ( $-50$  dB  $> S_v > -85$  dB) measured during all of the towed echosounder surveys as a function of lunar illumination. A linear regression (blue line) has been added..... 66

Figure 5.2-1. Panel ‘a’ shows a typical commercial FAD (grey oval) with a single receiver directly underneath it to collect residence (presence and absence) and depth data (if the transmitter is equipped with a pressure sensor), utilized by several recent studies. This represents the limits of previous applications. Panel ‘b’ represents the moored sub-surface FAD used in the development of the vertical component of the VAR, with three receivers aligned down the taut mooring line which can be used to calculate depth and distance from the FAD array. Panel ‘c’ shows the final iteration of our array development, combining the vertical and horizontal components suspended beneath a free-drifting buoy to calculate depth, distance away, and bearing of a tagged animal. .... 73

Figure 5.3.1-2. A Vemco VR2Tx receiver in a mounting cup. (Left) A 3” (7.62 cm) PVC pipe was cut to length as a protective receiver cup. Short tethers were tied through holes drilled in the top and bottom of the pipe and attached to longline snaps that were used to quickly attach and detach the cup from the array’s main six mm line at predetermined intervals. (Bottom right) A 3.8 cm long bolt was tightened through the bottom of the cup as a stopper. (Top right) Two additional holes in the top of the pipe were used to tie the receiver into the cup (connected with a snap swivel for easy removal and replacement) and to affix a rubber band around the top of the receiver to ensure a snug and motionless fit without impeding signal reception..... 75

Figure 5.3.2-3. Diagram (not to scale) of the vertical component of the VAR. The grey oval at the surface represents the FAD float used, a Zunibal Zunfloat (180 cm diameter, 150 kg of flotation). A 200 m length of Samson six mm AmSteel Dyneema line was tied through the holes in the float, and the receivers in the mounting cups were clipped to this line at 100 m intervals (top, middle, bottom). A three kg steel shackle was used as the bottom weight. .... 76

Figure 5.3.3-4. Diagram of the horizontal component of the VAR. The grey oval represents the FAD on the sea surface, and the vertical thick black line represents the line with a weight at the bottom. Receivers were spaced 15 m apart at 10 m depth using extendable poles (thicker grey lines) and spacer lines (thinner black lines): diagram is not to scale..... 77

Figure 5.4.1-5. Mean detection efficiency (with 95% confidence intervals) of transmissions from V9 transmitters to VR2Tx receivers during seven trials (TrialN). Receiver labels are across the x axis: the three receivers in Figure 5.3.3-4 were positioned in a 15-meter equilateral triangle on a horizontal plane at 10 m depth and are labeled as H1, H2, and H3. The three receivers in Figure 5.3.3-3 were positioned along a vertical line and are labeled V1 (15 m deep), V2 (100 m deep), and V3 (200 m deep). Transmitter depths are in the legend, and nine transmitters were used (fastened along a vertical line)..... 80

Figure 5.4.2-6. The top panel shows detection time difference (in milliseconds) of transmissions between receiver pairs at 15 m and 100 m in the vertical array over the course of the entire drift test (time across the y axis). The shaded grey bars represent the times the drift tests were occurring (white spaces between grey bars represent time between trials spent resetting the line for another drift). The large green and red dots are the DTD derived from sync tags built into the receivers and correlate to the distance between those receivers, therefore representing the

possible bounds of DTD of a transmission travelling an uninterrupted straight path. T.Station (T001 – T300) represents the different depths of transmitters during the drift test. The bottom panel shows the DTD error based on known GPS locations of the transmitters, where 1.534 ms equates to 1 m of error..... 82

Figure 5.4.2-7. The top panel shows detection time difference (in milliseconds) of transmissions between receiver pairs at 15 m and 200 m in the vertical array over the course of the entire drift test (time across the y axis). The large green and red dots are the DTD derived from sync tags built into the receivers and correlate to the distance between those receivers, therefore representing the possible bounds of DTD of a transmission travelling an uninterrupted straight path. T.Station (T001 – T300) represents the different depths of transmitters during the drift test, and the shaded grey bars represent the times the drift tests were occurring (white spaces between grey bars represent time between trials spent resetting the line for another drift). The bottom panel shows the DTD error based on known GPS locations of the transmitters, where 1.534 ms equates to 1 m of error..... 83

Figure 5.4.2-8. Detection time difference (in milliseconds) of a transmission between receivers H1, H2, and H3 on a horizontal plane roughly 15 m apart at 10 m depth. The large green and red dots are the DTD derived from sync tags built into the receivers and correlate to the distance between those receivers, therefore representing the possible bounds of DTD of a transmission travelling an uninterrupted straight path. T.Station (T001 – T300) represent the different depths of transmitters during the drift test, and the shaded portions of the figure represent the times the drift tests were occurring (white space between grey bars represents time between trials spent resetting the line for another drift)..... 85

Figure 5.4.2-9. Mean water temperature through the water column at the study site measured by TDR and VR2Tx receivers during the drift tests. .... 86

Figure 5.4.3-10. Calculated distance in meters from the array (top panel) and depth (bottom panel) of a tagged great barracuda (transmitter ID: A69-9006-7991) derived from the moored FAD-based vertical component of the array..... 87

## List of Tables

Table 2.2-1. Selected examples from a search of studies using anchored FADs that include information on materials or deployment, that are subsurface (or ‘midwater’), or that were deployed in depths $\geq 500$ m and therefore comparable to our proposed design. ‘Buoy Depth’ of 0 represents a surface FAD. Substantial and replicable information must be included on materials used or deployment processes to qualify as ‘Yes’ .....	13
Table 2.4.2-2. Species documented on these subsurface FADs in the Exuma Sound during the course of a 2.5-year camera survey (in preparation for publication elsewhere), separated into resident intransigent versus ephemeral circumnavigant species, compared to other epipelagic fishes documented in the Exuma Sound (personal communication: Z. Zuckerman, Cape Eleuthera Institute) but remain absent from our subsurface FAD surveys. An asterisk (*) denotes species present within the first six months after FAD deployment.....	26
Table 2.4.2-3. Recently utilized methods for FAD-based research that lend well to a stable, subsurface platform. ....	27
Table 3.4-1. Inventory list of all species that were present in the video or visual surveys that occurred at the two subsurface pelagic FADs studied.....	35
Table 4.4-1. List of all organisms collected during the light trap surveys. N represents the total number of individuals in a given Class, and Nsub is the number of individuals subsampled within a taxonomic group for total length, measured in millimeters plus and minus 95% confidence intervals (TL mm $\pm$ 95% CI).....	57
Supplementary Table 8.1-1. Output statistics of a generalized additive model (GAM) with a negative binomial distribution to analyze the effects of time (‘age’ of FAD), season, and survey method on shark abundance. Bold text highlights significant effects. ....	114
Supplementary Table 8.1-2. Analysis of variance (ANOVA) output table for the best fitting GAM model of shark abundance (output shown in Table 8.1-1). Bold text highlights significant effects.....	114

Supplementary Table 8.1-3. Output statistics of a generalized additive model (GAM) with a Poisson distribution to analyze the effects of time ('age' of FAD), season, and survey method on total fish abundance. Bold text highlights significant effects.. ..... 115

Supplementary Table 8.1-4. Analysis of variance (ANOVA) output table for the best fitting GAM model of total fish abundance. Bold text highlights significant effects..... 115

Supplementary Table 8.1-5. Output statistics of a generalized additive model (GAM) with a Gaussian distribution to analyze the effects of time ('age' of FAD), season, and survey method on Shannon's diversity. Bold text highlights significant effects..... 116

Supplementary Table 8.1-6. Analysis of variance (ANOVA) output table for the best fitting GAM model of Shannon's diversity. Bold text highlights significant effects..... 116

Supplementary Table 8.1-7. Output statistics of generalized additive models (GAMs) with Poisson distributions to analyze the effects of time ('age' of FAD), season, and survey method on the abundance of seven individual species (Bar jacks *Caranx ruber*, almaco jacks *Seriola rivoliana*, scad *Decapterus sp.*, *Clupeidae*, unicorn filefish *Aluterus monoceros*, wahoo *Acanthocybium solandri*, and mahi *Coryphaena hippurus*). Bold text highlights significant effects..... 117

Supplementary Table 8.1-8. Analysis of variance (ANOVA) output table for the best fitting GAM model of abundance of seven individual species (Bar jacks *Caranx ruber*, almaco jacks *Seriola rivoliana*, scad *Decapterus sp.*, *Clupeidae*, unicorn filefish *Aluterus monoceros*, wahoo *Acanthocybium solandri*, and mahi *Coryphaena hippurus*). Bold text highlights significant effects..... 119

Supplementary Table 8.2-1. Output statistics of a linear model (LM) to analyze the effects of distance away from FAD, lunar illumination, deployment time, depth, and the interactions between illumination and depth, and distance away and depth, on light trap log(CPUE) of all organisms at the North FAD. Significant terms are bolded..... 121

Supplementary Table 8.2-2. Analysis of variance (ANOVA) output table for the linear model (LM) to analyze the effects of distance away from FAD, lunar illumination, deployment time,

depth, and the interactions between illumination and depth, and distance away and depth, on light trap log(CPUE) of all organisms at the North FAD. Significant terms are bolded..... 122

Supplementary Table 8.2-3. Output statistics of a linear model (LM) to analyze the effects of distance away from FAD, lunar illumination, deployment time, depth, and the interactions between illumination and depth, and distance away and depth, on log(CPUE) of polychaetes at the North FAD..... 123

Supplementary Table 8.2-4. Analysis of variance (ANOVA) output table for the linear model (LM) to analyze the effects of distance away from FAD, lunar illumination, deployment time, depth, and the interactions between illumination and depth, and distance away and depth, on log(CPUE) of polychaetes at the North FAD..... 123

Supplementary Table 8.2-5. Output statistics of a linear model (LM) to analyze the effects of distance away from FAD, lunar illumination, deployment time, depth, and the interaction between illumination and depth on the log of total length of light trapped individuals at the North FAD..... 124

Supplementary Table 8.2-6. Analysis of variance (ANOVA) output table for the linear model (LM) to analyze the effects of distance away from FAD, lunar illumination, deployment time, depth, and the interaction between illumination and depth on the log of total length of light trapped individuals at the North FAD..... 124

Supplementary Table 8.2-7. Output statistics of a linear model (LM) to analyze the effects of distance away from FAD, lunar illumination, deployment time, depth, and the interaction between illumination and depth on the diversity (at order level) of light trapped individuals at the North FAD..... 125

Supplementary Table 8.2-8. Analysis of variance (ANOVA) output table for the linear model (LM) to analyze the effects of distance away from FAD, lunar illumination, deployment time, depth, and the interaction between illumination and depth on the diversity (at order level) of light trapped individuals at the North FAD..... 125

Supplementary Table 8.2-9. Output statistics of a linear mixed effects model (LME) to analyze the effects of distance away from FAD, lunar illumination, temperature, location (North FAD or

South FAD), and period (day or night) on logNASC in the ‘weak scatterer’ category (between -50 dB and -85 dB  $S_v$ ). Significant terms are bolded..... 126

Supplementary Table 8.2-10. Analysis of variance (ANOVA) output table for the linear mixed effects model (LME) to analyze the effects of distance away from FAD, lunar illumination, temperature, location (North FAD or South FAD), and period (day or night) on logNASC in the ‘weak scatterer’ category (between -50 dB and -85 dB  $S_v$ ). Significant terms are bolded..... 127

Supplementary Table 8.2-11. Output statistics of a generalized linear mixed effects model (GLM) to analyze the effects of distance away from FAD, period (day or night), temperature, location (North FAD or South FAD), and lunar illumination on the presence of strong scatterers (binomial NASC > -50 dB  $S_v$ ). Significant effects are bolded..... 127

Supplementary Table 8.2-12. Analysis of variance (ANOVA) output table for the generalized linear mixed effects model (GLM) to analyze the effects of distance away from FAD, period (day or night), temperature, location (North FAD or South FAD), and lunar illumination on the presence of strong scatterers (binomial NASC > -50 dB  $S_v$ ). Significant terms are bolded..... 128

## Acknowledgements

I would like to thank a number of people that have provided an immense amount of professional and personal support over the years. First, I would like to thank my advisors David Bailey and Shaun Killen. Even before my enrollment, Dave was willing to entertain a project proposal under unique circumstances, and I am very grateful that you persisted and made this whole arrangement work out. Thanks to both Dave and Shaun for trusting me to work somewhat independently, but also for the attentive and in-depth mentorship and feedback. I appreciate you making this work from a distance. Additionally, I would like to thank Travis van Leeuwen and Matthew Witt for their contributions to this thesis and more importantly to my professional development. I consider you both unofficial advisors and am very grateful for the time and effort you have put into this work. Frank Smith has also gone above and beyond in our collaboration to develop a new telemetry array, and I would like to thank you for your time and effort put into this project. The creativity involved in this work has been a really exciting part for me.

I would also like to Brendan Talwar and the rest of the Exuma Sound Ecosystem Research Project team over the years. Brendan, it's been great doing our work side by side and hopefully we can keep that going. And to everyone that has worked with us to build EXERP: Candace Fields, Alexa Hoffman, Samantha Russell, Jessica Dehn, Lauren Barnes, Savannah Ryburn, Claude Pressoir, Elyana Lafrance, Jawanza Small, Kenaro Malcolm, Bryce Gell, Natasha Hinojosa, Jack Dales, Danielle Orrell, Bailey Warren, Miranda Andersen, Juliette Lee, Matt Israel, Davis Huber, Phil Osborn, Cynthia Hsia, Ed Good, Greg Sayles, Dylan Grady, Will Barnes, and all of the students of the EXERP research classes and colleagues at the Cape Eleuthera Institute- thanks a ton, it's really been great working with you all. A huge thanks to Dave Philipp and Julie Claussen for supporting this idea early on and being great mentors and friends.

This work would have also not been possible without the support of the Moore Charitable Foundation and the Moore Bahamas Foundation. You have given us the flexibility to try different things and get a lot of research done, involving many students along the way. Many thanks also go to Luke Madden for his media and graphics contribution to this research, making science engaging and exciting through your photos and videography. Thanks to the R/Vs Great White and Alucia and crews for helping us get the field work done.

Finally, a huge thank you to my family and friends that have supported me along the way. Candice, you have been incredibly supportive and have made sacrifices so that I can stay in school for an inordinate amount of time. I truly appreciate you and Tula for being great throughout this. I'd like to thank my parents Jill and Scott, and my siblings Carson, Clara, Lindsey, Shawn, and Allison for inspiring and sharing an interest in science and nature and encouraging me to pursue this career.

### **Author's declaration**

The thesis presented here is original work by E. Schneider. There are no conflicts of interest associated with this work. All research has been conducted under permits issued by the government of The Bahamas. Project ideas were conceptualized by a combination of E. Schneider, B. Talwar, D. Bailey, S. Killen, T. van Leeuwen, M. Witt, and F. Smith.

# 1. General Introduction

## *1.1 Pelagic Zone*

The pelagic ocean is the largest habitat on Earth by surface area and volume, but it has been largely understudied compared to coastal or terrestrial ecosystems (Webb et al., 2010). This zone of the ocean provides important ecosystem services such as food and oxygen production, carbon cycling and climate stabilization (Worm et al., 2006), and is known to harbor considerable biodiversity (Angel, 1993). However, most pelagic animals are inherently difficult to study due to the expanse of their habitat and their life history and behavior, resulting in a comparatively weak understanding of pelagic ecology and biology (Block et al., 2003). For example, even basic population trends of pelagic fishes are frequently debated or misunderstood (e.g., Burgess et al., 2005; Hampton et al., 2005). High level predators including scombrids (tuna, wahoo), billfish and pelagic sharks have been identified as the taxonomic groups that are most at risk of over-exploitation (Moyes et al., 2006), and more research is required to better understand how to conserve these animals.

## *1.2 Surveying Pelagic Fish Populations*

Surveying fish populations is an important tool that informs conservation activities and underpins fisheries management, and the techniques used vary depending on objectives, habitats, and target species. Data may be collected using fisheries-dependent or independent approaches, and both present advantages and disadvantages. Fisheries-dependent data leverages existing offshore activities at a scale that may be cost-prohibitive if not for the existence of that fishery but may be geographically biased as fishing fleets normally target known hotspots (Bradley et al., 2019). Conversely, fisheries-independent surveys can be carefully designed to randomly or systematically sample a given area and reduce certain biases but may be limited by research funding. Methodological limitations (e.g.s., cost and time) and fish behavioral biases are also important considerations when designing surveys, and multiple approaches are often used to add confidence to estimates or to effectively sample a wide range of species or life history stages that may not be possible to sample using one method. Trawl surveys are commonly used in both abundance and diversity surveys, and hydroacoustic sampling is a powerful tool for biomass

estimations (e.g., Letessier et al., 2022; Massé et al., 2018; Watanabe & Nishida, 2002), but these methods also have limitations. There are behavioral biases involved with trawling as trawl evasion and catchability varies between species and life stage (Fraser et al., 2007), and species-level identification using echosounder data (a form of hydroacoustics) alone is only possible if the species-specific ensonification signal has been characterized, which only exists for a limited number of pelagic marine fishes. More recently, environmental DNA barcoding (eDNA) has been developed and used to mitigate catchability biases, as all living organisms shed DNA into their surroundings and can in theory be sampled (Frajia-Fernandez et al., 2020). However, this is still a new technology and has limitations for estimating abundance, and organisms must exist in a known reference library to be identified. Other more targeted pelagic sampling methods exist, such as longline surveys and baited camera surveys (Santana-Garcon et al., 2014), but each present their own biases in relation to bait attraction, size, and feeding mode. The limitations of each approach should be considered when interpreting survey data.

### *1.3 Structure Affecting Animal Behavior*

Structure, including oceanographic, geologic, biological, and anthropogenic, also plays an important role in shaping pelagic ecology. Currents and clines have the potential to shape the abundance or distribution of many marine species. One common example is the resulting increase in localized pelagic biomass around seamounts. The deflection of a nutrient-rich current towards the surface provides a boost to primary production that is carried throughout the trophic levels (Morato et al., 2007). In other instances, this geologic structure (a submarine mountain) can also act to physically impede the downward movement of vertically migrating zooplankton, causing an accumulation of prey that can then support an abundance of predators (Genin, 2004). Additionally, marine animals are known to interact with thermoclines (Sogard & Olla, 1993) and gyres or eddies for various reasons. Examples include movement/transport (Gaspar et al., 2006; Lobel & Robinson 1986) and prey detection (Lokkeborg et al., 2014), and research is ongoing to better understand how fish interact with these oceanographic structures.

Marine species, particularly pelagic fish, are also drawn to floating biological (e.g., logs, seaweed) or anthropogenic (e.g., plastic crates, buoys) structures for a variety of reasons (Castro et al., 2002). Among numerous likely factors, the ‘indicator log’ and ‘meeting point’ hypotheses

are the most widely accepted (Orue et al., 2019). The ‘indicator log’ theory states that migratory fish may use floating objects to gauge the productivity of an area, and would have historically encountered floating debris (logs, etc.) at the highest concentrations near large estuaries, river mouths, or gyres which are typically highly productive (Castro et al., 2002). The ‘meeting point’ hypothesis states that schooling fish utilize structures to find conspecifics and reform larger schools and has been supported with some experimental evidence wherein fish often arrive at floating structures as individuals or in small groups and leave in larger schools (Soria et al., 2009). Additional factors also influence fish behavior around structures, such as grazing, hunting, or structural predator avoidance (Girard et al., 2004). A general structure for how fish communities assemble themselves around a floating object was proposed, and describes small, slow ‘intranatant’ individuals maintaining immediate proximity to the object, slightly larger ‘extranantant’ individuals ranging slightly further away but still within range of a quick retreat, and larger predatory ‘circumnatant’ individuals that can maintain association with an object even during excursions up to several kilometers away (Parin & Fedoryako, 1999). Vision, olfaction, and sound/vibration perception are all likely mechanisms used by fish to find different structures in the open ocean (Dempster & Kingsford 2003). Interestingly, physical characteristics such as size, material or color of the structure do not appear to significantly affect fish association or usage (Hall et al., 1992), although depth of material suspended off the structure (frequently used in fishing practices) does (Orue et al., 2019).

In pelagic habitats, the broad-scale horizontal and vertical range of migratory fishes is roughly bound by abiotic factors, mainly temperature and dissolved oxygen (Prince & Goodyear, 2006). However, much of their fine scale movements are based on tracking the sound scattering layer or other prey aggregations (Dagorn et al., 2000), in addition to interacting with geologic, biological, or anthropogenic structures. Therefore, many pelagic fishes are constantly influenced by both the biotic and abiotic environment in their daily activities (Josse et al., 1998).

#### *1.4 Animal Tracking in the Ocean*

Tracking the movement of marine animals is often a high research priority to understand their life history, ecology, and human interactions (Hussey et al., 2015), but the scale of movements varies greatly and must be assessed with different techniques and technology. For

example, tiger sharks undergo roundtrip migrations of up to 7,500 km crossing open-ocean habitats (Lea et al., 2015), but other species, such as the commercially important queen conch (*Lobatus gigas*) may have a home range as small as 6 ha in coastal habitats (Glazer et al., 2003). A range of different tracking methods have been developed to suit different species and contexts, including passive mark-recapture methods using numbered identification tags, light-based geolocating satellite tags, rapid acquisition GPS, and acoustic transmitters. Each method has advantages and disadvantages relating to tag size, cost, habitat, animal behavior, and type of data that can be generated (or precision thereof), and these factors must be considered to align the most appropriate technology with the study objectives. Tracking animals in the open ocean is particularly challenging based on the expanse of the habitat. More area and less human activity in this environment pose challenges for traditional mark-recapture studies, and the average water depth of the pelagic zone of the ocean prevents the use of most bottom-based tracking technology such as an acoustic telemetry array that uses receivers on the seafloor. Much of the pelagic animal tracking to date has been done with satellite tags, but data generated from these tags are prone to large error ranges (up to 120 km in some pelagic fish studies; Gatti et al., 2021) and are not well-suited for fine-scale behavioral investigations.

### *1.5 Fish Aggregating Devices*

Fishers have long exploited the natural association of fish to floating structure by targeting these objects to increase catch rates while decreasing their effort. In the last thirty years, the commercial tuna industry has deployed man-made floating structures (typically buoys) called fish aggregating devices (FADs) to further enhance their efficiency (Baske et al., 2012). At present, over 50% of the global tuna landing is caught using FADs (Miyake et al., 2010), and estimates suggest that 47,000 to 105,000 new drifting FADs are deployed into the world's oceans annually (Baske et al., 2012). With this sharp increase in this new fishing technology, the need for management strategies and research to understand the effects of FAD deployment and fishing has become obvious.

There are a number of aspects of fish biology that may be negatively impacted by FADs, and this area of research has been highlighted as an important avenue of pursuit as the FAD fishery continues to expand with few regulations. For example, there is some evidence that FADs

may be causing an ‘ecological trap’ for some species, during which some aspect of their fitness decreases resulting from the false incentives created by associating with a man-made FAD (Marsac et al., 2001). Examples include decreased body condition resulting from lower feeding efficiency, and altered migratory behavior (Hallier & Gaertner, 2008). This does appear to be context-specific because numerous examples have also found that fish association with FADs may not alter net migration. For instance, Indian Ocean tuna were shown to have similar movement characteristics when tagged in ‘high-FAD’ areas and ‘low-FAD’ areas, indicating that there was no net disruption to their migrations (Stehfest & Dagorn, 2010).

### *1.6 FADs in Research*

In addition to these broader studies, there has been an effort to understand the dynamics of aggregations and the fine-scale fish movements around floating structures such as FADs. However, technology and accessibility have limited the amount of research performed on this particular topic. Through a combination of direct visual, video or acoustic observation, single-receiver acoustic telemetry and satellite tagging, several aspects of assemblage and fish behavior around FADs have been observed. Some examples have shown that fish association distance roughly correlates to the size and trophic position of the animal (Taquet et al., 2008). Additionally, FADs typically have rough lateral bounds to their aggregation effects, in that most schools of fish will stay within a certain range (anywhere from 80-500 m) while associated with the FAD (e.g., Doray et al., 2007). There have been several studies attempting to describe the detailed temporal patterns and depth profiles of certain target and bycatch species, however these are typically short-term observation periods based on FADs that may be actively or recently fished (e.g.s., silky sharks in Filmalter et al., 2015; tuna, carangids and balistids in Forget et al., 2015 and Doray et al., 2007). Because much of the FAD-related research is either based off fisheries-dependent activities or is conducted on actively fished FADs, there has been a call for developing methods to collect fisheries-independent data to be used in management and stock assessments (Moreno et al., 2016).

Instrumented FADs have recently been identified as research priorities as they have high potential for facilitating data collection in an otherwise difficult to access environment (Moreno et al., 2016). One such project (FADIO: FADs as Instrumented Observatories) aimed to develop

this idea and has contributed significantly to the efforts of studying pelagic ecology (Dagorn et al., 2006). However, to date, all of these initiatives have used FADs that are actively fished as their platforms, potentially masking ecological phenomena due to the nature of this extractive process, or biasing findings towards geographical areas that are chosen by fishing fleets. There is a need to improve stock assessments and management guidelines with more fisheries-independent data (Moreno et al., 2016), and research-specific platforms are the next logical step to achieving these outcomes.

In 2017, we installed two moored FADs along the 600 m isobath in the Exuma Sound, eastern Bahamas. Unique in that the FAD structures (2 steel meter-wide buoys) remain 10 m beneath the surface of the ocean, these FADs were designed to be difficult to find without GPS, rendering them ‘off-limits’ to fishing activities. To our knowledge, these were the first deep-water (>200 m) sub-surface FADs designed strictly for research purposes and will hopefully act as a means to answer questions related to colonization, succession, and assemblage dynamics around FADs. A recent study reported the colonization process of drifting FADs over the course of 60 days, showing interesting differences in biomass accumulation based on size and taxonomic group (Orue et al., 2019). However, these changes were only studied over a relatively short time scale of two months, as many FAD-based investigations have been historically ephemeral. By deploying these research FADs, this opens the possibility of generating long time series datasets that can give further insight into assemblage dynamics, for example as they pertain to seasonality or wider effects a FAD may have on the surrounding ecosystem. As the call has arisen for more fisheries-independent data to support stock assessments and general ecological understanding, these research FADs have the additional advantage of potentially revealing phenomena that may have been otherwise masked by the fishing activity that occurs on other FADs (Orue et al., 2019). Insights into any potential associative patterns that might exist could help researchers, managers, and fishing fleets establish baselines for pelagic biodiversity and abundance, improve fishery selectivity, and generally refine research methods to improve the sustainability of these pelagic resources.

### *1.7 Objectives*

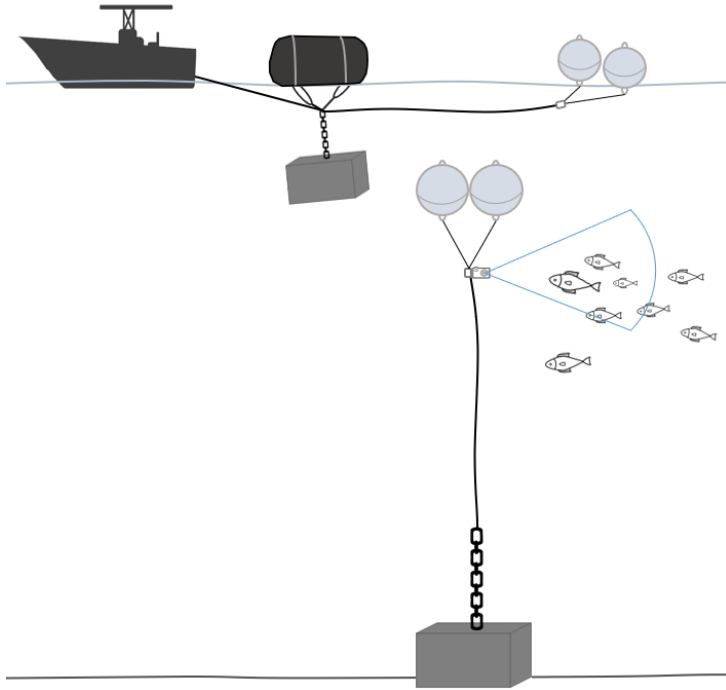
The goal of this thesis is to understand the associative behavior of pelagic fish to structure in the open ocean. In investigating this, we aim to determine whether FADs can be used as effective conservation tools by facilitating a better understanding of the association dynamics of pelagic animals around subsurface, deep-water FADs in the Exuma Sound, The Bahamas, and discussing how this behavioral information can be used for fisheries management and conservation. Four projects were conducted (Chapters 2-5) which are presented here and aim to address the following specific objectives.

- Chapter 2
  - a. Provide details and considerations for the design, construction, and deployment of an affordable and durable deep-water subsurface FAD that can be deployed using small boats
  - b. Highlight the potential for a long-lasting moored FAD to be used as a sustainable and reliable scientific platform for pelagic species research and conservation, lending specifically to several research applications
- Chapter 3
  - a. Determine the factors affecting fish association to FADs
    - i. Determine how quickly a new FAD is colonized
    - ii. Compare the effectiveness of video and visual survey methods
    - iii. Describe any seasonality and between-group (taxonomic or functional) associations that occur
- Chapter 4
  - a. Determine the influence of a FAD and other abiotic factors on pelagic animal assemblages
- Chapter 5
  - a. Design and test an array that can calculate distance away and bearing of a transmitter in relation to the array-affixed structure
  - b. Test detection efficiency and positioning error between various depth combinations of receivers and transmitters in the array (e.g., shallow receiver x shallow transmitter, shallow receiver x deep transmitter, etc.)
  - c. Track the movement of a wild fish through the array to test its performance

## 1.8 Methodological Outline

### 2. Design and Deployment

### 3. Visual and Video Surveys



### 4. Micronekton Survey

### 5. Acoustic Telemetry Array

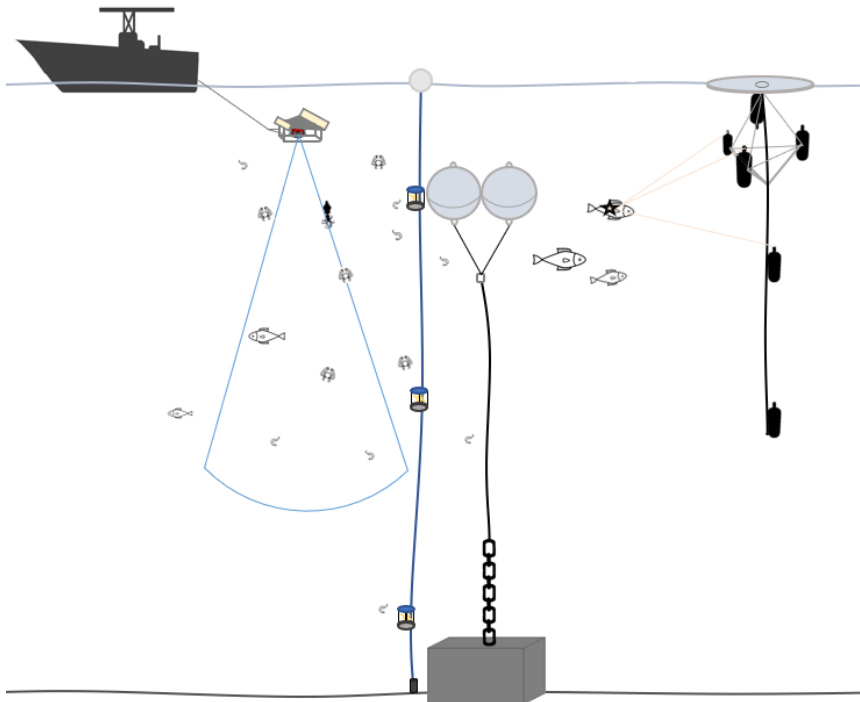


Figure 1.8-1. An illustration of each of the projects that are included in this thesis. The inset numbers refer to the corresponding chapter, along with a brief text description of that project. Chapter 2 (top left) details the design, construction, and deployment of the subsurface moored research FADs. A small boat is depicted towing the mooring anchor, which is suspended by a lift bag, with the trailing mooring line and buoys at the sea surface. Chapter 3 (top right) depicts the field of view of a video camera mounted on the FAD used during the visual and video survey project, after the FAD is in its subsurface placement. Chapter 4 (bottom left) depicts a small boat towing an echosounder mounted on a glider frame (with the area of ensonification shown as a downward facing cone). The vertical line depicts a series of small cylindrical light traps that sampled the micronekton throughout the water column around the FAD. Chapter 5 (bottom right) depicts a drifting FAD (grey oval at the sea surface) with six black acoustic receivers suspended beneath it using extendable poles and rope. A fish tagged with an acoustic transmitter (marked with a star) is depicted swimming near the array.

## **2. Design and deployment of an affordable and long-lasting deep-water subsurface fish aggregating device**

Published in Caribbean Naturalist (2021), Issue 83, pages 1-16.

Schneider EVC, Brooks EJ, Cortina MP, Bailey DM, Killen SS, van Leeuwen TE

### **2.1 Abstract**

Fish aggregating devices (FADs) are used worldwide to enhance the efficiency of various fisheries. Devices consist of a floating or subsurface component designed to exploit natural fish behavior, using species' attraction to structure (e.g., *Sargassum* spp.) to aggregate fish and increase capture success in open ocean environments. Concerns have arisen regarding the scale and management of FAD-associated fisheries, however, the efficiency of FADs to aggregate fish also introduces the possibility for FADs to be used as conservation tools to study pelagic species ecology. Building on two successful and several failed deployments of anchored deep-water (>500 m) subsurface (10 m) FADs over three years in The Bahamas, and observations from the subsequent FAD monitoring program, the objectives of the paper are to: 1) provide details and considerations for the design, construction, and deployment of an affordable and durable deep-water subsurface FAD that can be deployed using small boats; and 2) highlight the potential for a long-lasting moored FAD to be used as a sustainable and reliable scientific platform for pelagic species research and conservation, lending specifically to several research applications. This information will be useful for assessing the impacts that FADs and other anthropogenic marine infrastructure have on wild marine species, and their effectiveness for conserving pelagic fish through increased encounters for study.

### **2.2 Introduction**

The pelagic ocean is the largest habitat on Earth by both surface area and volume, however, it is largely understudied compared to coastal or terrestrial ecosystems (Webb et al., 2010). The pelagic zone of the ocean provides important ecosystem services such as food and oxygen production, carbon cycling, and climate stabilization (Robison, 2009), and is known to

harbor considerable biodiversity (Angel, 1993). With offshore habitats under intense fishing pressures (Dulvy et al., 2008; Verity et al., 2002) and many fish stocks reaching either fully exploited or over-exploited levels (FAO, 2018; Pons et al., 2017), the need for better science, management, and enforcement of the pelagic zone and its fisheries is evident and increasing.

One aspect of fish behavior, particularly seen in pelagic species, that has substantially contributed to their harvest is their propensity to aggregate around floating structure at a higher rate than they would otherwise in open water lacking structure (Girard et al., 2004; Castro et al., 2002; Deudero et al., 1999). Over the past several decades, intentionally constructed fish aggregating devices (FADs) have become a ubiquitous tool in pelagic purse seine fisheries (Moreno et al., 2016) with more than half of all tuna landed globally caught using FADs (Miyake et al., 2010). A wide range of epi-pelagic fishes have been documented aggregating to floating structures (Castro et al., 2002) including many high-level predators such as scombrids (e.g., tunas), billfish, and pelagic sharks which are groups of fishes most at risk of over-exploitation (Baum & Myers, 2004; Baum et al., 2003). It is estimated that 81,000 to 121,000 new FADs are deployed into the world's oceans annually, with many lost within the first year after deployment (Gershman et al., 2015). The scale of FAD use poses numerous challenges to ocean conservation and fisheries management, and such a rapid increase in fishing technology (e.g., FADs instrumented with GPS trackers and 'fish-finder' echosounders) has outpaced management developments (Baske et al., 2012). When working to manage an industry that utilizes such powerful fishing tools as FADs, extra attention must be paid to promote the sustainability of targeted stocks and bycatch species.

Recently, there has been a concerted effort to utilize instrumented FADs and to work cooperatively with fishing industries to increase the capacity for pelagic species research in this often difficult to access and vast habitat (Brehmer et al., 2019; Davies et al., 2014). However, these initiatives typically use FADs that are actively fished and free-floating which may bias ecological research towards geographical areas that are chosen by fishing fleets and potentially mask ecological phenomena due to the nature of this extractive process. Additionally, most drifting FADs are not accessible by small boats with shorter ranges and have a relatively short functional life of less than one year before degrading or washing out of range or ashore, limiting the feasibility of long-term biological studies or oceanographic monitoring (Lopez et al., 2017).

Therefore, to address these concerns, it is important to invest in the collection of fisheries-independent data utilizing long-lasting anchored FADs to better understand the status and trends of commercially important fish stocks (Moreno et al., 2016). Depending on location, anchored FADs may allow greater accessibility to undertake monitoring work, can facilitate a wide array of instrumentation both above and below the surface of the ocean, and will allow for longer studies to occur if designed properly (see examples in Table 2.2-1). Few resources exist on the design, construction, and deployment of anchored FADs for study, despite their widespread use in the fishing industry. Specifically, details on exact materials and costs are rare in the literature. When information is presented, some existing studies and manuals typically describe FADs deployed from large boats or using materials that are normally either expensive or difficult to ship to remote locations.

Here we detail the design, construction, deployment, and utility of an anchored deep-water, subsurface FAD that is durable and long-lasting, easily reproducible, and specifically intended to facilitate fish ecology and marine conservation research. The durability and moored nature of the design makes the FAD less prone to loss or damage, and the low cost of the FAD allows for the possibility of several to be deployed using small boats and facilitate much needed replication and manipulation in experimental designs, a component often lacking in this area of study. While the subsurface aspect of these FADs was designed to reduce surface-associated damage and tampering, and to facilitate specific research objectives, any potential trade-offs between constructing a subsurface FAD and fish attraction / aggregation are also a point of interest and are detailed below. In this study, we have not tested the attraction or aggregation effects of these FADs against that of surface FADs, but we draw in references from other regional projects.

Table 2.2-1. Selected examples from a search of studies using anchored FADs that include information on materials or deployment, that are subsurface (or ‘midwater’), or that were deployed in depths  $\geq 500$  m and therefore comparable to our proposed design. ‘Buoy Depth’ of 0 represents a surface FAD. Substantial and replicable information must be included on materials used or deployment processes to qualify as ‘Yes’.

<b>FAD Type</b>	<b>Bottom Depth (m)</b>	<b>Buoy Depth (m)</b>	<b>Materials Info</b>	<b>Deployment Info</b>	<b>Location</b>	<b>Reference</b>
Surface and subsurface	300-2000	0-?	Yes	Yes	Pacific Islands	Chapman et al., 2005
Surface	<200	0	Yes	Yes	Timor-Leste	Mills & Tilley, 2019
Surface	100-3000	0	Yes	Yes	Caribbean	Gervain et al., 2015
Surface and subsurface	1000-2000	50-100	Yes	No	Japan	Sokimi, 2006
Surface and subsurface	146-2761	0-18	Yes	No	Hawaii	Higashi, 1994
Surface	<5000	0	Yes	No	Pacific Islands	Itano et al., 2004
Subsurface	415	50	No	No	Taiwan	Weng et al., 2013
Surface and subsurface	50-2500	?	No	No	Pacific Islands	Taquet et al., 2011
Surface and subsurface	300-700	0-?	No	No	Pacific Islands	Bell et al., 2015
Surface	260-600	0	No	No	Puerto Rico	Merten et al., 2018
Surface	50-500	0	No	No	Canary Islands	Castro et al., 1999
Surface	1000-2200	0	No	No	American Samoa	Buckley & Miller, 1994
Surface	2000-2500	0	No	No	Martinique	Doray et al., 2007

## 2.3 Methods

### 2.3.1 FAD Design

The main design objectives were to create a long-lasting subsurface anchored FAD without any surface markers, deep enough to avoid surge-associated damage or navigational

hazards, while still shallow enough to be accessible to divers and avoid pressure-related damage to the steel buoys. Additionally, the FAD needed to easily facilitate equipment mounting to act as a stable platform for various fish ecology and marine conservation investigations.

The FADs used in our study consisted of a concrete anchor block (122 cm L x 122 cm W x 84 cm H = 1.25 m<sup>3</sup>; ~2900 kg weight on land, ~1620 kg weight in water), a vertical mooring line (600 m of 5,817 kg minimum tensile strength one inch polypropylene) and two tethered subsurface steel buoys (surplus naval buoys, 71 cm diameter, 54 kg weight / 181 kg buoyancy each; Figure 2.3.1-1). A depth of 10-15 m subsurface was decided to be an acceptable target range for the floats, although subsurface FADs are not commonly deployed at bottom depths > 600 m (study site depth) which is novel here (Chapman et al., 2005). At the time of writing, two of these FADs have remained in place for over five years (December 2017 – May 2023) and have withstood wind and surge from multiple passing hurricanes (<100 kph winds). The FADs were visited weekly for the first 2.5 years, and then monthly thereafter.

Existing designs found in scientific papers and technical reports did not conform to all our objectives, therefore a new and unique design was utilized here. For example, Weng et al. (2013) used a subsurface FAD at a bottom depth of 415 m, however, the buoy depth of 50 m was inaccessible to divers. Further, details of an array of subsurface FADs around Okinawa, Japan indicate subsurface FADs at bottom depths up to 2000 m. However, the materials and deployment were costly, and structure depth ranged from 20 m to 100 m subsurface which minimizes survey time available for divers or renders it inaccessible (Sokimi, 2006). The closest example to those used here is a subsurface FAD array in Hawaii described by Higashi (1994) with a bottom depth range of 366 m to 549 m and a buoy depth of 18 m to 21 m, but little detail describing the construction and deployment is available. From the limited information available, it suggests a large naval vessel was used for deployment and that the FAD construction used galvanized steel cable, suggesting neither a simple nor cheap construction and deployment process.

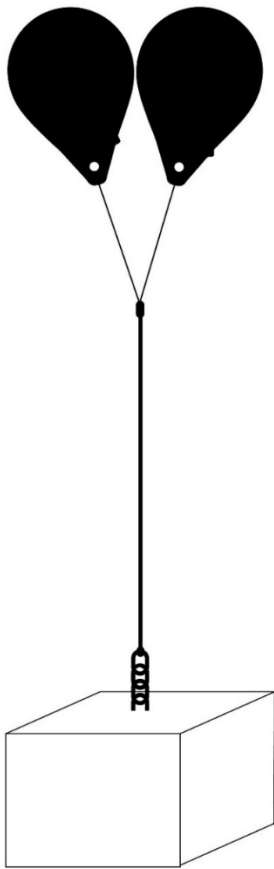


Figure 2.3.1-1. Schematic of the subsurface fish aggregating device (FAD) currently being used at The Cape Eleuthera Institute, The Bahamas. FAD design consists of a concrete anchor block, mooring line, and two steel buoys. Steel buoys are moored 10 m below the sea surface to prevent detection by fishers and to create tension and verticality in the mooring line for gear deployment. Diagram not to scale.

### *2.3.2 Construction*

Steel reinforcing lattice (#4 rebar) was laid as the concrete was being placed, and a stainless-steel round stock bail (Figure 2.3.3-2) was incorporated beneath the last layer of lattice so that the top of the bail protruded from the center of the block to aid in mooring line attachment. A shackle (7/8" [22.2 mm] bolt through) was used to attach four meters of 3/4" (19.1 mm) long-link chain to the bail anchor point between the block and mooring line. The chain was

used to prevent chaffing of the anchor line against the anchor block in the event of converting the structure to a surface FAD. However, this was determined to be unnecessary for subsurface orientation because the tension in the mooring line, by default, prevents the anchor line from contacting the anchor block. This was followed by a 7/8" (22.2 mm) bolt through shackle, a 7/8" (22.2 mm) eye by eye swivel, another 7/8" (22.2 mm) shackle and finally a size four rope connector (Samson Nylite, Ferndale, Washington, USA; Figure 2.3.3-3).

Eight-strand 1" (25.4 mm) polypropylene line (5,817 kg minimum tensile strength) was used as the mooring line and attached to rope connectors via an eye-splice. The rope connector prevented the eye splice from chaffing against the metal rigging. End-to-end splices were used any time the line needed to be extended. The same series of hardware was repeated at the end of the line (rope connector, swivel, and shackle). However, this series was then followed by a 7/8" (22.2 mm) master link (Figure 2.3.3-3).

The floating portion of the FAD structure was comprised of two round 71 cm diameter steel buoys (54 kg weight, 181 kg buoyancy each) tethered to the master link using two meters of 1/2" (12.7 mm) three-strand polypropylene line that was eye-spliced through a rope thimble. This is similar in size and surface area to the flotation component of drifting FADs used in some commercial tuna fisheries (personal observation). However, FADs used in commercial fisheries often incorporate subsurface netting, palm fronds, synthetic streamers, or other structure below the surface. These additions were not included in this design to avoid animal entanglement (Filmlalter et al., 2013) and to maintain clearance along the mooring line for equipment deployment (hydrophones, acoustic receivers, and oceanographic monitoring equipment) and retrieval during future stages of the research program.

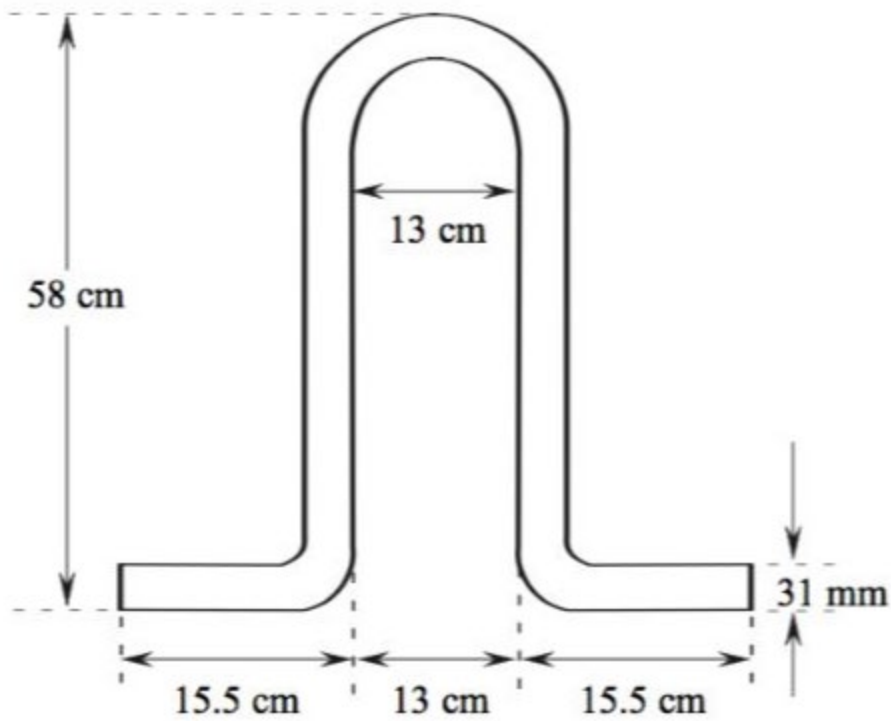


Figure 2.3.2-2. Stainless steel round stock bail that was incorporated into the top of the concrete anchor block to serve as the attachment point between the block and metal chain, which was the beginning of the mooring line.



Figure 2.3.2-3. Top end of the mooring line showing an eye splice to a rope connector, swivel, bolt through shackle, and 7/8" (22.2 mm) master link to which the buoys (and a safety line during deployment) were attached.

### *2.3.3 Deployment*

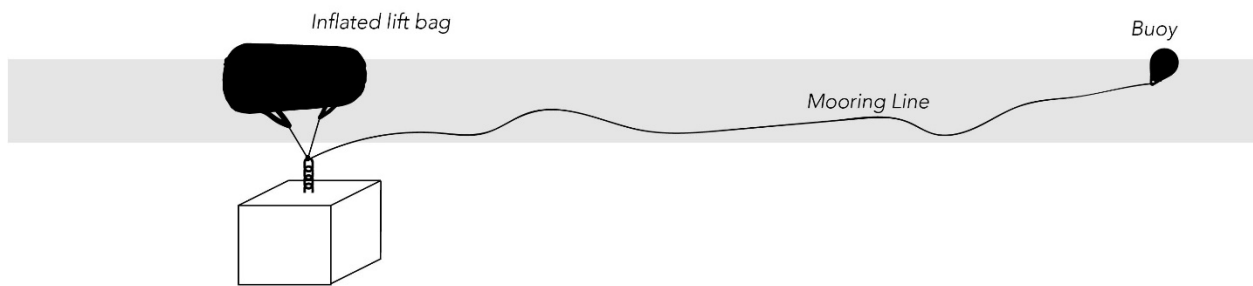
Several location parameters were taken into consideration when selecting locations for the subsurface FADs, and the Exuma Sound (near the Cape Eleuthera Institute and base of

research operations) was ideally suited for this. First, a deep-water drop off was located near-shore and accessible from the research station. Second, the area is a known migration route for pelagic fishes. Although the bathymetry had not been accurately described, several known depth points from previous deep-water research were used to select suitable locations and to predetermine mooring line lengths.

Following the construction of the individual components on land, the anchor was transported into shallow water at a nearby marina using a crane truck. Although in this case a crane truck was used, the block could be constructed on a platform at the edge of the water and deployed using rollers or a winch for simplicity. Once the anchor was submerged, three lift bags (SP2000, Subsolve, North Kingstown, Rhode Island, USA) were attached to the anchor bail using a release under load mechanism (Sea Catch TR7, MacMillan Design, Gig Harbor, Washington, USA). A safety line was attached between the block and lift bag to prevent premature deployment. Lift bags were inflated with compressed air and the anchor raised off the bottom for towing behind a small boat. The tow line was attached above the release mechanism so that if the anchor block dropped unexpectedly the weight of the anchor would not damage the boat. Once at the deployment location, a second small vessel slowly released the mooring line overboard and onto the surface of the water down-current and away from the anchor attachment point. A polyethylene ball float was attached to the free end of the mooring line to aid in visualization of the rope during and after deployment. Following the deployment of the mooring line from the vessel, snorkelers attached the anchor chain to the bail using a shackle, removed the safety line between the block and the lift bags, and released the load-bearing mechanism using a nylon rip cord thus dropping the block (Figure 2.3.3-4). The location of the drop was positioned to be 1/3 of the depth up-current of the targeted FAD location to account for drag on the line pulling the block in the down-current direction.

Following the anchor drop, the excess mooring line on the surface was recovered. The mooring line was then elongated using lift bags attached at depth to simulate the ultimate tension on the line from the FAD buoys. To do so, divers on SCUBA attached a lift bag to the mooring line using a Prusik hitch at 25 m depth and filled the lift bag with compressed air (Figure 2.3.3-5). Following the lift bag's ascent to the surface, this process was continued until the line was under approximately 600 kg of tension, evidenced by the 900 kg lift bag filled to approximately

66% of total volume, and positioned at a static depth of 10 m without further elongation. At least 24 hours were allowed for a complete tidal cycle, and to allow the mooring line to undergo phase one creep (stretching) to its ultimate length under load. If this time period resulted in reduced tension, or if the lift bags reached the surface, the mooring line elongation process was repeated. When the line was determined to have undergone all elongation, an eye-splice was used to attach a rope protector to the mooring line just above the lift bag. A shackle, master link, and a 15 m safety line with a fully inflated SP2000 lift bag were attached to the trailing end of the mooring line at the surface to further ensure the mooring line did not retract. Two individually rigged steel buoys were spliced onto the master link. After the attachment was complete, the lift bag under tension was released allowing the recoil of the mooring line to submerge the buoys to a depth of 10 to 15 m, at which point the inflated surface lift bag prevented any possible further descent. A small polyethylene buoy was finally attached to the master link and filled with compressed air as needed to fine tune buoyancy to the targeted 10 m depth resting point. Lastly, a safety line (3/8" [9.5 mm] Spectra 12-strand braided line, 6,305 kg minimum tensile strength) was tied to the master link, run through each eye-attachment point on the two buoys and tied back to the master link. In the case of eye-ring failure or a buoy tether being severed, this line provides a cut-resistant back-up to avoid the loss of a buoy or the entire FAD.



 Anchor block target

Figure 2.3.3-4. Initial stage of the FAD deployment process. The concrete anchor block is suspended by lift bags and attached to the mooring line that has been deployed overboard onto the sea surface down current from the anchor. The anchor is positioned 1/3 the length of the mooring line up current of the targeted resting location.

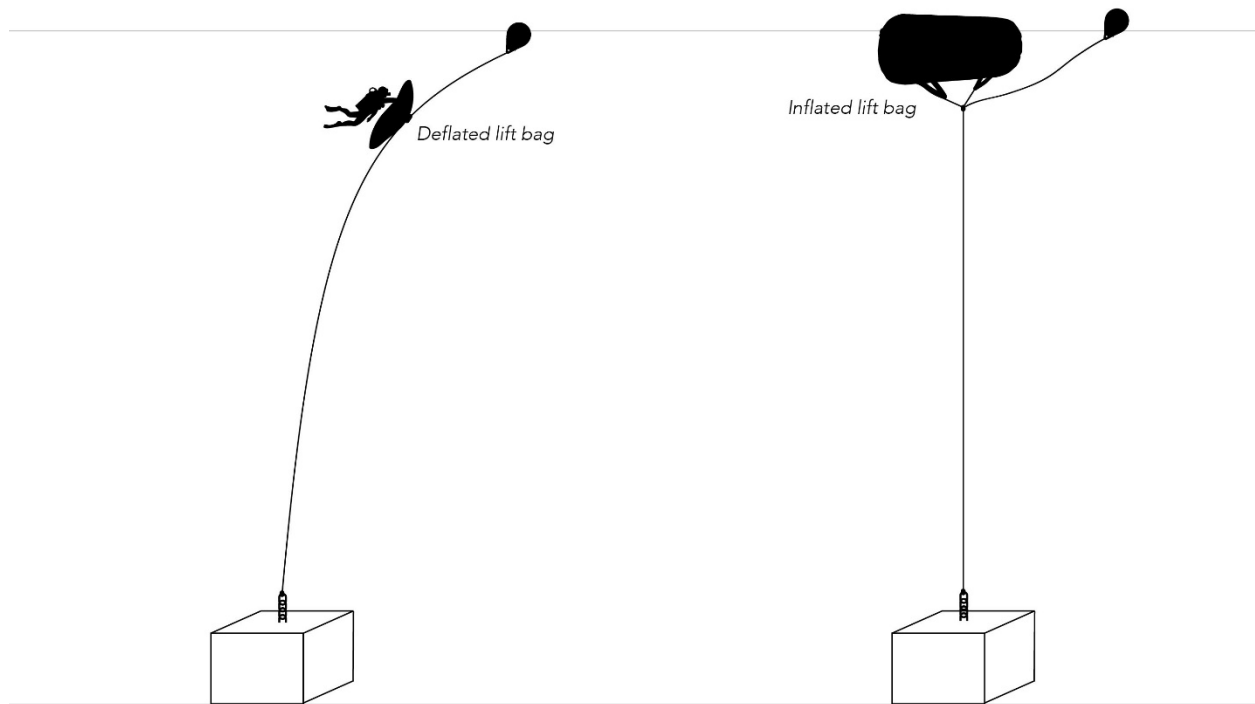


Figure 2.3.3-5. Schematic showing the process of removing slack from the mooring line following deployment. A diver attaches a deflated lift bag to the slack mooring line using a Prusik hitch and slowly inflates the bag. This process is repeated until the desired tension on the mooring line has been reached and the steel buoys are then attached.

#### *2.3.4 Removal Potential*

While the durability and moored nature of the FAD design presented here results in a robust and maintainable platform for longer time scales, these FADs are removable using the same equipment and process needed for deployment and users can therefore avoid contributing marine debris to the ocean following the conclusion of research activities. Although this would involve some effort, divers repeatedly deploying lift bags down the mooring line will slowly raise the anchor block which can then be towed to shallow water and allow for retrieval of the entire FAD.

## 2.4 Results and Discussion

### 2.4.1 Design Considerations

Materials and operations were all considered and selected to not only meet the project objectives, but to be accessible by a wide array of potential users including those at remote field stations or research groups with limited funding and resources. It has been shown that price is often a limiting factor during FAD creation and installation in remote island locations, and although this is typically documented in the scope of bolstering fishing communities (Bell et al. 2015), financial restraints will similarly apply to research groups. During the development and expansion of the Pacific FAD fishery, 2000 to 3000 USD was targeted for a reasonable total cost for a deep-water FAD intended to last approximately two years (Chapman et al., 2005), so the 5000 USD total cost per FAD in this project was deemed appropriate when designing for a durable longer-lasting structure. Longevity is also a high concern for surface FADs, with wave/weather damage or vandalism frequently leading to loss of the FAD in less than two years (Tilley et al., 2019; Chapman et al., 2005). Inspections in June 2019 (one and a half years after deployment), using deep sea submersible surveys in the area, revealed that all parts of the FAD design inaccessible to divers remain in good condition. The concrete anchor block, steel connections (shackles, chain, swivels, etc.), polypropylene mooring line and steel buoys were all considered to be affordable and possible to source and ship to a remote location and are standard options for offshore FADs (Chapman et al., 2005). Recently, there has been considerable effort to construct FADs from biodegradable materials to decrease marine debris and the potential negative impacts on wildlife such as entanglement (Moreno et al., 2018). Increasing longevity through careful design and robust synthetic materials was pursued during this project, although this could easily be adapted for a shorter-lived but biodegradable version. Additionally, the FADs were deployed using only SCUBA divers, a crane truck (or equivalent for pushing the anchor into the water), lift bags, and two eight-meter-long inboard panga vessels. One possible price reduction was tested by using three A-6 sized polyethylene buoys (Polyform A-6) instead of steel buoys when the first FAD was deployed, however this was quickly proven to not work. Flexible buoys expand or contract with minimal changes in water depth associated with the mooring line stretching or contracting, which in turn changes the buoyancy and prevents a stable target depth from being maintained. Additionally, several flexible buoys showed marks

consistent with teeth punctures by predatory fishes. Therefore, steel buoys soon replaced the flexible buoys after deployment of the first FAD and are highly recommended. Alternative mooring line materials were also considered, and materials such as Spectra or Dyneema are cut-resistant and would dramatically reduce phase one creep (stretching), making buoy placement at a target depth easier, however, these options are considerably more expensive and were avoided for this reason.

The subsurface aspect of the FAD design was chosen for several reasons related to the objectives of the project. First, 10 m depth was found to greatly minimize movement of the structure by surge or during windy weather, and would prevent any potential boat strikes, adding to the longevity of the infrastructure. Additionally, 10 m is an easily accessible and safe depth for both SCUBA and freedivers to work or deploy/retrieve equipment and does not pose any serious pressure-related stress to the buoys or equipment (at two atmospheres).

#### *2.4.2 Research Applications and Conclusions*

The subsurface anchored design of the FADs used in this study has proven to be a stable and diverse scientific platform for more than five years. Although this project did not conduct fish surveys away from the FADs to establish non-FAD-associated baselines, many of the epipelagic fish species that are known to occur in the region (either through other publications, fishing records, or anecdotal evidence) have been documented at the FADs, ranging in trophic level and size (Table 2.4.2-2). These anchored FADs allow the fish community to be continually monitored over long temporal scales and can facilitate short and long-term experimental studies through increased accessibility that would not be possible when using conventional offshore drifting FADs. It is possible that these long-term stationary fish censuses could be representative of actual population trends, and these data would therefore be useful to fisheries managers. Additionally, Dagorn et al. (2010) previously argued that anchored FADs are acceptable and useful proxies for drifting FADs to address research questions such as the ecological trap hypothesis, and that they pose accessibility advantages while maintaining contextual similarities to their drifting counterparts. A variety of methods that have been recently performed on surface FADs and would be well-suited to this FAD design, many of which were proposed by Moreno et al. (2016) as research priorities, are detailed in Table 2.4.2-3.

The subsurface aspect of the FADs used in this study, combined with the buoyancy of the buoys used (362 kg of lift total), resulted in a taut mooring line. Therefore, this design presents several unique opportunities for research activities. First, equipment can be shuttled up and down the mooring line with a simple rigging system, enabling fixed depth/location deployment of various instruments. This would otherwise be difficult without a taut mooring line. Additionally, keeping the structure underneath the surface and away from any surge or waves results in a nearly silent structure, presenting opportunities for investigation into fish sensory biology in the open ocean, and for better hydroacoustic data collection (e.g., hydrophone deployment for cetacean surveys). Finally, this tension ensured that the FAD buoys remained at the known GPS location and did not sway with tidal or current flow. Although this study area does not experience significant currents, locations with strong tidal flow should consider the impact of horizontal forces on the FAD and mooring line.

Strategically designed FADs that are not open access can act as useful research platforms to develop new monitoring approaches while maintaining the integrity of the study population and enhance our understanding of how anthropogenic activity is affecting marine biodiversity. For example, many animals that utilize pelagic FADs are fish species known to undergo long migrations (Hallier & Gaertner, 2008) and can be difficult to study. Whether following seasonal changes in food abundance, thermal windows, or breeding opportunities (Alerstam et al., 2003), this migratory behavior most likely exposes them to various fisheries pressures and potential overexploitation. Knowledge of how migratory animals respond to variable conditions experienced during migration is a central component to understanding long-distance movement patterns and their management. If data are collected consistently, this information can help estimate population size, increase understanding of demographic variables needed in the development of population viability models, reveal how wild fish species are impacted by anthropogenically altered habitats, and can potentially be used for novel conservation applications. These include the construction of scientific platforms (such as deep-water subsurface FADs) along known migration routes to aid in the study of elusive migratory animals, or the ability to alter movements of migratory animals through protected seascapes by enhancing habitat preferences in these areas to minimize harvest. By utilizing FAD-based equipment such as video cameras or acoustic telemetry receivers, information on behavior during migration can be collected and used in fisheries conservation.

Pelagic animals are inherently difficult to study due to the expanse of their habitat, life history, and behavior, resulting in a comparatively weak understanding of pelagic species ecology and biology (Block et al., 2003). Therefore, in response to the recent call for developing methods to collect fisheries-independent data to be used in management and stock assessments (Moreno et al., 2016), a network of economical, instrumented, research-oriented subsurface FADs such as those proposed here could provide substantial ecological and fisheries data that is desperately needed to effectively conserve pelagic ecosystems and their biodiversity.

Table 2.4.2-2. Species documented on these subsurface FADs in the Exuma Sound during the course of a 2.5-year camera survey (in preparation for publication elsewhere), separated into resident intransatant versus ephemeral circumnatant species, compared to other epipelagic fishes documented in the Exuma Sound (personal communication: Z. Zuckerman, Cape Eleuthera Institute) but remain absent from our subsurface FAD surveys. An asterisk (\*) denotes species present within the first six months after FAD deployment.

Present on subsurface FAD surveys		Absent from subsurface FAD surveys
Intranatant	Circumnatant	Recorded in Exuma Sound
<i>Aluterus Monoceros</i> *	<i>Acanthocybium solandri</i> *	<i>Carcharhinus longimanus</i>
<i>Balistes capriscus</i> *	<i>Carcharhinus falciformis</i> *	<i>Istiophorus albicans</i>
<i>Cantherhines</i> spp.*	<i>Carcharhinus obscurus</i>	<i>Kajikia albidus</i>
<i>Canthidermis sufflamen</i> *	<i>Cheilopogon melanurus</i>	<i>Makaira nigricans</i>
<i>Carangidae</i> spp.*	<i>Coryphaena hippurus</i> *	<i>Scomberomorus cavalla</i>
<i>Caranx latus</i> *	<i>Elagatis bipinnulata</i> *	
<i>Caranx ruber</i> *	<i>Galeocerdo cuvier</i> *	
<i>Decapterus</i> spp.*	<i>Hemiramphus</i> spp.	
<i>Decapterus macarellus</i> *	<i>Sarda sarda</i>	
<i>Peprilus triacanthus</i>	<i>Sphyrna barracuda</i> *	
<i>Seriola rivoliana</i> *	<i>Sphyrna mokorran</i>	
	<i>Thunnus albacares</i>	
	<i>Thunnus</i> spp.	

Table 2.4.2-3. A summary of recently utilized methods for FAD-based research that lend well to a stable, subsurface platform.

<b>Examples of surface FAD-based methods</b>				
<b>Method</b>	<b>Species</b>	<b>Data Collected</b>	<b>Potential Influence of Data</b>	<b>References</b>
Acoustic telemetry receiver attachment	Fish	Residence (presence/absence), some behavioral patterns	Reduction in fisheries interactions and bycatch	Tolotti et al., 2020 Filmlalter et al., 2015 Dagorn et al., 2007
Video survey	Humans, fish	Fishing activity, species presence/aggregation dynamics	Managing FAD use, understanding aggregation	Merten et al., 2018 Doray et al., 2007
Echosounder/modelling	Any	Biomass	Understanding ecosystem effects of FADs	Lopez et al., 2016
Animal collection	Bivalve	Muscle tissue for stable isotope analysis, stomach contents	Characterize low levels of pelagic food web, ecosystem-based management, diet analysis	Unpublished data (B. Talwar, Cape Eleuthera Institute)

### **3. Colonization, diversity, and seasonality at pelagic fish aggregating devices (FADs) assessed using visual and video surveys**

Schneider EVC, Talwar BS, Killen SS, Russell S, van Leeuwen TE, Bailey DM

#### **3.1 Abstract**

The pelagic zone of the ocean can be a challenging environment to conduct research in, and as a result we lack robust baseline abundance and diversity data compared to what is available in more accessible coastal habitats to be able to track changes or stressors to the biota in this environment. Many large-scale fisheries target pelagic fish, and much of the information available on these species is based on fisheries-dependent data that may be biased towards hotspots and commercially valuable fishes. Here, a long-term video and visual fish survey was conducted on two subsurface moored FADs in the pelagic waters of the central Bahamas to determine the feasibility of using moored pelagic FADs as tools for collecting fish abundance and diversity data. A wide range of species were documented, including large migratory fish that are the focus of commercial and recreational fisheries, and smaller often overlooked species on which little abundance or seasonality information exists. We found that FADs colonize quickly and reach a peak stable (albeit seasonally cyclical) abundance and diversity within the first several months after deployment. Species richness was higher in video surveys and abundance was higher in visual surveys, except for sharks. Our results highlight the need to tailor survey methods to fit the context and study objective and provide further evidence for the importance of fisheries-independent data in monitoring pelagic species.

#### **3.2 Introduction**

Measuring biodiversity in the open ocean is integral to the effective conservation of pelagic ecosystems. We benefit from an array of ecosystem services provided by the open ocean, including a diversity of fish species that support some of the largest fisheries on the planet (FAO, 2022). However, many of these species are transient and live far from shore, making efforts to study their biology and abundance costly and logistically complicated (Worm et al., 2003; Webb

et al., 2010). Research methods studying pelagic fishes have included fisheries-dependent approaches such as analyzing catches on deck (Escalle et al., 2019), logbook records (Ménard et al., 2000), and fisheries echosounder data (Lopez et al., 2016), but this may be biased towards fishing hotspots or target species. Fisheries-independent longline surveys have occurred but typically target specific taxonomic or functional groups (e.g., pelagic sharks in Simpfendorfer et al., 2002). Baited remote underwater videos (BRUVs) may have the potential to observe a wider diversity of species and are rarely dependent on fishery activity but are also less common in the pelagic habitat (e.g., Heagney et al., 2007; Santana-Garcon et al., 2014). Because standardized sampling of pelagic fishes is logistically challenging, paired with the fact that these habitats often exist far from shore and across multiple national jurisdictions (or entirely in international waters), the effects of various stressors including fishing (Dulvy et al., 2021), climate change (Petrik et al., 2020), and pollution (Chouvelon et al., 2019) on pelagic fish communities may go unnoticed.

Fish aggregating devices (FADs) have become a ubiquitous tool in many tuna fisheries in the last 20 years, as many species of epipelagic fish are drawn to natural and artificial floating objects (Davies et al., 2014). FADs serve to concentrate otherwise sparsely distributed individuals or schools around a floating object (Girard et al., 2004) and can greatly increase capture efficiency in the fisheries that use them (Friedlander et al., 1994; Tilley et al., 2019). Recently, FADs have served as useful research platforms to understand the biology and ecology of various fish species as well as fisheries' impacts on target and bycatch populations (Moreno et al., 2016; Schneider et al., 2021). And while this field of research is relatively new, the idea of utilizing FADs as data hubs in the pelagic zone is gaining traction (Brehmer et al., 2019). Despite FADs presenting their own biases in relation to whether the behavior of attraction and aggregation occurs across all pelagic fishes, prior research has documented a wide range of taxonomic and functional groups associated with FADs, from small planktivores up to large sharks (Taquet et al., 2007). Still, a better understanding of temporal dynamics and survey methodologies tailored to monitoring biodiversity will be useful to effectively design, implement and track the outcomes of conservation measures.

In The Bahamas, the diversity and abundance of oceanic fishes is poorly studied despite pelagic sportfish accounting for the largest proportion (41%) of the nation's catch from 1950 to

2010 (Smith & Zeller, 2015). Fishery-dependent data are limited by a lack of commercial oceanic fisheries (Sherman et al., 2018) and poor reporting by the recreational fishing sector, which is historically responsible for the majority of the country's total fishery catches (Smith & Zeller, 2015). Fishery-independent surveys have occurred in The Bahamas' coastal (Alevizon et al., 1985; Layman et al., 2004; Grimmel et al., 2020) and deepwater habitats (Clark and Kristof, 1990; Brooks et al., 2015), but rarely in the open ocean. To address this gap, and to assess the feasibility of using FADs to monitor biodiversity and fish abundance, we conducted video and visual surveys at two pelagic moored FADs in the central Bahamas to (i) determine the factors affecting fish abundance and diversity at a FAD, (ii) determine how quickly fish colonize a new FAD to understand if and when a FAD reaches a plateau of abundance or diversity so that effects of FAD age can be accounted for during future investigations, (iii) determine if fish abundance and diversity differ when sampling using two different survey methods (video and visual surveys), indicating a potential behavioral bias, and (iv) describe any seasonality and between-group (taxonomic or functional) associations that occur and whether temperature influences abundance and diversity. These two survey methods (video and visual surveys) were included to compare their relative effectiveness and understand any survey bias that each present. For example, shy species might avoid boat or swimmer activity, like some adult pelagic sharks, and may be undercounted in visual surveys (Heagney et al., 2007). We hypothesize that there will be a difference in the total fish abundance and diversity based on survey method (we expect diversity to be higher using video surveys and abundance to be higher during visual surveys). We expect a higher diversity during the cold dry season and expect that a FAD will be colonized within the first year (i.e., abundance and diversity will not increase after 1 year).

Fisheries-independent data are important because they can provide a consistent unit of effort which is challenging to standardize in rapidly evolving fisheries processes (Moreno et al., 2016). To address the need for accurate, fisheries-independent data to track fish stocks and establish baselines of lesser-studied species, our results provide insight into the effectiveness of different survey techniques and how to best match data needs with methodological approaches.

### **3.3 Methods**

Video and visual surveys were performed on two deep-water moored subsurface FADs in the Exuma Sound offshore from the Cape Eleuthera Institute, Eleuthera, The Bahamas, under Department of Marine Resources permit numbers MAMR/FIS/17, MA&MR/FIS/9, and MAMR/FIS/2/12A/17/17B. As described in Schneider et al. (2021), the FADs were moored in 600 m depth and 13 km apart, and each consisted of two large steel buoys (71 cm diameter) held 10 m beneath the sea surface. The northernmost of the two FADs (further referred to as North FAD) was installed on 14 August 2017, and the southernmost of the two (South FAD) was installed on 5 October 2017. Visual surveys occurred between installation and the end of 2017 in both locations (n = 8 at North FAD, n = 1 at South FAD).

Weekly video and visual surveying commenced in January 2018 and continued until March 2020. As open-water FAD-based visual fish surveys are uncommon and standardized methods have not been established, we designed our visual survey to fit within the process of deploying the video cameras. At each location, a free diver entered the water directly above the FAD. To begin the survey the free diver surveyed at the surface for two minutes scanning in 360° from the surface down past the FAD and recorded the abundance of all fish species visible onto a slate. Two minutes was used as it is typically the time it took for our divers to prepare for their free-dive. They then dove (duration approximately one minute) to deploy the camera, still scanning for fish, and returned to the surface for an additional one minute, resulting in four minutes spent surveying. Visibility at the site was typically 25 meters in all directions. As standardized visual pelagic fish surveys are uncommon, and our goal was to conduct a rapid visual survey, and this four-minute process was used. This survey presents a distinctly different amount of effort and introduces different biases than the video surveys but was used to understand the effectiveness of an intentionally rapid, easy to perform visual survey. All observers received fish identification training prior to conducting any surveys using both traditional identification guides as well as video survey footage and in-water training and testing. Observer ID was not recorded for each survey, and therefore was not included as a random effect in the modelling.

During the process, the diver mounted a GoPro Hero 4 on a D-ring at the top of one of the FAD buoys (10 m depth). The camera's underwater housing was fitted with a float to keep it vertical and a swivel and vane to maintain a consistent downstream orientation. Following

deployment, the boat departed the area and did not return for at least two hours to avoid affecting the video survey (mean video survey duration =  $76.0 \pm 2.8$  minutes). During camera retrieval, the free diver conducted another visual survey as described above. Wind speed, wind direction, cloud cover, and time were recorded before each survey. A temperature logger (DS1921H Thermochron iButton High Resolution, Maxim Integrated, San Jose, CA, USA) was attached to the same D-ring used to mount the camera rig onto each FAD and recorded temperature hourly for the duration of the study.

Videos were watched and annotated by trained project team members, and MaxN (maximum number of individuals of a species visible in a frame of the video) was recorded for each species during each survey (Ellis & DeMartini, 1995).

Statistical analyses were conducted in R (R Core Team, 2022) using R studio version 1.3.1093. Species accumulation curves and Chao's diversity estimator was used to estimate total species richness of the population (r package 'vegan'; Oskanen et al., 2022), and a t-test was used to compare species richness between the two survey methods to test for behavioral biases that might lead to higher or lower richness estimates. Initially, we planned to measure colonization by analyzing trends in abundance and diversity from deployment onwards, however during data exploration it became apparent that substantial intra-annual variability existed in the data. Because of this, any appearance of colonization may have simply been part of an intra-annual cycle (seasonality) and not just colonization of the FAD. So, to understand the colonization process and determine if diversity or total abundance changes year over year, one-way ANOVAs with post-hoc Tukey tests were used to compare video survey results from soon after FAD deployment- January and February 2018- to the same timeframe in the two successive years (Jan + Feb 2018 vs. Jan + Feb 2019 vs. Jan + Feb 2020). The two months were pooled to increase the number of surveys being compared, and the comparison period started in January 2018 as it was the earliest month that consistent video surveys occurred following deployment. A one-way ANOVA was also used to compare visual survey results from the North FAD in the same manner from August of each year, as this was the earliest that visual survey data were collected (immediately following the deployment of North FAD).

GAMs were selected to test the effects of predictive factors on fish abundance and diversity after inspecting the residual plots which violated the assumption of a normal

distribution, precluding the use of linear models. Generalized additive models (GAMs) were used to analyze the effects of time (FAD age), survey method (visual or video), season (warm or cold: warm season in The Bahamas is May 1 – October 31), and location (North FAD or South FAD) on total fish abundance (with a Poisson distribution) and diversity (with a Gaussian distribution, using the Shannon diversity index [H'] to measure species diversity in the community at a given time) (r package 'mgcv' and 'gam'; Wood, 2011 & Hastie, 2022, respectively). A GAM with a negative binomial distribution was used for analyzing the effects of time (FAD age), season (warm or cold), and survey method (visual or video) on shark abundance due to a high frequency of zero counts. The Pearson estimate was calculated for the dispersion parameter to check for overdispersion.

The Akaike information criterion (AIC) was used to determine the best fit model following removal of various terms, and figures are presented for species or groups where significant effects were seen. No collinearity was expected between any of the explanatory variables, yet ACF plots were inspected to test for autocorrelation in the response variables and was low throughout. Linear models were used to analyze the effects of video survey length on abundance and diversity, and the effects of temperature on diversity (H'). A correlation plot and lag correlation analysis were used to investigate relationships between species and groups (Stoffer, 2019).

### **3.4 Results**

From August 2017 to March 2020, 174 video surveys were performed (93 at North FAD and 81 at South FAD) and 340 visual surveys were performed (183 at North FAD and 157 at South FAD). Twice as many visual surveys occurred because two were conducted on each video survey day: one during deployment of the camera and one during retrieval. The video surveys observed 8,041 individual fish from 21 species in 10 families and the visual surveys observed 40,924 individual fish from 22 species in 12 families (total 27 species in 14 families) (Table 3.4-1). Sea surface temperature ranged from 22.2 ° C to 34.0 ° C throughout the surveying period (Figure 3.4-1).

There were no significant differences in diversity or total abundance on visual surveys at the North FAD when comparing the first month after deployment (August 2017) to the same month one year later (August 2018), however a significant increase was seen in both diversity and total abundance when comparing August 2017 to August 2019 ('Diversity' one-way ANOVA:  $F = 4.068$ ,  $p = 0.03$ , Tukey 2017 vs 2019  $p = 0.03$ ; 'Abundance' one-way ANOVA:  $F = 6.284$ ,  $p < 0.01$ , Tukey 2017 vs 2019  $p < 0.01$ ). There were no significant differences in Shannon diversity on video surveys in January and February compared between the years 2018, 2019, and 2020 (one-way ANOVA:  $F = 0.43$ ,  $p = 0.65$ ). There was a significant difference in total abundance in this two-month period among years (one-way ANOVA:  $F = 13.23$ ,  $p < 0.001$ ) with a post-hoc Tukey test indicating a significantly greater total abundance in 2018 compared to both successive years (2018 vs. 2019:  $p = 0.02$ ; 2018 vs. 2020:  $p = 0.001$ ).

Species accumulation curves are shown in Figure 3.4-2 for both locations and both survey methods. When surveys from the two FADs are grouped, Chao's diversity estimator predicted  $25.65 \pm 3.47$  species in the total population based off the video surveys (21 species were actually observed), and  $27.99 \pm 5.23$  species in the population based off the visual surveys (22 species were actually observed). The measured species richness in individual surveys that occurred at the same location and began at the same time was significantly higher in the video surveys ( $2.65 \pm 0.11$ ) than the visual surveys ( $1.96 \pm 0.09$ ) (t-test  $p < 0.001$ ). Figure 3.4-3 highlights the detection probability of different groups when using video or visual surveys. Most notably, a GAM with a negative binomial distribution found that shark abundance was significantly higher when using video surveys, and that time (FAD age) was a significant predictor as well (Figure 3.4-4 & Figure 3.4-5; Supplementary Table 8.1-1).

A GAM including time (FAD age), survey method, and season showed a significant effect of all three predictor variables on total abundance (Figure 3.4-6) and was a better fit than a model that also included location, determined using the Akaike information criterion (AIC). The model showed higher total abundance when using visual surveys and higher total abundance during the warm season (Supplementary Table 8.1-3). Season and FAD age had significant effects on diversity, with a more diverse assemblage observed during the warm season (Figure 3.4-8 & Figure 3.4-9; Supplementary Table 8.1-5). We found no effect of video survey length on total abundance or diversity (linear model:  $p = 0.34$  and  $p = 0.18$ , respectively).

Temperature had an effect on Shannon’s diversity index observed by the video surveys, with species diversity increasing as temperature increases (linear model:  $p < 0.001$ ; Figure 3.4-10). Further, a number of individual species exhibited changes in seasonal abundance between the warm and cold months. Bar jacks (*Caranx ruber*), almaco jacks (*Seriola rivoliana*), scad (*Decapterus sp.*) and clupeids were more abundant in the warm months, whereas unicorn filefish (*Aluterus monoceros*), wahoo (*Acanthocybium solandri*) and mahi (*Coryphaena hippurus*) were more abundant during the cold months (Figure 3.4-11; Supplementary Table 8.1-7). A correlation and lag correlation analysis did not reveal any strong occurrence correlations between species or groups.

Table 3.4-1. Inventory list of all species that were present in the video or visual surveys that occurred at the two subsurface pelagic FADs studied.

Family	Scientific Name	Common Name	Video Survey	Visual Survey
Balistidae	<i>Balistes capriscus</i>	Grey Triggerfish	✓	✓
Balistidae	<i>Canthidermis sufflamen</i>	Ocean Triggerfish	✓	✓
Belonidae	<i>Tylosurus crocodilus</i>	Houndfish		✓
Carangidae	<i>Elagatis bipinnulata</i>	Rainbow Runner	✓	✓
Carangidae	<i>Seriola rivoliana</i>	Almaco Jack	✓	✓
Carangidae	<i>Caranx ruber</i>	Bar Jack	✓	✓
Carangidae	<i>Caranx latus</i>	Horse-Eye Jack	✓	✓
Carangidae	<i>Decapterus sp.</i>	Scad	✓	✓
Carangidae	<i>Caranx hippos</i>	Creville Jack	✓	✓
Carangidae	<i>Seriola drumerili</i>	Amberjack	✓	✓
Carcharhinidae	<i>Carcharhinus falciformis</i>	Silky Shark	✓	✓
Carcharhinidae	<i>Carcharhinus obscurus</i>	Dusky Shark	✓	
Carcharhinidae	<i>Galeocerdo cuvier</i>	Tiger Shark	✓	
Clupeidae	<i>Clupeidae</i>	(many)		✓
Coryphaenidae	<i>Coryphaena hippurus</i>	Mahi Mahi	✓	✓
Echeneidae	<i>Echeneidae sp.</i>	Remora	✓	
Exocoetidae	Likely <i>Cheilopogon melanurus</i>	Flying Fish		✓
Hemiramphidae	<i>Hemiramphus brasiliensis</i>	Ballyhoo		✓

Monacanthidae	<i>Aluterus monoceros</i>	Unicorn Filefish	✓	✓
Monacanthidae	<i>Cantherhines pullus</i>	Orangespotted Filefish	✓	
Monacanthidae	<i>Cantherhines macrocerus</i>	Whitespotted Filefish	✓	✓
Scombridae	<i>Acanthocybium solandri</i>	Wahoo	✓	✓
Scombridae	<i>Scomberomorus sp.</i>	Mackerel		✓
Scombridae	<i>Katsuwonus pelamis</i>	Skipjack Tuna		✓
Sphyraenidae	<i>Sphyraena barracuda</i>	Great Barracuda	✓	✓
Sphyrnidae	<i>Sphyrna spp.</i>	Hammerhead Shark	✓	
Stromateidae	<i>Peprilus triacanthus</i>	Atlantic Butterfish	✓	✓

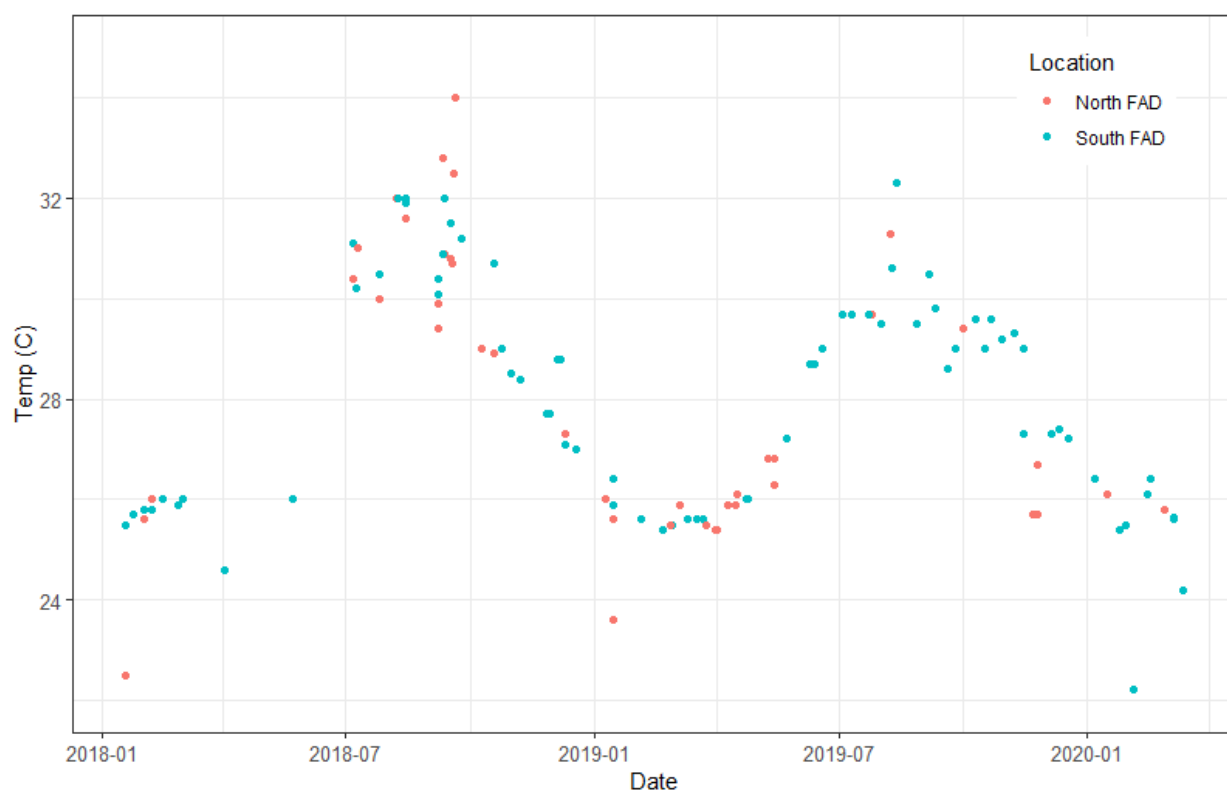


Figure 3.4-1. Water temperature ( $^{\circ}$  C) measured at the two FAD locations taken at the beginning of each survey, from January 2018 to March 2020. Red dots indicate measurements taken at the North FAD and blue dots indicate measurements taken at the South FAD.

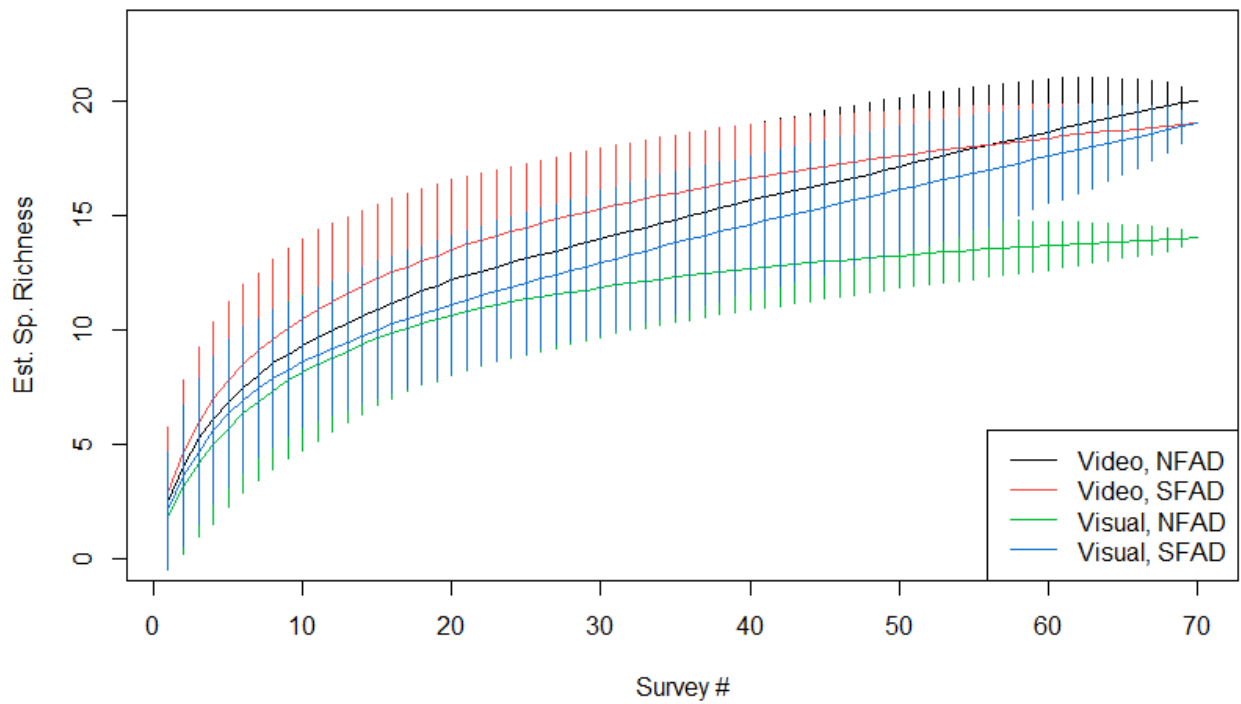


Figure 3.4-2. Values of estimated species richness in relation to survey number are shown here using species accumulation curves that have been calculated based on video (black and red) and visual (green and blue) surveys at each FAD location, with bars representing 95% confidence intervals. The two survey locations are the North FAD (NFAD in legend) and the South FAD (SFAD in legend).

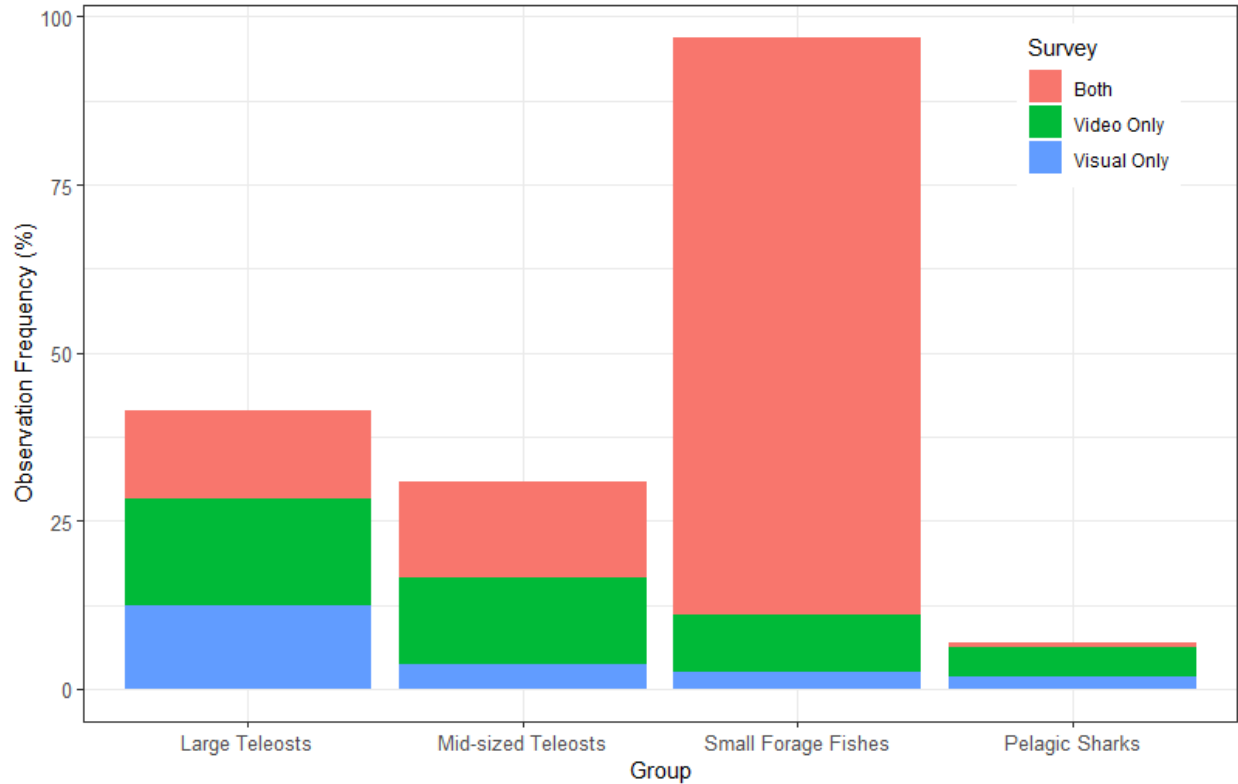


Figure 3.4-3. Stacked bar chart showing observation frequency of different taxonomic or functional groups during the two types of surveys (i.e., what type of survey was more effective at surveying a given group). On days when video and visual surveys both occurred at the same location, the bars represent the percentage of surveys that each listed taxonomic or functional group was seen in. For example, small forage fishes were seen in 96.9% of all surveys: they were seen *only* in visual surveys (and not on the video survey that occurred at the same time) 2.5% of the time, only in video surveys (and not on the visual survey that occurred at the same time) 8.6% of the time, and in both surveys (visual and video surveys that occurred at the same time) 85.8% of the time.

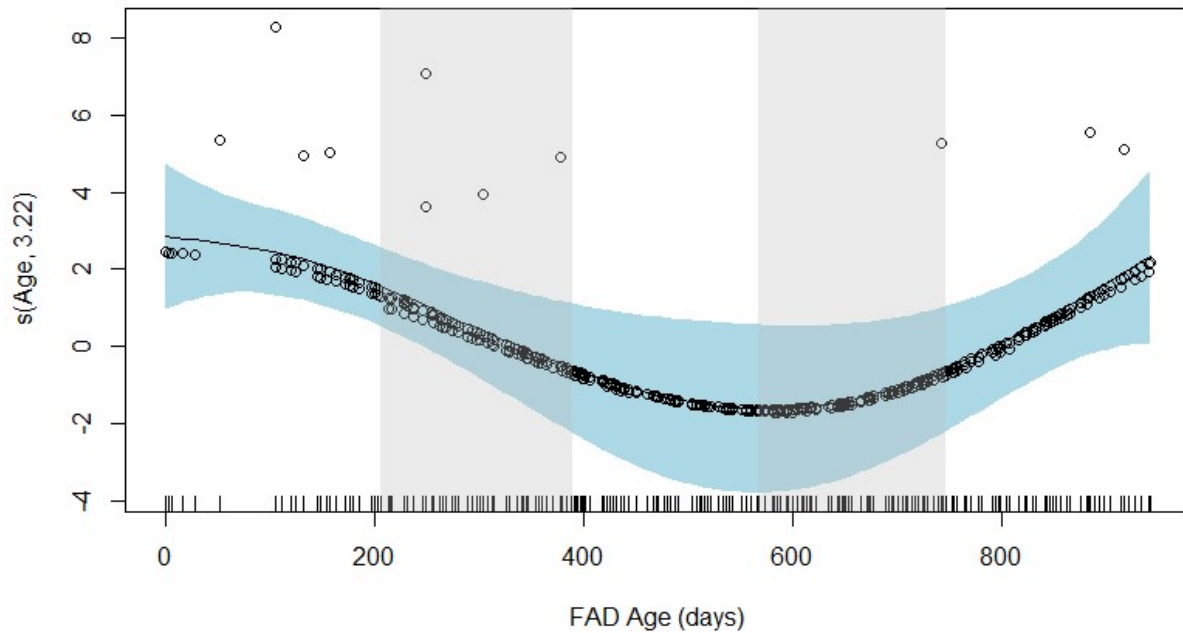


Figure 3.4-4. Cubic spline generated plot of smoothed fit from the GAM showing the partial effect of time (FAD age) on shark abundance with partial residual points plotted. The hash marks above the x axis indicate the distribution of observed values, and the grey shaded columns highlight the warm/wet season (May 1 – Oct 31) of each year. The y axis represents the smooth term contribution to the GAM (edf = 3.22), which is the scaled partial effect of age on shark abundance and is centered around the model’s constant term. The shaded blue area represents 95% confidence intervals.

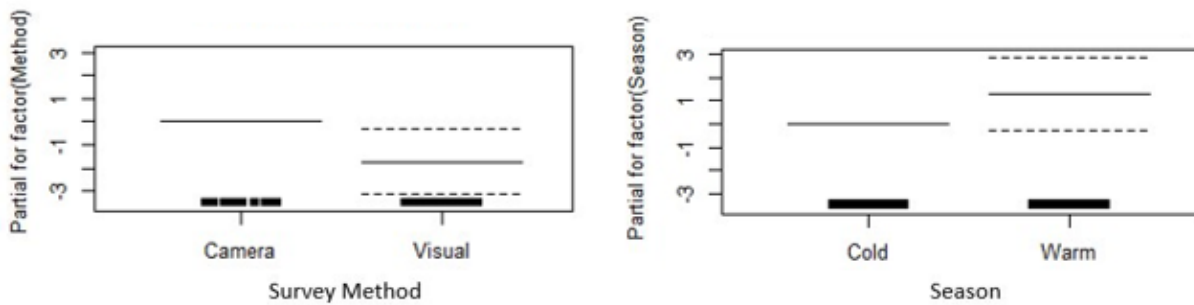


Figure 3.4-5. Partial effects of survey method and season on the variation in shark abundance predicted by a GAM. Because survey method and season are categorical variables, the horizontal solid black lines above each factor show the predicted partial effect on shark abundance for that variable centered around the model's constant term. The dashed lines above and below the solid black lines represent 95% confidence intervals. The carpet of black ticks above each variable on the X axis denotes each measurement and appears as a solid line.

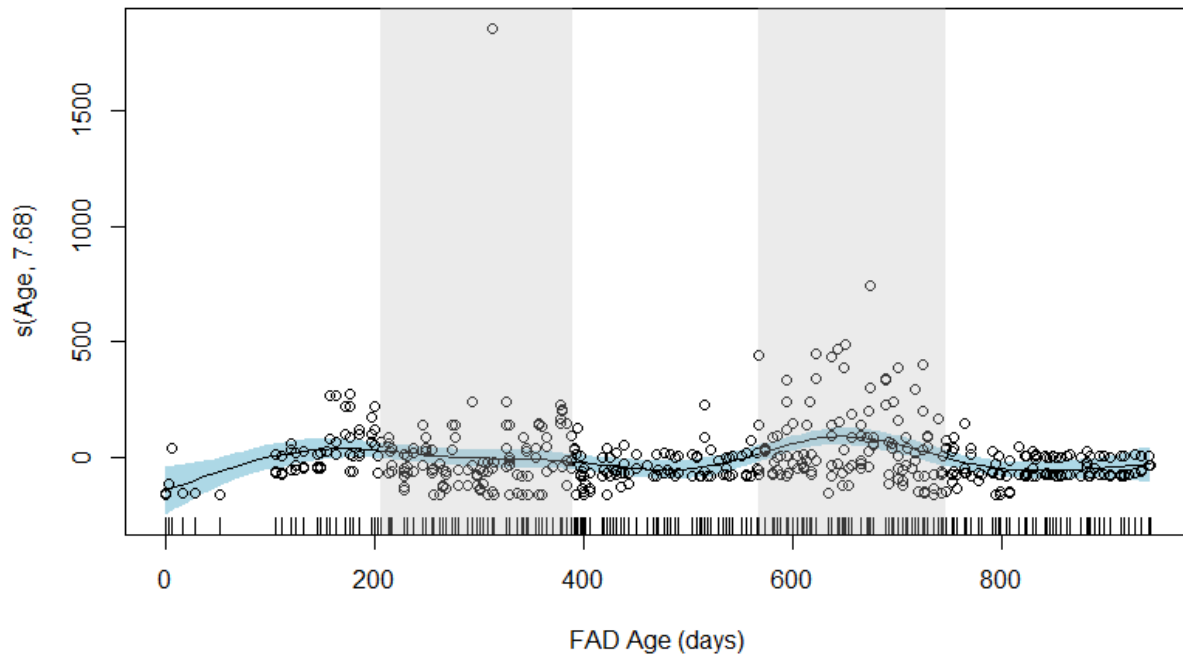


Figure 3.4-6. Cubic spline generated plot of the smoothed fit from the GAM showing the partial effect of time (FAD age) on total fish abundance with partial residual points plotted. The hash marks above the x axis indicate the distribution of observed values, and the grey shaded columns highlight the warm/wet season (May 1 – Oct 31) of each year. The y axis represents the smooth term contribution to the GAM (edf = 7.68) centered around the model's constant term. The shaded blue area represents 95% confidence intervals.

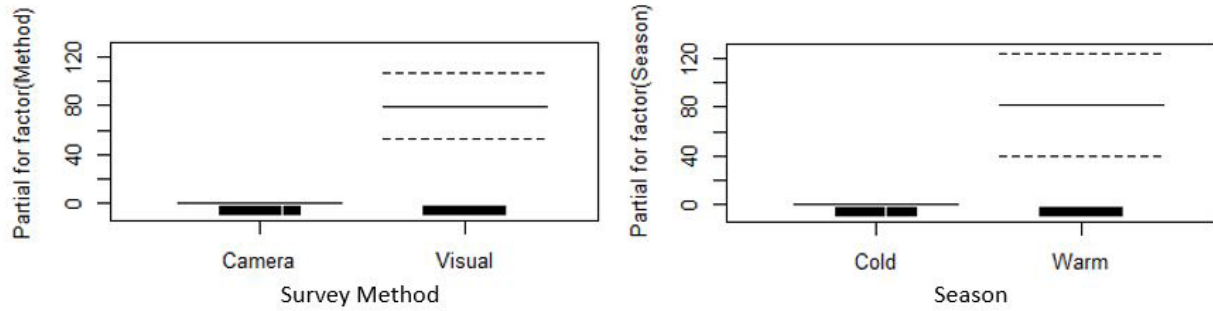


Figure 3.4-7. Partial effects of survey method and season on the variation in total fish abundance predicted by a GAM. Because survey method and season are categorical variables, the horizontal solid black lines above each factor show the predicted partial effect on fish abundance for that variable centered around the model’s constant term. The dashed lines above and below the solid black lines represent 95% confidence intervals. The carpet of black ticks above each variable on the X axis denotes each measurement and appears as a solid line.

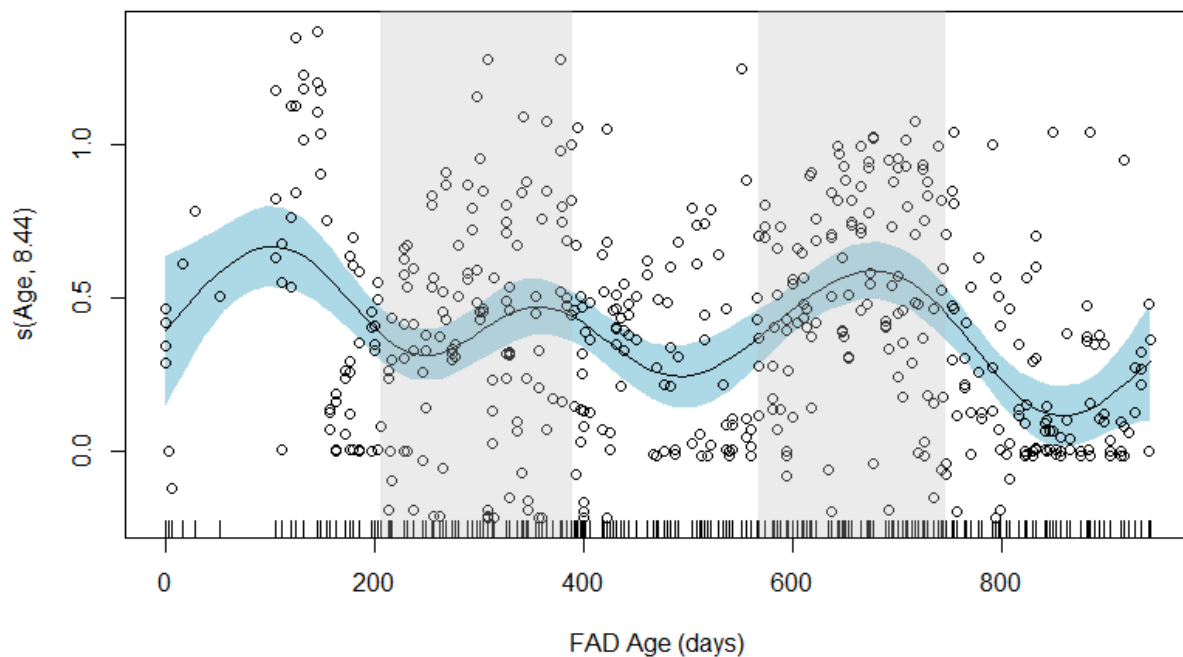


Figure 3.4-8. Cubic spline generated plot of the smoothed fit from the GAM showing the partial effect of time (FAD age) on Shannon diversity with partial residual points plotted. The hash

marks above the x axis indicate the distribution of observed values, and the grey shaded columns highlight the warm/wet season (May 1 – Oct 31) of each year. The y axis represents the smooth term contribution to the GAM (edf = 8.44) centered around the model’s constant term. The shaded blue area represents 95% confidence intervals.

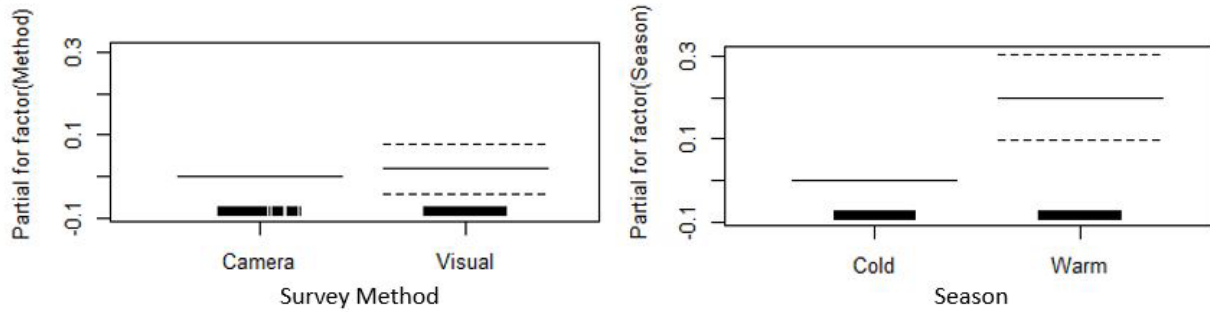


Figure 3.4-9. Partial effects of survey method and season on the variation in Shannon diversity predicted by a GAM. Because survey method and season are categorical variables, the horizontal solid black lines above each factor show the predicted partial effect on Shannon diversity for that variable centered around the model’s constant term. The dashed lines above and below the solid black lines represent 95% confidence intervals. The carpet of black ticks above each variable on the X axis denotes each measurement and appears as a solid line.

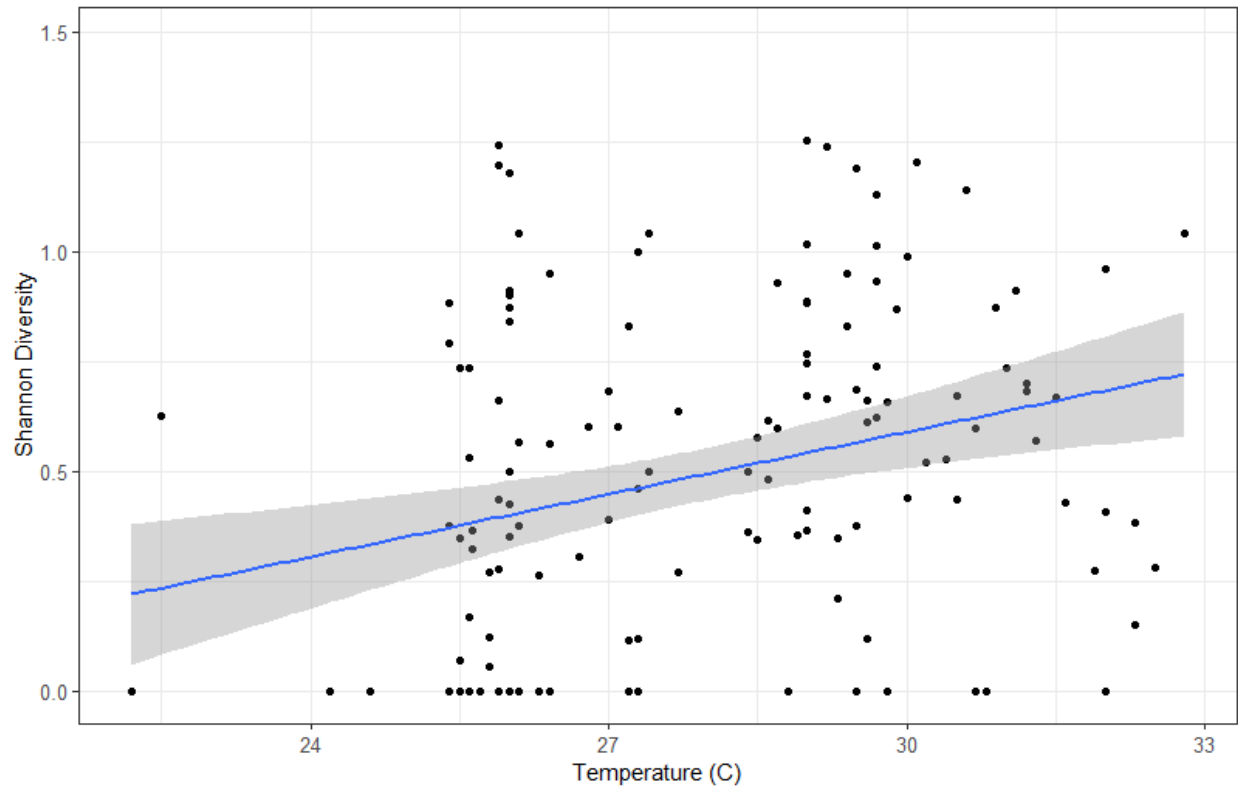


Figure 3.4-10. Linear regression showing the measured Shannon diversity observed using video surveys in relation to water temperature measured at the surveyed FAD. The shaded region represents 95% confidence intervals.

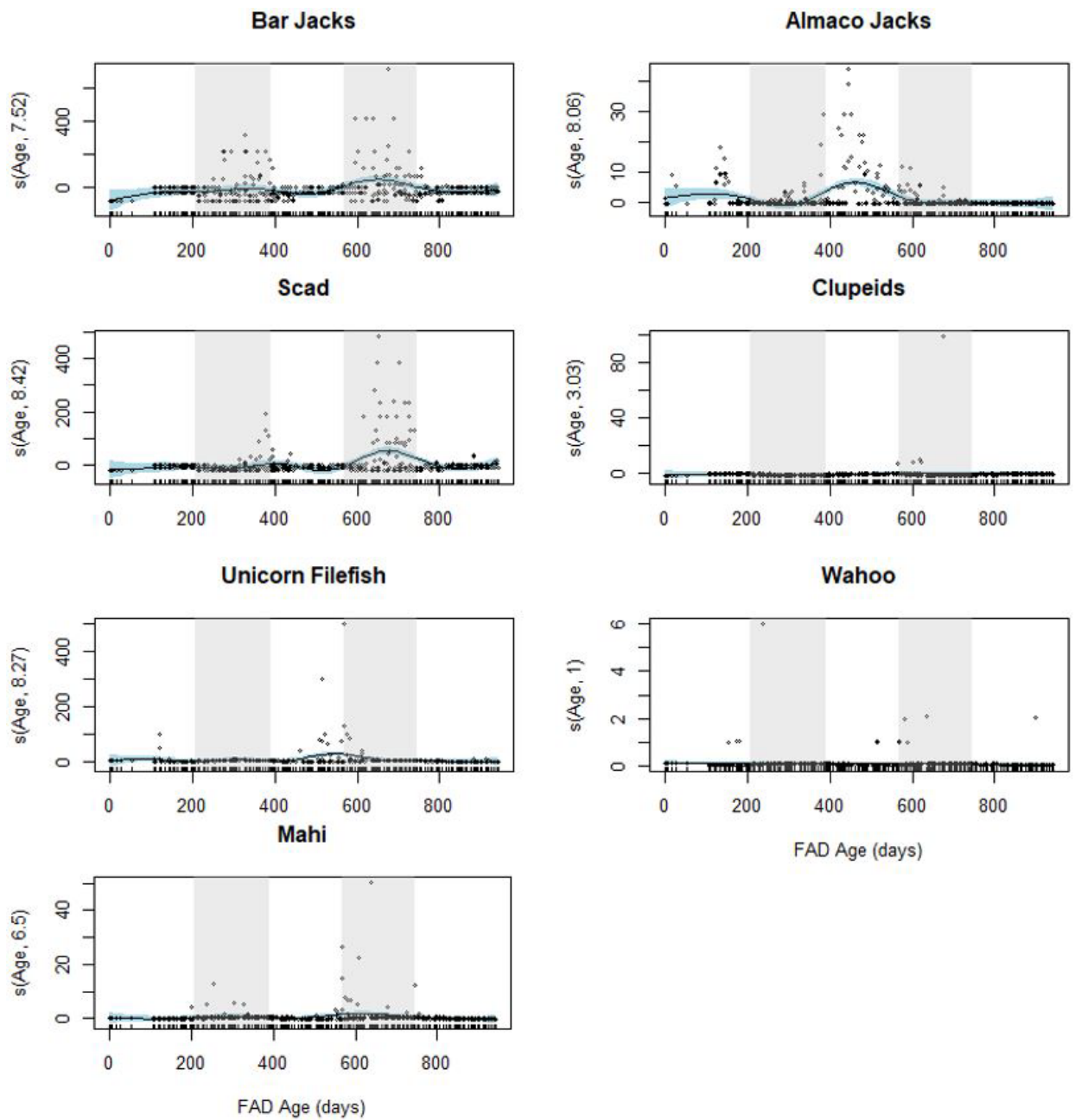


Figure 3.4-11. Cubic spline generated plot of the smoothed fits from the GAMs showing the partial effect of time (FAD age) on abundance of individual fish species with partial residual points plotted. The hash marks above the x axes indicate the distribution of observed values, and the grey shaded columns highlight the warm/wet season (May 1 – Oct 31) of each year. The y axes represent the smooth term contribution to the GAMs centered around the model’s constant term, with edf indicated in the y axis labels. The shaded blue areas represent 95% confidence intervals. Figures are shown for all species with significant effects.

### 3.5 Discussion

Fisheries-independent data are important for establishing baselines and uncovering patterns such as seasonality that may be masked by the bias of fisheries-dependent sampling. Behavioral biases likely exist in that all pelagic fish species are probably not attracted to or aggregate around FADs, but a wide range of taxonomic and functional groups have been documented associating with these structures (Taquet et al., 2007; Deudero et al., 1999; Rountree, 1989). The results from over two years of weekly FAD-based fish surveys demonstrate that survey method and effort can be tailored towards specific target species and research objectives and have revealed several interesting and new insights into pelagic fish seasonality around FADs.

In total, 48,965 individuals comprising 27 species were observed on the surveys. The species observed on the video and visual surveys add insight into an interesting narrative, both published and anecdotal, that subsurface FADs may attract a different assemblage than surface FADs. Previous research in the region has found that similarly located subsurface FAD assemblages were predominantly comprised of coastal-pelagic species such as great barracuda (*Sphyraena barracuda*), cero mackerel (*Scomberomorus regalis*), little tunny (*Euthynnus alletteratus*), and bar jacks (*Caranx ruber*), where nearby surface FAD assemblages were comprised of more obligate pelagic species including mahi (*Coryphaena hippurus*), skipjack (*Katsuwonus pelamis*) and blackfin tuna (*Thunnus atlanticus*), along with barracuda (*Sphyraena barracuda*), cero mackerel (*Scomberomorus regalis*) and little tunny (*Euthynnus alletteratus*) (Friedlander et al., 1994). While our surveys did observe some obligate pelagic species including mahi, wahoo (*Acanthocybium solandri*), and several oceanic sharks, several species of tuna and all billfishes were notably absent from all of our surveys and have never been encountered on our surveyed subsurface FADs, despite white marlin (*Kajikia albida*), blue marlin (*Makaira nigricans*), Atlantic sailfish (*Istiophorus albicans*), and yellowfin tuna (*Thunnus albacares*) being popular sportfishing targets with numerous confirmed catches in the study area. Additionally, the aforementioned study comparing FAD designs also saw a significantly lower CPUE when trolling around subsurface FADs than surface ones (Friedlander et al., 1994), so there may be differences in attraction or aggregation mechanisms based on the position of the structure in the water column that should be investigated with further studies.

When visual surveys were compared from August 2017 (immediately following deployment of the North FAD) to August of successive years, there were no significant differences in diversity or total abundance between 2017 and 2018, although there was a significant increase in both metrics between August 2017 and 2019. Video surveys from January and February of each year were pooled and compared across years, and there were no significant differences in diversity among years. There was a significant decrease in total abundance for the January/February 2019 and 2020 periods compared to 2018. Together, this suggests that the FADs were colonized within the first month, and peak diversity and total abundance occurred at or before the first 3 - 4.5 months. An echosounder-based aggregation study on commercially fished drifting FADs (DFADs) in the Indian Ocean determined that tuna species first arrived at the DFADs after 12.2 ( $\pm$  7.7) days and non-tuna species arrived after 21.7 ( $\pm$  15.1) days (Orue et al., 2019), and this length of time to colonization for non-tuna species is similar to that seen in the present study. One notable difference in the Indian Ocean study was the early presence of tunas which were largely absent from our surveys. However, multiple studies have demonstrated that FAD-associated tunas are commonly found at 25 m or deeper and often oriented upstream of the FAD (Robert et al., 2013; Lopez et al., 2017; Orue et al., 2019), so our downstream-facing video survey with a camera mounted horizontally at 10 m and surface-based visual surveys with an average visibility of 25 m could have missed any tunas present. And while other aggregation studies that have found similar timescales to colonization focus mainly on commercially important tunas (Macusi et al., 2017), our findings establish arrival times and diversity curves that include a range of lesser studied species which are equally as important when monitoring pelagic biodiversity. It is important to understand these colonization processes if FADs are to be used in future standardized surveys such as stock assessments. For example, a month-old FAD may not have the same diversity or fish abundance compared to a four-month-old FAD simply because of its age, and by quantifying the colonization process, FAD age can be accounted for during analysis or interpretation of survey data.

Species richness was significantly higher in video surveys than visual surveys, but we found visual surveys observed a significantly higher total abundance. Because these surveys were conducted simultaneously, this indicates that behavioral differences including association distance to the FAD and bold or shy behavior (i.e., sensitivity to presence of a diver or boat) might influence whether a species is observed using a specific survey method. For example,

sharks were significantly more likely to be seen in video surveys which observed four total shark species, whereas only silky sharks (*Carcharhinus falciformis*) were seen during visual surveys. Juvenile sharks have been known to approach oceanic marker buoys more often and closely than adults and are therefore possibly bolder (Heagney et al., 2007), and all of the individuals seen during our visual surveys were estimated between 1 – 1.5 m total length (juvenile to sub-adult for this species) which could explain why only silky sharks were seen during visual surveys. Despite this specific example, sharks are generally circumnavigant to FADs (Parin & Fedoryako, 1999; Taquet et al., 2007), having a looser association with the structure, and show avoidance behaviors to artificial sound (Chapuis et al., 2019) so are therefore less likely to be seen during a short visual survey compared to a longer remote video survey. Additionally, species richness was lower using visual surveys at the North FAD than at the South FAD (Figure 3.4-2). This was interesting because the North FAD had the higher richness when estimated using the video survey data, and video surveys are better at documenting rare and cryptic species, so it is possible but unlikely that the North FAD had a lower true species richness. It is possible that slight differences exist in assemblages between the two locations due to some unknown factors, or that random variations led to a lower richness measured in the North FAD visual surveys.

A higher total fish abundance observed on visual surveys matches results from other studies as it is generally accepted that differences in life history strategies and fish reactions to human surveyors may influence measured abundances (Wetz et al., 2020). Video surveys and abundance metrics derived from them (such as MaxN used here) may also underestimate true abundance of certain species based on a limited field of view (Kilfoil et al., 2017; Campbell et al., 2018). A limitation in this study was that our surveys were conducted with a single horizontal-facing camera that was mounted 10 m deep on top of a subsurface FAD. Even this short distance from camera to surface would likely preclude any strictly surface-oriented bait fishes from appearing on the video surveys (such as ballyhoo, *Hemiramphus brasiliensis*, and flying fish, *Cheilopogon melanurus*, which were only present on visual surveys). Additionally, multi-camera units that record 360 degrees have been used to quantify fish assemblages around other marine structures and would have likely resulted in higher abundance estimates than those from our single-camera videos that had a limited field of view (Hemery et al., 2022). This improvement could be made in future studies, and it will therefore be important to tailor survey

methods to fit the behaviors and location of target species to best represent the sample population of interest.

Total abundance was significantly higher in the warm season (May 1 – October 31), and temperature had a significant positive effect of diversity. The increase in abundance was largely driven by carangids, of which bar jacks, almaco jacks, scads, and clupeids (not part of *Carangidae*) were significantly more abundant during the warm season. We found no significant correlations or lagged correlations between any species or groups, so it is likely that temperature or other factors such as recruitment cycles drive seasonal presence and absence of each group. *Carangidae* was the most abundant and diverse family observed during these surveys, but little information exists on their population or life history. Nearly all carangids observed in our visual surveys were estimated to be juveniles between 10-20 cm total length (TL), including our single most abundant species, bar jack *Caranx ruber*. A similar species to the bar jack but not seen in our surveys, blue runner *Caranx crysos*, is known to reach sexually maturity at 33.1 cm TL (de Oliveira et al., 2017) and reach 21.5 cm TL at one year old (Goodwin & Johnson, 1986). Bar jacks have been documented to spawn in June and July in The Bahamas (Cushion & Sullivan-Sealey, 2008), so there is a chance that the individuals we observed in the summer months are one year old individuals, possibly using the FADs as an intermediary structure before moving from their pelagic phase into coastal habitats where they are more commonly found as adults. We found three species to be significantly more abundant during the cold season: unicorn filefish, wahoo, and mahi. Little has been published on the movements of unicorn filefish in the region, although they are taken as bycatch in FAD-based seine fisheries elsewhere (Lezama-Ochoa et al., 2017). The seasonality of mahi and wahoo seen in our surveys aligns with prior knowledge, as both mahi and wahoo undertake seasonal migrations that appear to be temperature-driven, moving from more northern latitudes into the Caribbean in the winter months (Oxenford et al., 2003; Schlenker et al., 2021). There was evidence of some heteroscedasticity in the total fish abundance and individual species abundance models, which can increase the chances of Type I error, but it frequently expected with seasonally cyclical data such as this.

Fisheries-independent data must be collected on a broad scale to keep pace with the increased use of FADs worldwide in order to ensure the conservation of the pelagic ecosystem

and the careful use of its fisheries resources. Uncovering seasonal patterns allows for targeted sampling of certain groups throughout the year and behavioral differences highlight methods that are better suited for certain species (e.g., sharks are better surveyed using videos). Additionally, understanding the abundance and diversity of lesser studied species is an important step in reaching sustainable management and biodiversity targets. As we strive to see and predict the effects of anthropogenic and natural factors on pelagic biodiversity, this study also contributes to the optimization of open-ocean fish surveying such that a range of taxonomic and functional groups can be studied in a non-extractive manner. Future work should continue to test the viability of using similar methods to track fish stocks over longer temporal scales in this habitat that is often more challenging to access than others.

## **4. Invertebrate micronekton aggregation around a pelagic moored fish aggregating device (FAD)**

Schneider EVC, Talwar BS, Killen SS, Bailey DM, Bicknell AWJ, Witt MJ

### **4.1 Abstract**

Structure in the marine environment can influence the distribution and abundance of fauna through a number of mechanisms. A wide range of fish species are attracted to or aggregate around floating structure, particularly fish aggregating devices (FADs), which can lead to more efficient capture and a range of potential ecological consequences. However, little investigation has occurred into the aggregation effect of these structures on lower trophic level organisms, specifically micronekton that is part of the diet of a wide range of pelagic fishes. Here, light trap surveys investigate the aggregation of invertebrate micronekton around a moored pelagic FAD. In combination with echosounder surveys, we aim to describe the biomass aggregation around these structures in an oligotrophic subtropical ecosystem.

### **4.2 Introduction**

The structures that exist in the pelagic marine environment play an important role in shaping the distribution, abundance, and behavior of the organisms that live there. Oceanographic structures such as fronts, eddies, and clines facilitate the proliferation, aggregation, and entrainment of pelagic plankton (Kimura et al., 2000) and micronekton (organisms from 2-20 mm that can swim freely against ocean currents; Sabarros et al., 2009). Geologic structures such as seamounts also aggregate these low trophic level organisms through the interruption of their daily vertical migration, along with other upwelling-related processes (Genin, 2004). Any of these areas of concentrated prey can then typically support hotspots of larger predators (Worm et al., 2005). Surface biological or anthropogenic structure, such as *Sargassum spp.*, natural debris, or artificial fish aggregating devices (FADs), are also known to attract a wide range of marine species, mainly fishes (Taquet et al., 2007; Casazza & Ross, 2008). However, most research has been focused on larger species that interact with fisheries,

and our understanding of the patterns of association for other groups, and the mechanisms behind these aggregating effects, is still lacking.

The biotic assemblage around FADs is typically segregated by size and behavior, and a general structure was proposed by Parin and Fedoryako (1999): intranant species are small, often juveniles, frequently slow, and maintain immediate proximity to the FAD. Extranant species are quicker and may range slightly further but within distance of a quick retreat to the FAD. Circumnant species are large and active predators that may move far away from the FAD for periods of time while remaining associated. This pattern has been observed and is generally accepted (e.g., Taquet et al., 2007; Tolotti et al., 2020), and a number of reasons likely contribute to the associative behavior. For example, there is evidence that FADs can aid in reforming dispersed schools of conspecifics (Soria et al., 2009), can provide navigational aid in locating rich foraging grounds (Castro et al., 2002), and provide shelter for smaller fish to avoid predation (Gooding & Magnuson, 1967). Additionally, juvenile silky sharks have been shown to make excursions away from FADs to feed on non-associated prey, presumably in the scattering layer (Filmlalter et al., 2016), but it is usually assumed that those prey items are ubiquitous in the mesophotic region and not necessarily concentrated because of the FAD. There is evidence that lunar illumination affects some micronektonic organisms, such as those in the deep scattering layer, as organisms that undergo a diel vertical migration move closer to the surface on darker nights (Benoit-Bird et al., 2009). Additionally, the deep scattering layer is generally known inhabit a cool band of deep water (around 18 C) in the tropical western Atlantic, and therefore might spend more time in shallower, warmer waters around the FAD structure during the winter months (Cole et al., 1970). However, there has been little investigation into whether FADs aggregate these lower trophic level organisms that might attract and support FAD-associated fishes.

To understand what a FAD-associated assemblage looks like across multiple trophic levels, we conducted surveys using light traps and a towed fisheries echosounder around pelagic moored FADs to determine the influence of a FAD and other abiotic factors on pelagic animal assemblages. Light traps have been shown to effectively sample a wide range of marine organisms from plankton to juvenile fish that are costly or difficult to otherwise sample (McLeod & Costello, 2017). The size of these traps targeted the micronekton, a group of particular interest

from an ecological perspective as they have been overlooked in most FAD-based studies to date. Additionally, light trap surveys were more feasible to conduct than trawl surveys that could have been designed to target a similar group of species. We hypothesize that micronekton catch per unit effort (CPUE) will increase as distance to the FAD decreases (both horizontally and vertically). To complement the fine resolution that live-sampling in a light trap allows for, an echosounder was used as a more powerful and wide-reaching sampling tool. Echosounding reduces behavioral biases that might lead to selective sampling because anything in the water column that is dense enough to reflect sound energy is measured. We hypothesize that biomass will be greater closer to the FAD, and that there will be negative temperature and lunar effects as well. Our results will provide insight into aggregation dynamics around a pelagic moored FAD in a tropical oligotrophic ecosystem and provide new evidence into the potential mechanisms by which FADs aggregate fish.

## **4.3 Methods**

### *4.3.1 Study Location*

This study was performed in the northeast Exuma Sound, a semi-enclosed deep basin near the Cape Eleuthera Institute (CEI), South Eleuthera, The Bahamas. The two sub-surface FADs that were surveyed (hereafter called ‘North FAD’ and ‘South FAD’) were installed along the 600 m isobath by the Cape Eleuthera Institute in 2017 as detailed in Schneider et al., 2021. They were comprised of two 71-cm steel buoys anchored 10 m beneath the surface and were located 13 km apart.

### *4.3.2 Light Trap Survey*

Light trap surveys were performed on the North FAD weekly or biweekly from February to May 2019. Trapping was done with a combination of a quadrafoil trap (Aquatic Research Instruments, USA) and a tube trap that were fastened together to allow a breadth of sizes of organisms to be captured, as tube traps and quadrafoil traps can have size bias based on design and width of trap opening. Each quadrafoil trap consisted of five mm-wide openings and

contained a flashing multi-color LED fishing light and a 20 cm Lumistick green glow stick. Each tube trap consisted of a 45 cm long section of 15 cm diameter PVC pipe, with one mm mesh covering one end and an inverted funnel with a 13 mm opening on the other end. These traps were fitted with a green deep drop LED fishing light and a programmable white LED light ('Lanternfish', Blue Turtle Engineering, Melbourne Beach, USA).

Traps were deployed at one of three sampling locations: at the North FAD, 500 m away, or 1,000 m away. On a given trapping night, a weighted, pre-marked line was lowered with the traps attached such that they would be suspended at depths of 10 m (FAD depth), 200 m, 400 m, or 600 m. A weight anchored the line to the bottom, and a buoy kept the traps suspended at the appropriate depths and ensured the line stayed vertical and in the correct location. The three trapping locations fall along the 600 m isobath that runs parallel to the near-vertical shelf-break nearby to standardize bottom depth and distance from the wall. The trap line was left to soak for at least 1.5 hours and the surface buoy was never more than 30 m from the target deployment location. Traps were hauled and placed into individual coolers, and all organism sampling occurred at the CEI wetlab. We attempted to visually identify all animals to the family level, however several were only identified to class or order. Total length was measured for a subset of each.

#### *4.3.3 Echosounder Survey*

Towed echosounder surveys were performed biweekly around each of the two FADs from October 2018 to May 2019, alternating haphazardly between FADs and between day and night. A Simrad EK80 echosounder (Kongsberg Maritime, Norway) with a wide band transceiver and split beam transducer were used to survey the water column around each FAD. The echosounder was calibrated using a tungsten calibration sphere prior to surveying. The echosounder was mounted within a metal glider frame with adjustable wings and tail rudders, and a 12 m cable was used to tow the glider behind the boat at a depth of five meters. Visual observation and wing adjustment was used to ensure the glider was towed horizontally (not pitched up or down), and the Hobo logger confirmed a mean tow depth of five meters. Surveys were conducted in a radial star pattern with a FAD at the center, extending one km away in each cardinal and intercardinal direction at a speed of four knots (Figure 4.3.3-1), and acoustic data

were collected at 70 kHz in narrowband CW mode. During each survey, water quality parameters were recorded by an RBR Concerto CTD (RBR Global, Ottawa, Canada) that was mounted on the glider frame, measuring temperature, conductivity, salinity, and depth six times per second. Abiotic conditions were also recorded on the boat, and environmental and echosounder data was downloaded after each survey.

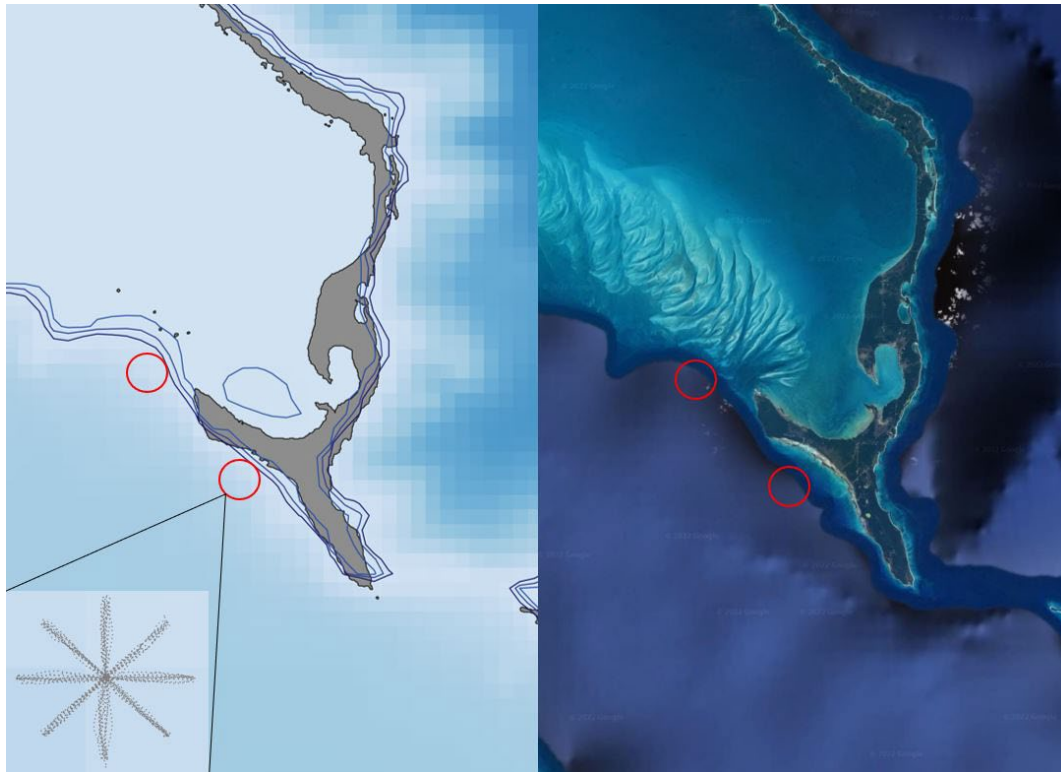


Figure 4.3.3-1. Study location showing the island of Eleuthera, the Exuma Sound (deep water that is shaded darker blue in the bottom left of each map), and the approximate location of each surveyed FAD circled in red. The inset frame shows the radial star survey pattern with each point representing a geolocated data point collected by the echosounder.

#### *4.3.4 Echosounder Data Processing*

Raw data from the echosounder was processed using Echoview 11.1 (Echoview, Hobart, Australia) following the dataflow in Figure 4.3.4-2. Transducer geometry was set to reflect the towed position of the glider, and monthly calibration files were used based on mean monthly

abiotic values because the absorption coefficient was expected to change based on the range of seasonal temperatures during the study.

A horizontal line was added at six meters to exclude the ringdown that was visible on the echograms. The near field (Fresnel zone) was calculated for each survey, however the ringdown exclusion depth was greater than any near field values, so further exclusion was not necessary. The background noise removal operator was used with a cell size of 20 pings by 10 m depth (per De Robertis & Higginbottom, 2007). The data were then smoothed using the XxY Statistic operator to calculate the means of three ping by three sample grids. Finally, the Processed Data operator was used to only display ‘good’ data regions. Plots of individual pings were inspected to assess the signal-to-noise ratio in each survey to determine the maximum reliable depths used in the analysis.

Each survey was exported three times with a 50 m horizontal by 25 m vertical (depth) grid overlaid- first without any threshold on volume backscattering strength ( $S_v$ ), then with a -50 dB minimum  $S_v$  threshold, and finally with a -85 dB minimum plus a -50 dB maximum  $S_v$  threshold. These thresholds were selected to separate  $S_v$  into two general categories: strong scatterers (more dense, often larger, may contain a swim bladder) and weak scatterers (likely invertebrates, often smaller and less dense) (Benoit-Bird & Au, 2001; Warren et al., 2001; Benoit-Bird & Lawson, 2016; Madirolas et al., 2016).

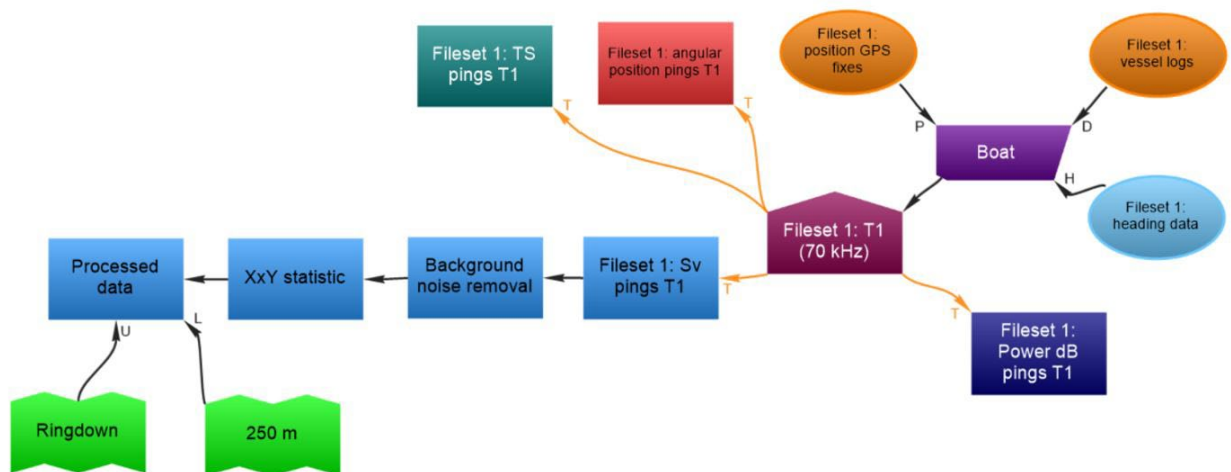


Figure 4.3.4-2. Dataflow, or series of processes followed using the echosounder data processing software Echoview, to prepare the raw acoustic data for analysis. The magenta pentagon labeled

‘Fileset 1: T1 (70 kHz)’ represents the echosounder towed behind the boat. The arrows leading away from the bottom left of the echosounder icon represent the order of the data processing operators used.

#### *4.3.5 Data Analysis*

Light trap catch per unit effort (CPUE: total individuals of any species trapped per hour) data were calculated to standardize effort between sampling events and were log-transformed to fit a normal distribution. Linear models were used to analyze the effects of distance from the FAD, depth, lunar illumination, trap deployment time, and the interactions between illumination and depth, and distance away and depth, on  $\log(\text{CPUE})$  of all individuals, and  $\log(\text{CPUE})$  of all polychaetes. A linear model was also used to analyze the effects of distance from the FAD, depth, lunar illumination, trap deployment time, and the interaction between illumination and depth on total length (TL) of all light-trapped individuals.

A linear mixed effects model (LME, r package *lme4*; Bates et al., 2015) was used to analyze the effects of distance from the FAD, temperature, lunar illumination, location (North or South FAD), and period (day or night) on the log of nautical area scattering coefficient ( $\log\text{NASC}$ ), a proxy for biomass, of weak scatterers (between -50 and -85 dB  $S_v$ ). A correlation structure with a continuous distance covariate (*corCAR1*) was added into the models to account for the expected autocorrelation resulting from successive measures in the ‘distance from the FAD’ variable, and site index (number assigned to each successive one km ‘spoke’ of the surveys at each location) was included as a random effect. Only data from the top 25 m depth bin was used, as including the next bin down to 50 m would surpass the maximum reliable depth based on signal-to-noise ratios.

Due to the high incidence of zero measures with the -50 dB threshold applied, the strong scatterer category was treated as a binomial measure, and all non-zero values were assigned a ‘one’. A generalized linear mixed effects model (GLM, r package *nlme*; Pinheiro et al., 2023) with a binomial distribution was used to analyze the effects of distance from the FAD, temperature, time period (day or night), location (North FAD or South FAD), and lunar illumination (with site index included as a random effect as in the previous model) on  $\text{NASC}$  of strong scatterers (louder than -50 dB  $S_v$ ) in the top 25 m of the water column, where we expected

to see an aggregating effect of the FADs that were located at 10 m depth. All analyses were conducted in R using R studio version 1.3.1093 (R Core Team, 2022).

#### 4.4 Results

From February to May 2019, a total of 1,119 individuals representing six classes and at least 21 families were collected in the light traps (Table 4.4-1). A linear model revealed significant negative effects of distance from the FAD, lunar illumination, and depth on total CPUE (Figure 4.4-3 & Figure 4.4-4, Supplementary Table 8.2-1). There was also a significant negative effect of distance from the FAD on the CPUE of polychaetes, the most abundant group (Supplementary Table 8.2-2). A linear model also revealed significant negative effects of distance from the FAD and trap deployment time on the total length of trapped individuals (Supplementary Table 8.2-3). None of the factors tested had a significant effect on the diversity (compared at ‘Order’ level) of organisms trapped (Supplementary Table 8.2-4).

Temperature was measured during each echosounder survey and is shown in Figure 4.4-5. There was a positive effect of period on the presence of strong scatterers (higher presence during the night) (Figure 4.4-6, Supplementary Table 8.2-7), and no other significant effects.

All of the tested factors except for distance away from the FAD had significant effects on the biomass of weak scatterers ( $-50 \text{ dB} > S_v > -85 \text{ dB}$ ; Supplementary Table 8.2-5). Temperature had a positive effect on NASC, lunar illumination had a negative effect on NASC, and NASC was higher at the South FAD and during night surveys. (Figures 4.4-7 to 4.4-10).

Table 4.4-1. List of all organisms collected during the light trap surveys. N represents the total number of individuals in a given Class, and Nsub is the number of individuals subsampled within a taxonomic group for total length, measured in millimeters plus and minus 95% confidence intervals (TL mm  $\pm$  95% CI).

Phylum	Subphylum	Class	Subclass	Order	Suborder	Family	Genus	N	Nsub	TL
										mm $\pm$ 95% CI

Annelid		<b>Polychaet</b>					<b>81</b>	
a		<b>a</b>					<b>7</b>	
Annelid		Polychaeta	Phyllodoci	Aphroditifor	Polynoida		1	5.3
a			da	mia	e			
Annelid		Polychaeta	Phyllodoci	Nereidiform	Nereidida		96	12.0 ±
a			da	ia	e			1.0
Annelid		Polychaeta	Phyllodoci	Nereidiform	Syllidae			
a			da	ia				
Annelid		Polychaeta	unknown					
a								
Arthrop	Crustace	<b>Malacostr</b>					<b>28</b>	
oda	a	<b>aca</b>					<b>8</b>	
Arthrop	Crustace	Malacostr	Amphipod	Hyperideia	Vibiliidae	Vibilia	1	8.7
oda	a	aca	a					
Arthrop	Crustace	Malacostr	Amphipod	Hyperideia	unknown		19	4.5 ±
oda	a	aca	a					1.2
Arthrop	Crustace	Malacostr	Amphipod	Senticaudat	Caprellid		1	7.6
oda	a	aca	a	a	ae			
Arthrop	Crustace	Malacostr	Amphipod	Senticaudat	Gammari			
oda	a	aca	a	a	dae			
Arthrop	Crustace	Malacostr	Amphipod	unknown			10	6.7 ±
oda	a	aca	a					2.2
Arthrop	Crustace	Malacostr	Decapoda	Dendrobran	Sergestid		12	13.3 ±
oda	a	aca		chiata	ae			1.0
Arthrop	Crustace	Malacostr	Decapoda	unknown			2	13.1 ±
oda	a	aca						2.9
Arthrop	Crustace	Malacostr	Euphausia				5	24.0 ±
oda	a	aca	cea					8.0
Arthrop	Crustace	Malacostr	Isopoda	Cymothoida	Cirolanid		2	5.8 ±
oda	a	aca			ae			0.4
Arthrop	Crustace	Malacostr	Isopoda	unknown				
oda	a	aca						
Arthrop	Crustace	Malacostr	Stomatopo				2	18.9 ±
oda	a	aca	da					3.7
Arthrop	Crustace	<b>Hexanau</b>					<b>6</b>	
oda	a	<b>plia</b>						
Arthrop	Crustace	Hexanaupl	Copep					
oda	a	ia	oda					
Chordat		<b>Actinopte</b>					<b>1</b>	
a		<b>rygii</b>						

Chordata		Actinopterygii	Scombriformes	Scombridae		1	17
Chordata	Tunicata	<b>Thaliacea</b>				<b>4</b>	
Chordata	Tunicata	Thaliacea	Salpida	Salpidae	unknown		
Mollusca		<b>Cephalopoda</b>				<b>3</b>	
Mollusca		Cephalopoda	Oegopsida	Lycoteuthidae	Lycoteuthis		
Mollusca		Cephalopoda	Myopsida	Loliginidae	Pickfordiuthis	1	35.7
Mollusca		Cephalopoda	Octopoda				
<b>Total</b>						<b>11</b>	
							<b>19</b>

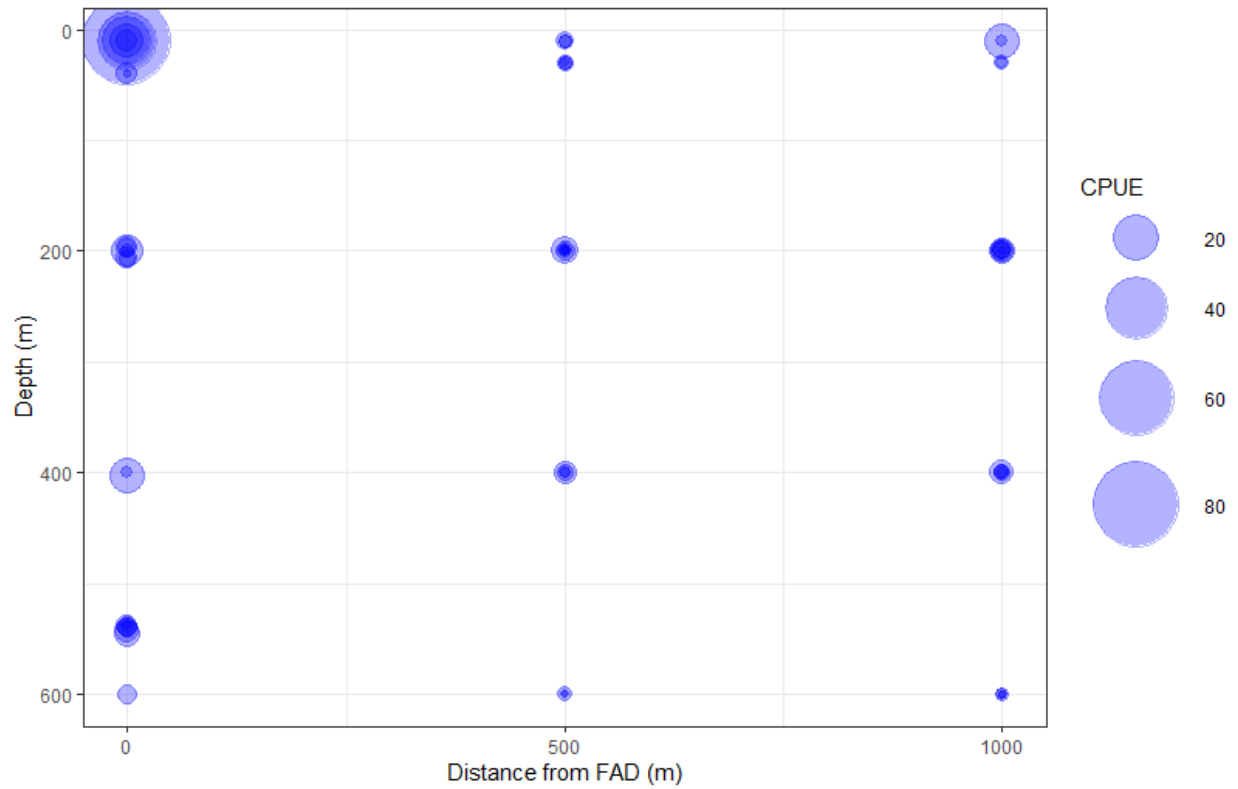


Figure 4.4-3. Catch per unit effort (CPUE: total individuals of any species trapped per hour) in relation to distance away from the FAD for all of the light trapping stations (at the FAD = 0, 500 and 1000 m away). The intersection of the zeros on each axis in the top left of the figure represents the position of the FAD.

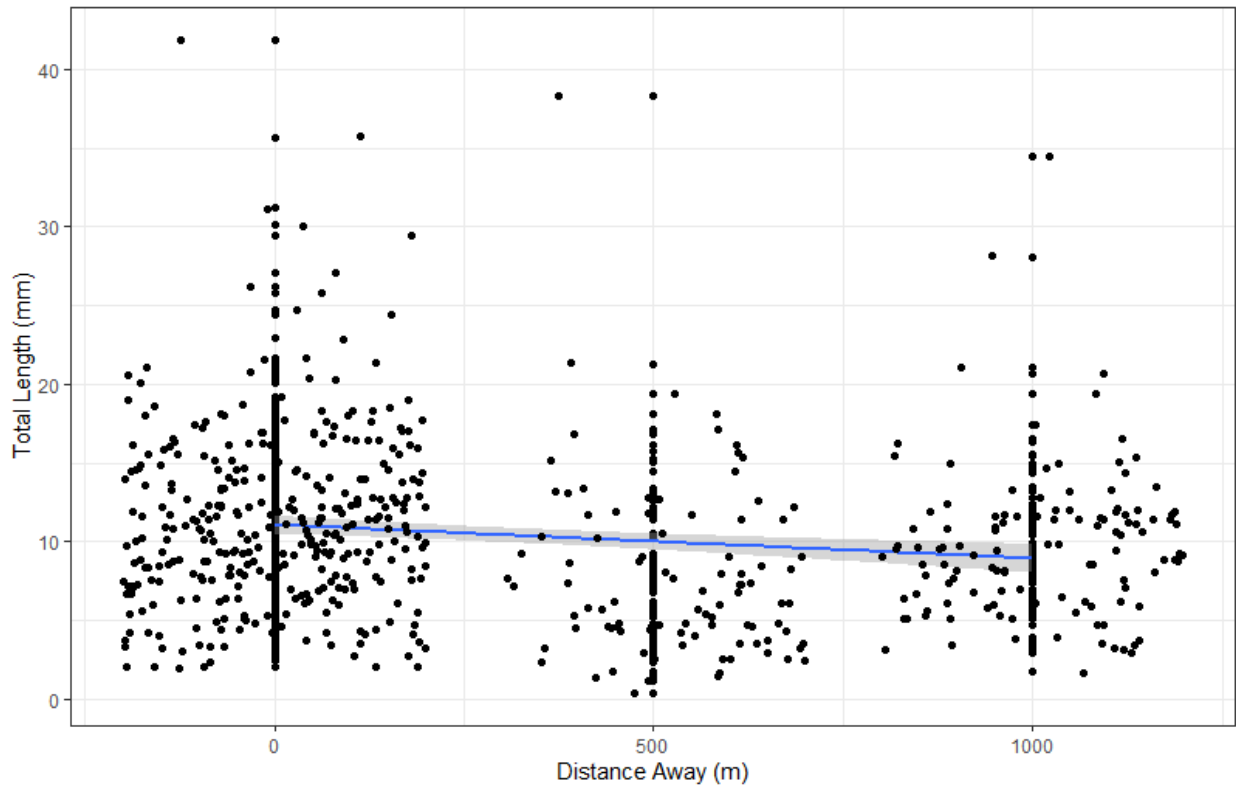


Figure 4.4-4. Total length (mm) of all individuals trapped, with data points jittered around the three distances away from the FAD where traps were deployed. A linear regression (blue line) with 95% confidence intervals shaded around it has been added.

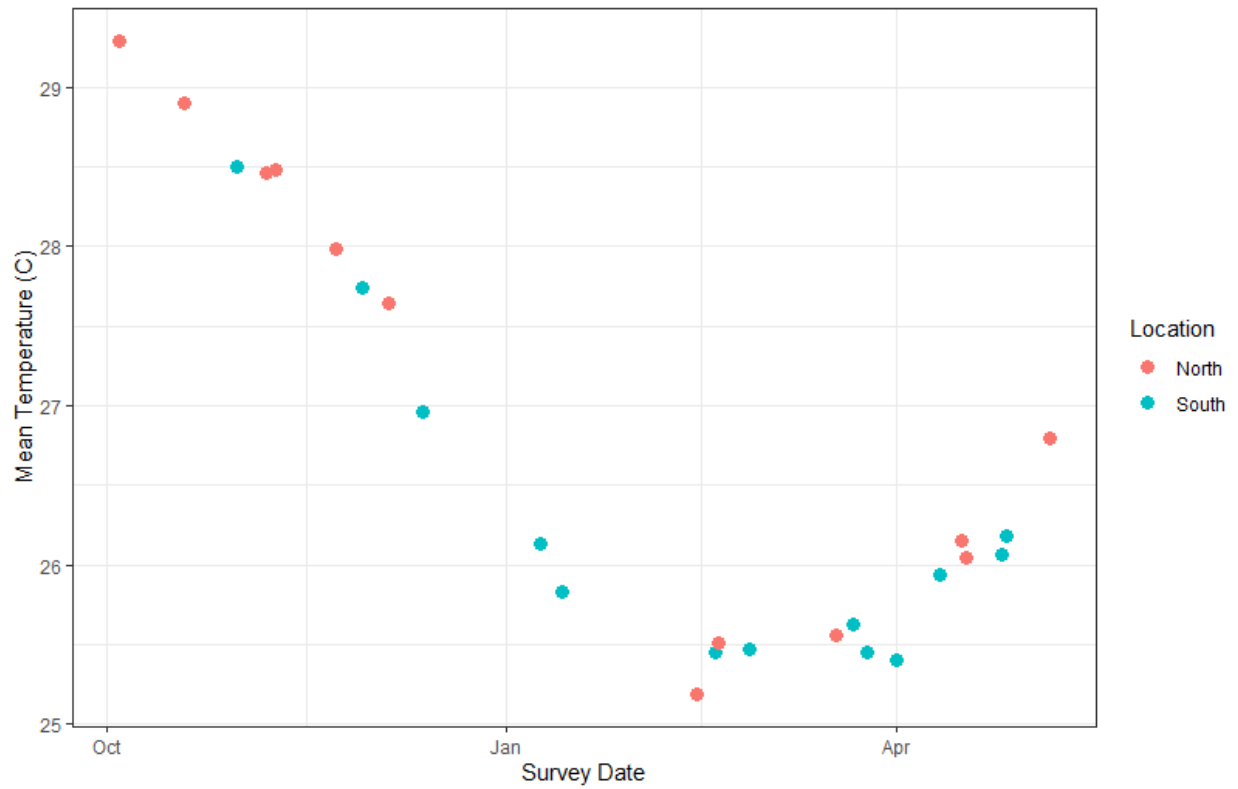


Figure 4.4-5. Mean temperature during each echosounder survey over time (October 2018 to May 2019) measured by the Hobo logger attached to the echosounder glider frame at five meters depth. Red dots represent temperatures during surveys at the North FAD and blue dots represent temperatures during surveys at the South FAD.

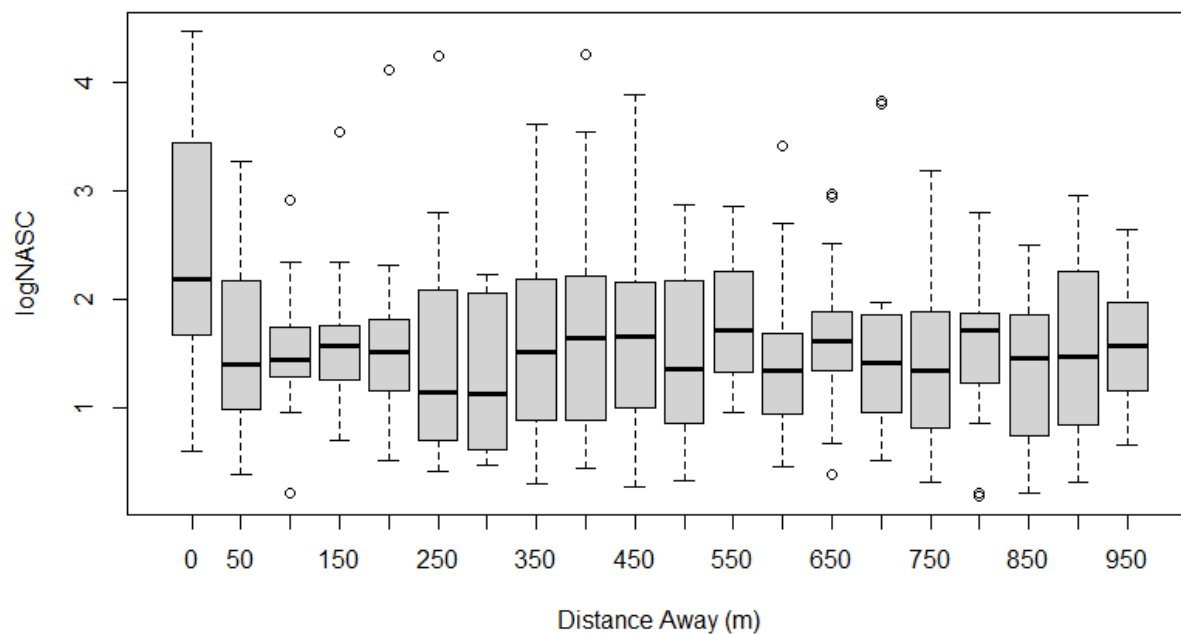


Figure 4.4-6. Boxplot showing biomass (represented by logNASC [nautical area scattering coefficient] which is unitless) of strong scatterers ( $S_v > -50$  dB) measured during the towed echosounder surveys at both locations shown over varying distances from the FADs. Values were binned every 50 m for visual clarity due to the large number of raw points.

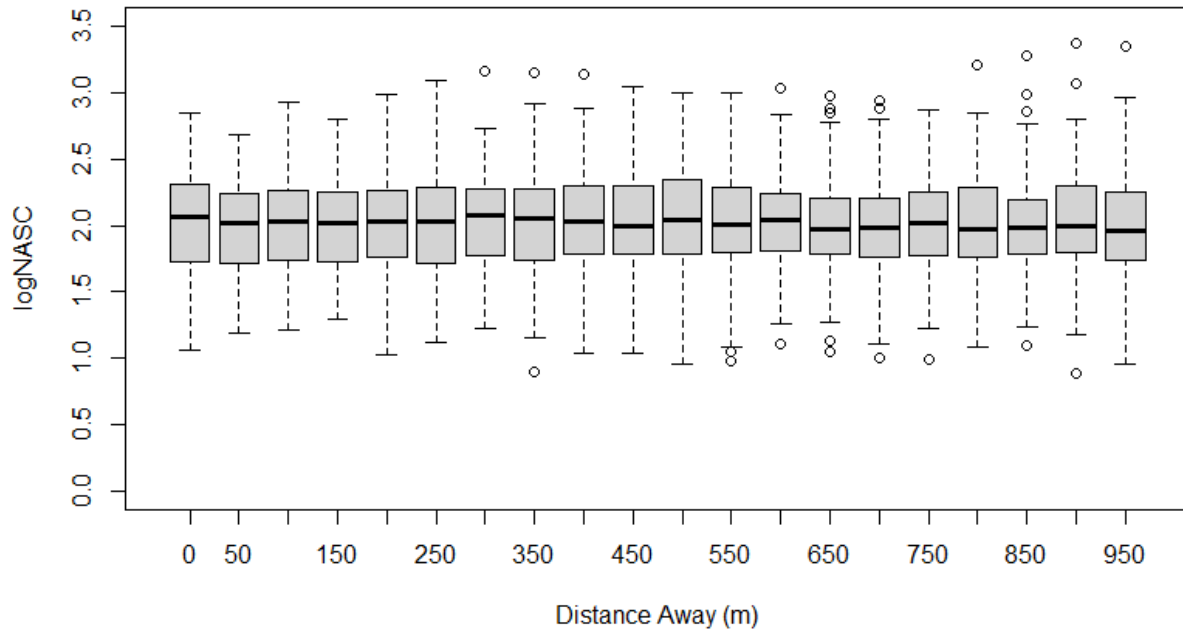


Figure 4.4-7. Boxplot showing biomass (represented by logNASC [nautical area scattering coefficient] which is unitless) of weak scatterers ( $-50 \text{ dB} > S_v > -85 \text{ dB}$ ) measured during the towed echosounder surveys at both locations shown over varying distances from the FADs. Values were binned every 50 m for visual clarity due to the large number of raw points.

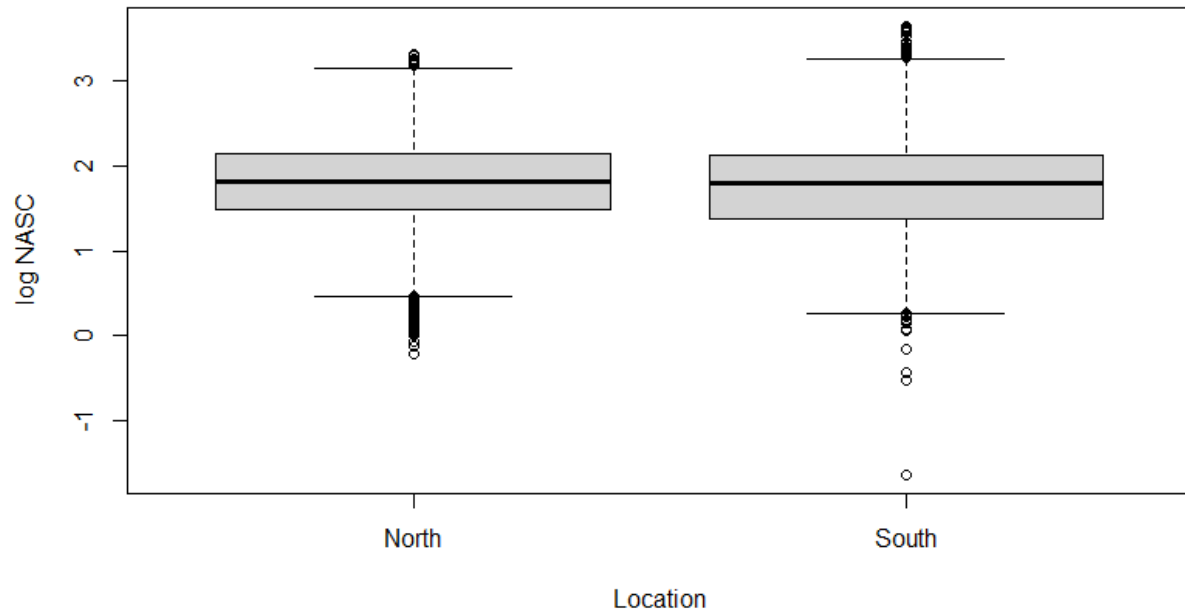


Figure 4.4-8. Boxplot showing biomass (represented by logNASC [nautical area scattering coefficient] which is unitless) of weak scatterers ( $-50 \text{ dB} > S_v > -85 \text{ dB}$ ) measured during the towed echosounder surveys grouped by location- North (North FAD) and South (South FAD).

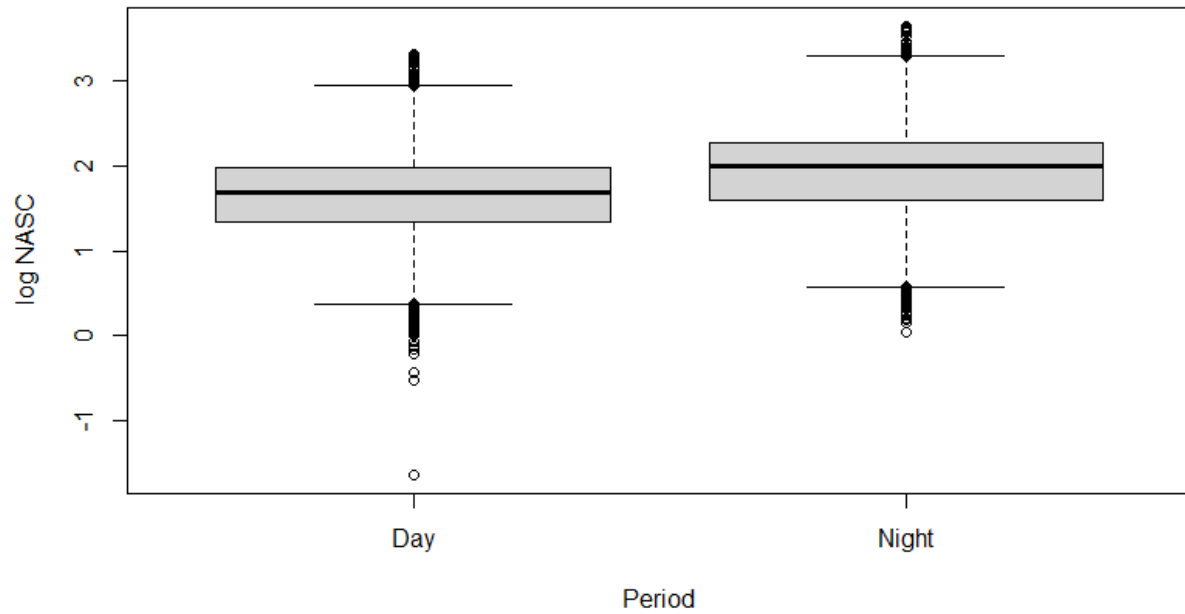


Figure 4.4-9. Boxplot showing biomass (represented by logNASC [nautical area scattering coefficient] which is unitless) of weak scatterers ( $-50 \text{ dB} > S_v > -85 \text{ dB}$ ) measured during the towed echosounder surveys at both locations grouped by period- day and night.

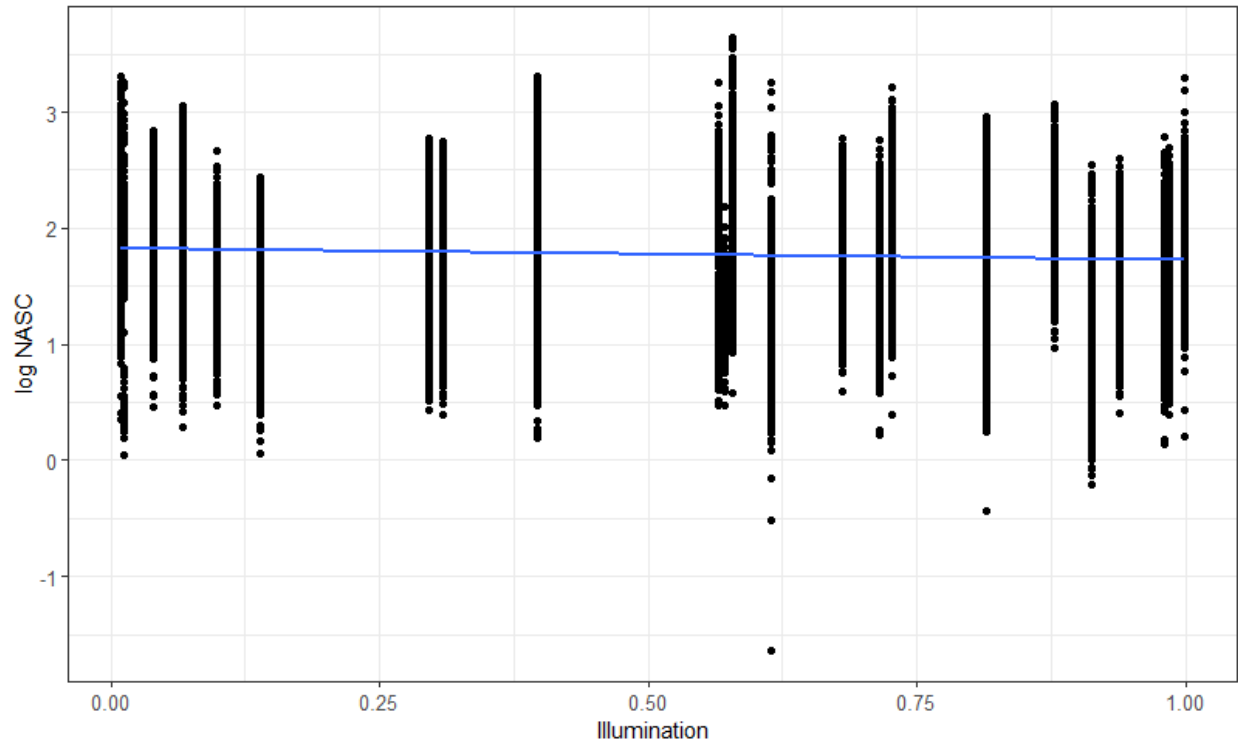


Figure 4.4-10. Biomass (represented by logNASC [nautical area scattering coefficient] which is unitless) of weak scatterers ( $-50 \text{ dB} > S_v > -85 \text{ dB}$ ) measured during all of the towed echosounder surveys as a function of lunar illumination. A linear regression (blue line) has been added.

#### 4.5 Discussion

Understanding the effects and mechanisms behind fish aggregation to floating structure is an important aspect of the management of pelagic fisheries, measuring and maintaining marine biodiversity, and understanding the impacts of anthropogenic activity such as FAD deployment on these habitats. A number of hypotheses have been presented to explain fish aggregation to floating structure in the pelagic zone, and here we provide weak evidence of a micronekton aggregation around a FAD. These data show the need to further test the potential for a predation-based mechanism for fish attraction or aggregation.

In conducting light trap surveys around the North FAD, we found a significant negative effect of distance from the FAD on CPUE of all trapped individuals. And while we did not find

the same significant effect on polychaete CPUE (the most abundant group, comprising 71% of all individuals), there was a relatively strong trend with distance and more sampling would be likely to show that this factor is important at this taxonomic level as well. This may suggest that the micronekton community of invertebrates that were sampled using this method exhibits aggregating behavior around the FAD, a phenomenon widely thought to exist only in fishes. Pelagic invertebrates are known to form various types of aggregations (Ritz, 1994), however many of these aggregations previously described form for social purposes such as mating, or to follow prey (e.g., Nowacek et al., 2011). It is understood that some FAD-associated fish species feed in the close vicinity of the structure and some make excursions away from FADs to feed, as evidenced by a range of prey items in the stomachs of FAD-associated tunas (Buckley & Miller, 1994; Menard et al., 2000; Jaquemet et al., 2011), although these prey species are not thought to be concentrated because of the FAD structure. One study specifically noted the unlikelihood of an aggregating effect of a FAD on a pelagic decapod (*Opliphorid* shrimp) because it was only found in the stomach of one tuna species sampled from the FAD and would have been expected to be preyed upon by other FAD-associated species if it was indeed more abundant around the structure (Brock, 1985). However, our findings provide evidence to the contrary based on the higher CPUE seen at the FAD structure compared to 500 m and 1000 m away. Floating *Sargassum* seaweed, for example, supports a diverse community of invertebrates, many of which almost exclusively associate with this genus of algae (Abe et al., 2013; Sehein et al., 2014). There are protective and foraging advantages for those invertebrates to be associated with floating *Sargassum*, and while the species surveyed in the light traps are not commonly found in *Sargassum*, it is possible that they may also perceive some benefit from association with structure, be it protection from predators, a fixed aggregation point for interaction with conspecifics, or to prey upon the sessile organisms there. A distinct limitation of this study, however, is that we only had one experimental unit (one FAD) that was surveyed. Because the effects seen here on CPUE could have been part of wider, FAD-unrelated patterns, further investigation is needed using more replicates and a larger sample size. However, our data presented here justifies this interesting and potentially important avenue of study.

Additionally, we found that depth and lunar illumination also had negative effects on the CPUE of light trapped individuals. The negative effect of depth on CPUE was expected based on the behavior of many pelagic micronekton. Many pelagic polychaetes, which comprised

approximately 70% of all individuals trapped in this study, undergo a nocturnal ascent diel vertical migration (Amei et al., 2021). As the light traps were deployed at night, more of the vertically migrating fauna would be expected to be in shallower depths and thus captured at a higher rate in these traps. The negative effect of lunar illumination on CPUE across all trapping stations was also to be expected, and this finding may be related to the potential decrease in effectiveness of light traps on brighter nights, or to anti-predatory behavior. For example, while abundance of micronekton may also be tied to lunar illumination, it has been established that the effectiveness of light traps decreases with higher lunar illumination (Gregory & Powles, 1985; Hickford & Schiel, 1999). This is likely due to a lower ability to discriminate the trap's light source with more background lunar illumination but could also be tied to anti-predator behaviors. Some species have been shown to concentrate their movements into 'antipredation windows', typically crepuscular periods when light levels make detection most difficult (Scheuerell & Schindler, 2003), and while this example derives from a different habitat, it is plausible that less movement (and therefore less individuals being trapped) could explain this relationship in the data.

There were negative effects of distance from the FAD and time of deployment on the total length of trapped individuals. Trapping larger individuals closer to the FAD and on shorter trap deployments could be explained by the higher mean swimming velocity in scattering layer groups that are generally larger (Ignatyev, 1997), hence the increased ability for a larger individual to maintain its position around the FAD or quickly move towards the trap. However, due to the pooled data and the breadth of modes of movement by different taxonomic groups of micronekton, it is also possible that there are other explanations for this size pattern that we have not investigated. For example, smaller individuals may be sufficiently mobile but could be avoiding the risk of predation around the FAD or light source which could also lead to this size distribution seen here.

The echosounder survey revealed a significant effect of period (night or day) on the NASC of strong scatterers, with higher biomass measured at night, and significant effects of temperature, lunar illumination, location, and period on the NASC of weak scatterers. However, the correlation structure included in the models did not fully correct for the expected autocorrelation, which can result in effects appearing stronger than they actually are. Due to the

unique situation in the present study where the source of the autocorrelation, successively occurring measurements across the ‘distance away’ metric, is also the variable we are interested in the effect of, the standard approach for addressing autocorrelation in the models was minimally effective, thus potentially enhancing effects that might not be significant.

With this caveat noted, there was a positive effect on the presence of strong scatterers when surveys occurred at night. The diel vertical migration is a well-documented movement of micronekton towards the surface at night, and there is some evidence that larger pelagic fish might follow this prey field as tuna especially tend to stay closer to the surface at night and deeper during the day, possibly explaining this finding (Cayré, 1990). Interestingly, we found no significant effect of distance away from the FADs on these strong scatterers, despite ample previously published evidence of this phenomena elsewhere. Several studies that have measured the distribution of strong scatterers such as tunas around moored FADs in the Caribbean detected large schools of tuna around 250 – 600 m away from the FAD on average (Doray et al., 2007; Trygonis et al., 2016), which would be in the middle lateral range of the echosounder survey we conducted. In these and other studies, tuna fall into the circumnatanant category proposed by Parin and Fedoryako (1999), in that they are infrequently within the immediate visual vicinity of the FAD structure and have been shown to stay associated while up to 15 km away (Girard et al., 2004), however this was not supported by our findings. It is possible that due to the oligotrophic nature of the Exuma Sound and lack of any upwelling features that would support substantial pelagic fish biomass, the overall abundance of strong scattering targets (large fish) is so low that the FADs have a minimal aggregation effect over the surveyed distances (1 km radius from each FAD). The NASC values of strong scatterers in the present study are approximately two orders of magnitude lower than those collected in the known presence of commercially targeted tuna schools (Moreno et al., 2019), so any attraction or aggregation effects may be difficult to truly distinguish if present at all. We also note again that there were only two experimental units (two FADs) in the echosounder surveys, so our conclusions are limited by this low level of replication.

When investigating the NASC of weak scatterers, we found a significant effect of location, temperature, period, and lunar illumination. We measured significantly higher NASC at the South FAD, which was unexpected. The two FADs are separated by only 13 km, are of

identical design, and both sit on the 600 m isobath, so the only notable difference is the potential exposure of the North FAD to tidal effluent from the Bight of Eleuthera that the South FAD would be less directly exposed to (Figure 4.3.3-1, right panel). We also found significantly higher weak scatterer biomass at night and during lower lunar illumination. This aligns with well-documented diel vertical migration patterns in pelagic plankton and micronekton, as an entire deep scattering layer community ascends in the water column at night (Ringelberg, 2009), and this migration is lessened (individuals stay deeper) during periods of high lunar illumination around the full moon (Hernandez-Leon et al., 2002). A limitation to this backscatter data is that the breadth of the threshold applied to the weak scatterer category is too wide to discern group-specific patterns. The threshold used, between -50 and -85 dB  $S_v$ , was designed to capture all biomass apart from large fish (Benoit-Bird & Lawson, 2016). It is therefore difficult to make any connections between what was sampled in the light traps and what was measured using the echosounder. It is likely that the samples from all of the light trap surveys, more than 99% of which were invertebrates between 0.4 and 41.9 mm in length, fall within a narrower band of  $S_v$  and therefore might not fully represent the NASC pattern at our designated ‘weak scatterer’ category.

Here, we provide weak evidence, hampered by low experimental unit replication, for an interesting example of invertebrate aggregation around a moored FAD. In assessing the impacts that a growing number of FAD deployments could have on pelagic fauna, it is important to understand the mechanisms that underpin fish attraction and aggregation in the first place. Plankton and micronekton form the base of pelagic food webs and support a diversity of fisheries, and it is therefore important to further our understanding of the behavior and responses of these organisms to anthropogenic change (Girard et al., 2004; Ballon et al., 2011). Furthermore, the identification of insonified targets is an important step in interpreting echosounder-derived biomass data (Madureira et al., 1993), so further incorporation of coupled sampling techniques such as sonar and light trapping, to target lesser studied but highly important low tropic level organisms, will be beneficial in developing our understanding of predator prey dynamics and fish aggregations.

## **5. Fine-scale acoustic positioning of structure-associated pelagic fishes using a 3-D acoustic telemetry array**

Schneider EVC, Talwar BS, Bailey DM, Killen SS, van Leeuwen TE, Smith F

### **5.1 Abstract**

Many ecologically and commercially important species exist in the epipelagic marine environment, but the scale and relative lack of structure (i.e., seafloor) of this habitat pose logistical challenges to tracking the fine-scale movement and behavior of these species. Acoustic telemetry can provide highly detailed positioning data for tagged animals in contexts and habitats that can facilitate an array of receivers with overlapping fields of detection, however this technique has yet to transfer to open-water scenarios. Here, we detail the developments and challenges of a new acoustic telemetry array that can be mounted on or suspended from various structures in the open ocean, thus facilitating more detailed tracking of tagged epipelagic animals. Consisting of a horizontal and vertical component that can be deployed separately or in tandem, this new ‘vertical acoustic array’ (VAR) is able to reliably calculate distance from the array and depth, and can theoretically calculate bearing, although multipath signals currently result in unacceptable error estimations and require further physical and analytical development before use. An acoustic telemetry array that can precisely position animals in open water will have important implications for bycatch mitigation, animal behavior around anthropogenic and natural structures, and pelagic species interactions in general.

### **5.2 Introduction**

Tracking the movement of marine organisms is of wide interest and is an actively evolving field (e.g., Aspillaga et al., 2021; Weinz et al., 2020; Guzzo et al., 2018). Fine-scale movements of fishes in the open ocean are particularly challenging to measure (Block et al., 2003), but understanding these movements is often necessary for effective fisheries management and more general species conservation (Hays et al., 2019; Nathan et al., 2022). For example,

understanding how pelagic fish behave around structure- a common phenomenon- can improve our understanding of their ecology, lead to better monitoring and more selective study, and inform best practices in certain fisheries. Blue-water net fisheries, for instance, that use fish aggregating devices (FADs) to target tunas operate across the world's tropical oceans and routinely capture mixed-species assemblages, often including imperiled species. An improved understanding of fine-scale fish behavior and potential interactions between species could lead to more selective fishing strategies. Other artificial structures such as aquaculture pens or offshore energy platforms also recruit and hold significant fish biomass (e.g., Claisse et al., 2014), and therefore interest and technology are developing to study fish movement in these challenging contexts.

Acoustic telemetry has been used to understand the association between pelagic fish and structures that facilitate capture (e.g., FADs in Filmalter et al., 2015; Filmalter et al., 2011). The current state of passive acoustic telemetry research conducted in open water utilizes a single acoustic receiver mounted beneath a floating (e.g., FAD) or fixed (e.g., oil rig) object to collect residence and depth data (if the transmitter is equipped with a pressure sensor) (see Forget et al., 2020 or Tolotti et al., 2020; Figure 5.2-1A). Whereas in nearshore environments where a well-designed array of receivers placed on the seafloor can generate positions and tracks of tagged animals, the deep water prevents the deployment of receivers on the bottom, and the unique nature of these structures prevents the deployment of numerous receivers spread in such a way that would facilitate more specific position calculations (i.e., an array). Basic residence (presence-absence) data can provide substantially more behavioral information than traditional visual or camera-based observations, even if limited inferences can be made, especially when fish exhibit similar residence patterns. But, understanding target and bycatch or predator and prey species movements and associations is a high priority to building an understanding of pelagic fish ecology (Tolotti et al., 2020), so working towards multidimensional positioning for pelagic species may open the door to a suite of useful research endeavors.

While acoustic telemetry-derived positioning data is most reliable in closed system applications (e.g., Watson et al., 2018), the homogeneity of the pelagic habitat- including its relatively stable environment, lack of structure (except for thermoclines), and absence of many of the sound-generating organisms of the benthos- is particularly conducive to acoustic signal

transmission (Claisse et al., 2011; Mathies et al., 2014; Kraus et al., 2018). Here, we detail a new acoustic telemetry array orientation (hereafter referred to as the vertical array [VAR]) that is designed to facilitate the collection of more specific positioning data in pelagic habitats. Our objectives were to: (i) design and test an array that can calculate distance away and bearing of a transmitter in relation to the array-affixed structure, (ii) test detection efficiency and positioning error between various depth combinations of receivers and transmitters in the array (e.g., shallow receiver x shallow transmitter, shallow receiver x deep transmitter, etc.), and (iii) track the movement of a wild fish through the array to test its performance. Comprised of a horizontal component to calculate bearing and a vertical component to calculate distance and depth, this modular technique aims to greatly improve the type and amount of positioning data generated for a tagged animal in an epipelagic environment. The ability to passively discern behavior around a structure will facilitate in-depth investigations into pelagic fish ecology and fisheries interactions.

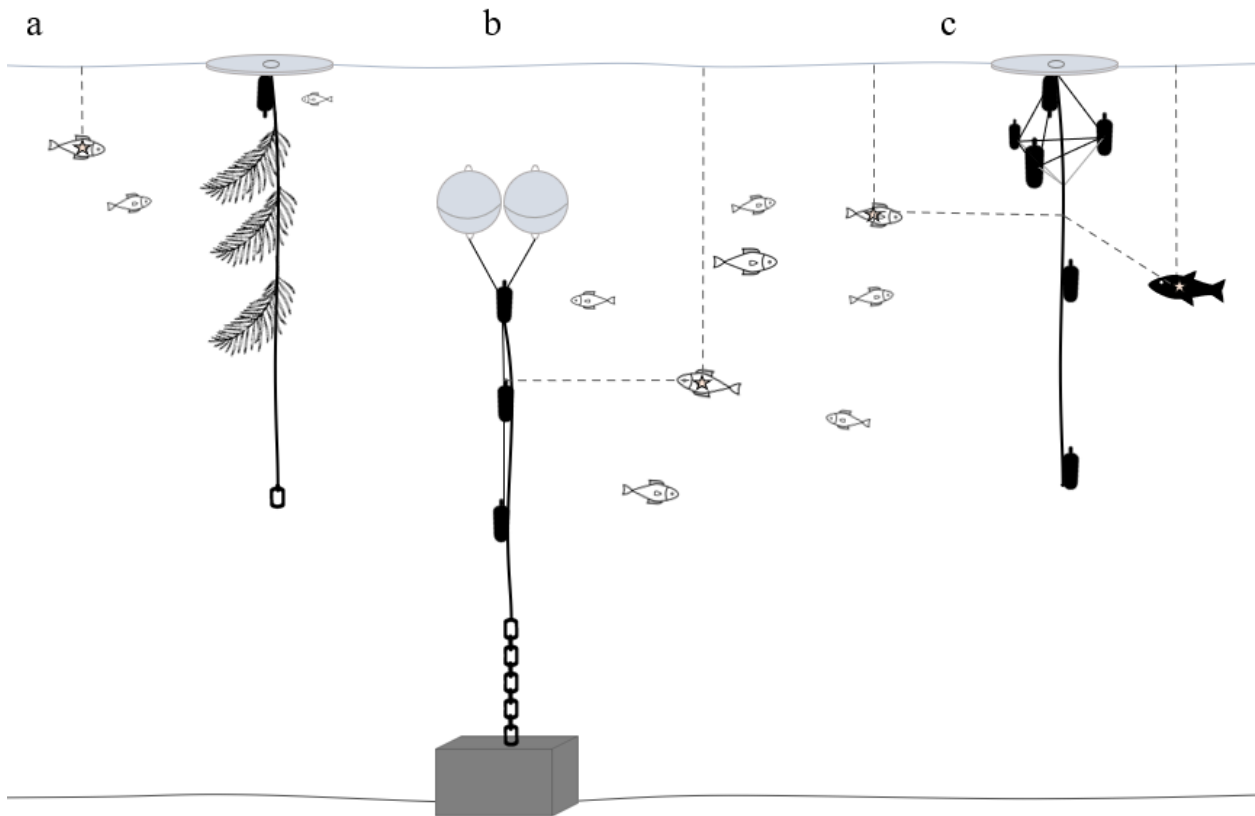


Figure 5.2-1. Panel 'a' shows a typical commercial FAD (grey oval) with a single receiver directly underneath it to collect residence (presence and absence) and depth data (if the

transmitter is equipped with a pressure sensor), utilized by several recent studies. This represents the limits of previous applications. Panel ‘b’ represents the moored sub-surface FAD used in the development of the vertical component of the VAR, with three receivers aligned down the taut mooring line which can be used to calculate depth and distance from the FAD array. Panel ‘c’ shows the final iteration of our array development, combining the vertical and horizontal components suspended beneath a free-drifting buoy to calculate depth, distance away, and bearing of a tagged animal.

### **5.3 Methods**

Field trials and the development of the VAR were conducted offshore from the Cape Eleuthera Institute in the Exuma Sound in the central Bahamas. The VAR has two main components: a horizontal frame of three receivers and a vertical drop line of three receivers. A subsurface moored FAD (Figure 5.2-1B. Bottom depth 600 m, buoy depth 10 m; described in Schneider et al., 2021) was used as a platform on which the vertical component of the array was first constructed. The full VAR can be deployed on either a moored/fixed structure or suspended underneath a free-drifting buoy. Details on both applications are included as the horizontal and vertical components of the VAR can be used together or separately.

#### *5.3.1 Vertical Component- Moored FAD*

The moored FAD used in this component of the array trials was constructed with a subsurface (10 m) flotation buoy that resulted in the mooring line being taut and vertical in the water column. This allowed for a shuttle-like rigging system to deploy receivers down the length of the mooring line. First, three VR2Tx receivers were initialized and set to record ‘fast diagnostics’, with the internal transmitter set to ‘sync tag’ on ‘very high’ power. Each receiver was individually secured in a protective holder (Figure 5.3.1-2) and attached to the beginning, middle, or end of a 200 m line (6 mm potwarp) such that 100 m separated each receiver. At 50 m intervals (at and between each receiver), a 50 cm diameter hoop made of one inch vinyl hose was attached to the receiver line with a small cable tie that had been cut half-way through with snips. Scuba divers opened and re-closed each hoop around the top of the mooring line directly beneath

the FAD flotation buoys, and the rigging was slowly lowered using the weight of the receivers. Once the entire rigging line had been lowered, the end was tied off beneath the FAD buoy. Receiver target depths and spacing were confirmed following retrieval by checking the recorded depths logged by each receiver. In this orientation, the vertical component of the array is designed to calculate a transmitter's depth and distance from the array or equipped structure.

Following the diagnostic trial that confirmed the performance of the shuttle rigging at positioning the receivers to the desired depths, the receivers were redeployed. A great barracuda (*Sphyraena barracuda*, fork length = 92 cm) was then angled at the FAD and externally tagged with a Vemco V9 acoustic transmitter using a traditional dart tag crimped through the external attachment cap. The fish was quickly released, was observed returning to the FAD structure, and the receivers were collected seven days later.



Figure 5.3.1-2. A Vemco VR2Tx receiver in a mounting cup. (Left) A 3" (7.62 cm) PVC pipe was cut to length as a protective receiver cup. Short tethers were tied through holes drilled in the top and bottom of the pipe and attached to longline snaps that were used to quickly attach and detach the cup from the array's main six mm line at predetermined intervals. (Bottom right) A

3.8 cm long bolt was tightened through the bottom of the cup as a stopper. (Top right) Two additional holes in the top of the pipe were used to tie the receiver into the cup (connected with a snap swivel for easy removal and replacement) and to affix a rubber band around the top of the receiver to ensure a snug and motionless fit without impeding signal reception.

### 5.3.2 Vertical Component- Drifting Buoy

The previous rigging was then adapted to suspend the vertical component of the array under a drifting buoy. Three VR2Tx receivers were individually secured in protective holders (Figure 5.3.1-2) and attached to the beginning, middle, and end of a 200 m line (Samson six mm AmSteel Dyneema) such that 100 m separated each receiver. A three kg weight was fixed to the end of the line, and the top of the line was fixed to a fish aggregating device (FAD) buoy (Zunibal Zunfloat, 180 cm diameter, 150 kg of flotation). This combination of bottom weight, thin line (6 mm), and a low-profile surface float (7.5 cm thick Zunfloat) reduced windage and drag such that the three receivers remained in a vertical line as the array drifted (Figure 5.3.2-3) and was confirmed using the depth sensors in the receivers.

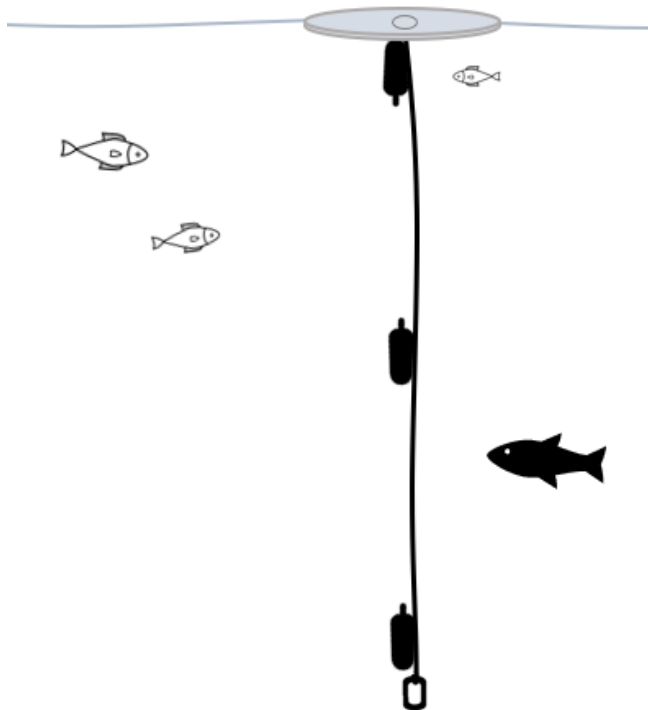


Figure 5.3.2-3. Diagram (not to scale) of the vertical component of the VAR. The grey oval at the surface represents the FAD float used, a Zunibal Zunfloat (180 cm diameter, 150 kg of flotation). A 200 m length of Samson six mm AmSteel Dyneema line was tied through the holes in the float, and the receivers in the mounting cups were clipped to this line at 100 m intervals (top, middle, bottom). A three kg steel shackle was used as the bottom weight.

### 5.3.3 Horizontal Component- Drifting Buoy

Three receivers were spaced 15 m apart oriented in a horizontal plane 10 m beneath the sea surface. To accomplish this and keep the receivers equidistant, three extendable poles (DocaPole 7-30 ft extension pole) were attached to a central custom-made hinge. A protective receiver cup (Figure 5.3.1-2) was attached to the opposite end of each pole, and spacer lines allowed for the protracted poles to splay out evenly. The central hinge was attached to a line suspended underneath a FAD buoy such that the receivers were suspended 10 m beneath the surface (Figure 5.3.3-4). In this orientation, the horizontal component of the array is designed to calculate a transmitter's bearing in relation to a reference point, such as another transmitter, or a vector from the origin to 'Receiver A' that could be set as 0°.

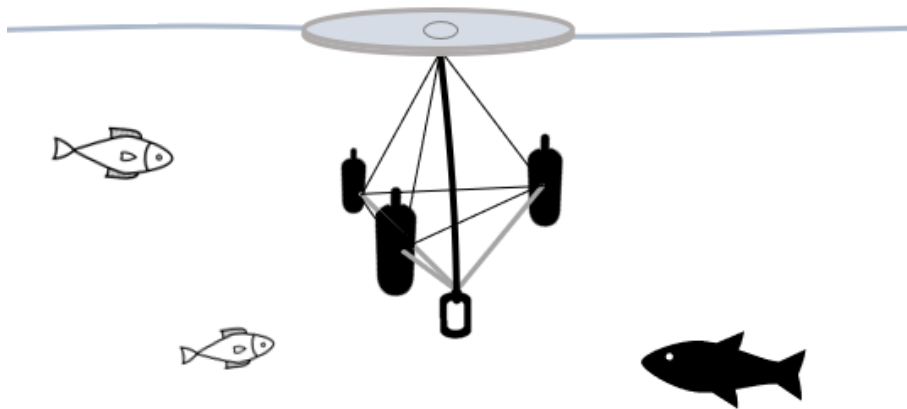


Figure 5.3.3-4. Diagram of the horizontal component of the VAR. The grey oval represents the FAD on the sea surface, and the vertical thick black line represents the line with a weight at the bottom. Receivers were spaced 15 m apart at 10 m depth using extendable poles (thicker grey lines) and spacer lines (thinner black lines): diagram is not to scale.

#### *5.3.4 Full Array*

The horizontal and vertical components of the array were combined by attaching all elements to a single vertical line suspended underneath a free-drifting FAD buoy. Drift tests were then conducted to measure detection range and to compare the position calculations of the array against known GPS-based locations during the drift (i.e., testing the array's functionality). All results reported hereafter are based on drift tests around the full VAR suspended beneath a free-drifting buoy. To conduct the drift tests, a transmitter line was assembled consisting of a large spherical buoy, 300 m of line (6 mm potwarp), and a three kg steel weight at the end. The line was outfitted with nine Vemco V9 transmitters spaced along the 300 m, affixed using rubber bands and cable ties. Each transmitter had an archival temperature and depth recorder (TDR) (Lotek LAT-1400) directly adjacent to it on the line to record actual transmitter depth for comparison to the array-calculated depths. A handheld GPS (Garmin eTrex 10) was attached to a one-meter pole mounted onto the surface buoy to record the transmitter line's location, and the line was released into the water one km upwind from the receiver array. The spherical buoy had more windage than the FAD buoy that the array was suspended from, allowing the transmitter line to drift faster than the receiver array. The transmitter line was collected after it moved past the receivers by approximately one km. This test drift was repeated seven times over the course of a five-hour period, during which the bearing from the origin of the horizontal component to a designated 'receiver A' was manually measured to track any rotation of the array throughout the drift tests. Following the trials, the receivers were retrieved, and the data downloaded.

#### *5.3.5 Data Analysis*

To assess transmission efficiency during the trials, a detectability analysis was performed. For each receiver-transmitter combination, the number of logged transmissions was

divided by the number of transmissions that should have occurred based on ping rate over a given time (length of each drift).

Next, detection time difference (DTD) was calculated for each transmitter by 2-receiver pairing. This underpins the hyperbolic positioning calculation by creating hyperbolas of possible locations that a transmitter can be in for each transmission, the intersection of which (with other hyperbolas as calculated by other 2-receiver pairings) represents the actual position of the transmitter. DTD was calculated as:

$$DTD_{R_a, R_b} = DT_{R_a} - DT_{R_b}$$

with DT denoting detection time and  $R_a$  and  $R_b$  denoting two receivers in the array. DTD error was then calculated by subtracting the observed DTD from the predicted DTD that is calculated using known GPS-based locations of the array and the transmitters during the trial. This DTD error was then converted from time to distance using the speed of sound in water (1,534 m / s when temp = 25 C and salinity = 35 ppt). The internal sync tags within each receiver are used to generate the maximum DTD for each receiver pairing, and values greater than those were expected to have encountered multipath error and were deemed unreliable.

## 5.4 Results

### 5.4.1 Detectability Analysis

Over the course of the seven drift tests using the full array suspended beneath a drifting FAD, detection efficiency was calculated for each combination of receiver and transmitter (Figure 5.4.1-5). Receivers at 10 m and 15 m (H1-H3 in the horizontal component [depth = 10 m], and V015 in the vertical component [depth = 15 m]) detected transmitters at 100 m and shallower at a rate of 13.7% ( $\pm 1.1\%$  SE) of total transmissions compared to a rate of 3.8% ( $\pm 0.6\%$  SE) for transmitters deeper than 100 m (Figure 5.4.1-5). Transmitters at 1 m depth were heard at an average rate of 7.5% ( $\pm 1.1\%$  SE) across all receivers and were heard roughly as frequently as the next shallowest (25 m) transmitter, likely due to the close proximity to the sea surface. The deepest receiver, at 200 m, detected transmissions from the deep transmitters (100, 150, 200, 250, and 300 m) at a rate of 18.7% ( $\pm 1.6\%$  SE), whereas it only detected transmissions

from the shallow transmitters (1, 25, 50, and 75 m) at a rate of 7.7% ( $\pm 1.9\%$  SE). A thermocline was present between 100 m and 150 m (Figure 5.4.2-9), and in general, detection rates between receivers-transmitter pairs that were on opposite sides of the thermocline were much lower than pairs on the same side of the thermocline.

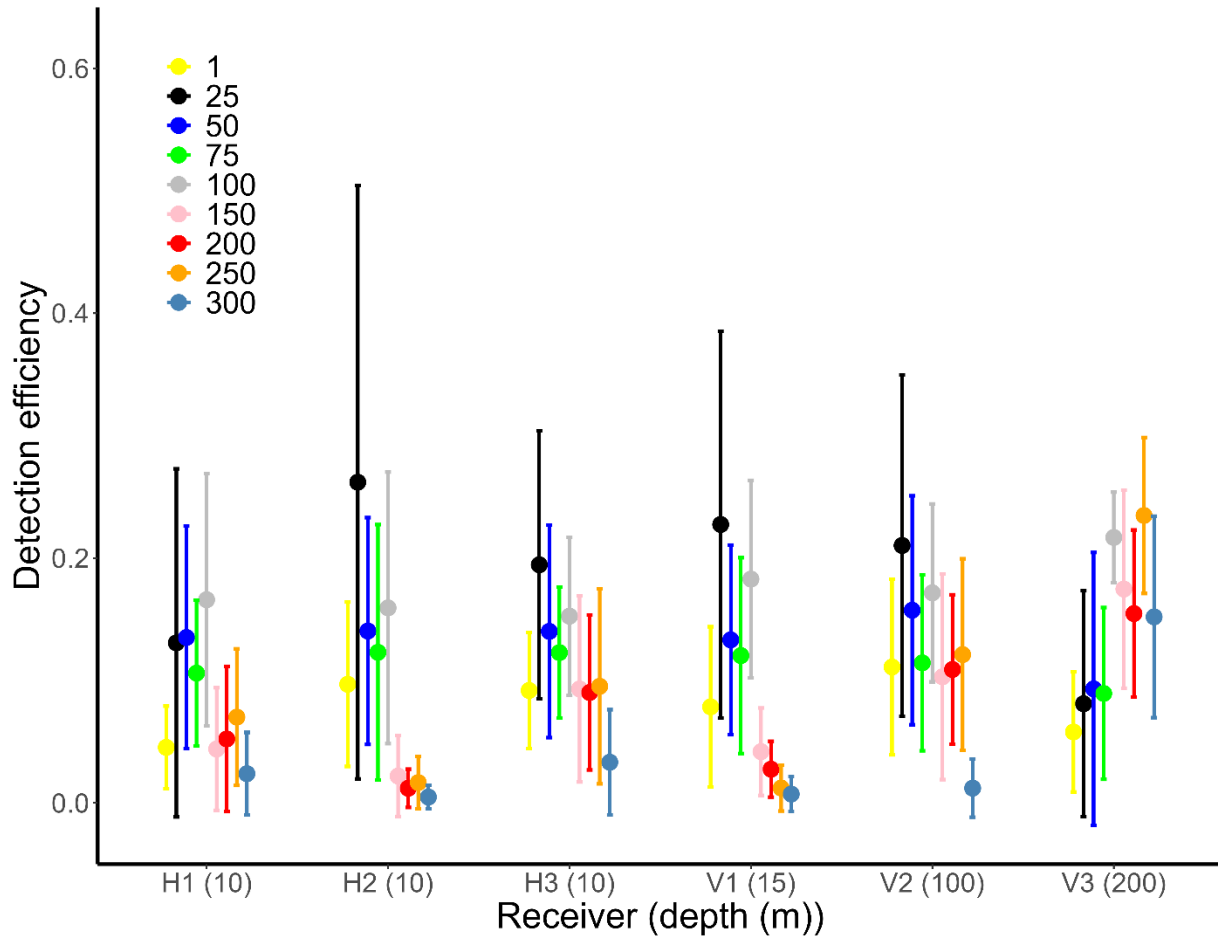


Figure 5.4.1-5. Mean detection efficiency (with 95% confidence intervals) of transmissions from V9 transmitters to VR2Tx receivers during seven trials (TrialN). Receiver labels are across the x axis: the three receivers in Figure 5.3.3-4 were positioned in a 15-meter equilateral triangle on a horizontal plane at 10 m depth and are labeled as H1, H2, and H3. The three receivers in Figure 5.3.3-3 were positioned along a vertical line and are labeled V1 (15 m deep), V2 (100 m deep), and V3 (200 m deep). Transmitter depths are in the legend, and nine transmitters were used (fastened along a vertical line).

#### *5.4.2 Detection Time Difference*

Detection time differences (DTD) between the vertical receiver pairings are shown in Figure 5.4.2-6 and Figure 5.4.2-7. The built-in sync tags within the receivers are used to calculate the maximum valid DTDs for receiver pairings and are proportional to the distance between the receivers. The absolute value of the DTD for the sync tag transmissions between receivers V015 and V100 was 57.43 ms (88.1 m corrected to distance) and was 122.1 ms (187.3 m) between receivers V015 and V200, representing an error margin of 3.6% and 1.2% respectively. Two of the nine transmitters produced DTD values outside of the sync tag DTD range for both the V015 / V100 and the V015 / V200 receiver pairings. This only occurred during the first of seven drifts and accounted for 5.6% of all calculations within the vertical component during the whole trial. The GPS-based distances between transmitters and the array were then converted into times and subtracted from these calculated DTD values to determine DTD error which is also shown in Figure 5.4.2-6 and Figure 5.4.2-7. On average, the vertical component of the array had an error of 6.5 m and was therefore deemed to be reliably calculating accurate positions.

Detection time differences (DTD) between the horizontal receiver pairings are shown in Figure 5.4.2-8. The absolute value of the DTD for the sync tag transmissions between receivers H1 and H2 was 11.91 ms (18.3 m corrected to distance), was 12.52 ms (19.2 m) between receivers H2 and H3 and was 12.9 ms (19.8 m) between receivers H1 and H3 (Figure 5.4.2-8). Three of the nine transmitters produced DTD values outside of the sync tag DTD range for the H1 / H2 receiver pairing, five of nine transmitters produced DTD values outside this range for the H2 / H3 receiver pairing, and four of nine transmitters produced DTD values outside this range for the H1 / H3 receiver pairing. These occurred over the first four drifts and accounted for 9.1% of all calculations within the horizontal component during the whole trial. Based on this, and a visual inspection of the trends in the DTD plot, transmitter positions and DTD error were not calculated as the values would be unreliable.

Mean water temperature at the study location, measured by TDRs along the transmitter line and receivers in the array, increased slightly from 25 C near the surface to a peak of 25.56 C at 53 m, and then decreased steadily to 19.1 C at 310 m (Figure 5.4.2-9).

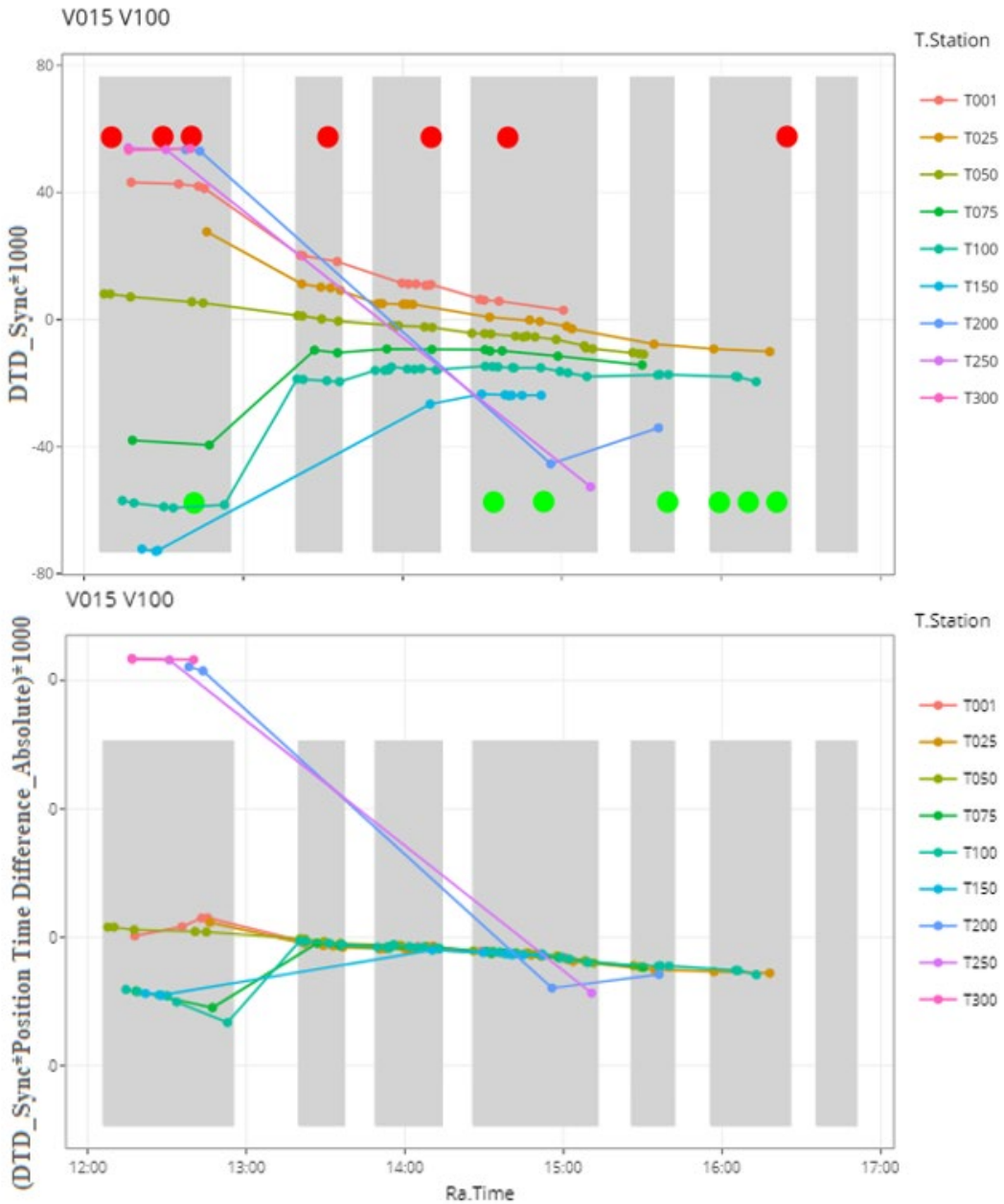


Figure 5.4.2-6. The top panel shows detection time difference (in milliseconds) of transmissions between receiver pairs at 15 m and 100 m in the vertical array over the course of the entire drift test (time across the y axis). The shaded grey bars represent the times the drift tests were occurring (white spaces between grey bars represent time between trials spent resetting the line for another drift). The large green and red dots are the DTD derived from sync tags built into the receivers and correlate to the distance between those receivers, therefore representing the possible bounds of DTD of a transmission travelling an uninterrupted straight path. T.Station

(T001 – T300) represents the different depths of transmitters during the drift test. The bottom panel shows the DTD error based on known GPS locations of the transmitters, where 1.534 ms equates to 1 m of error.

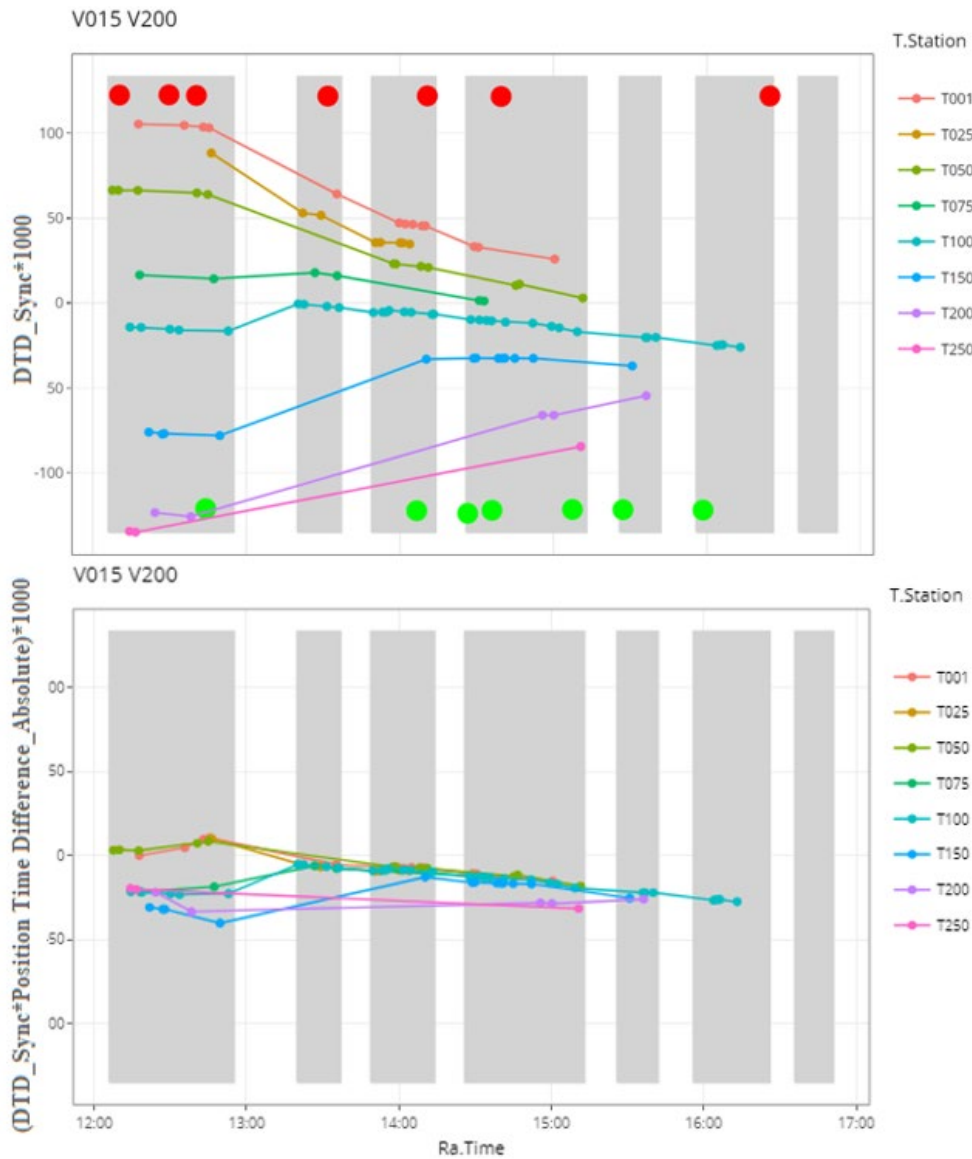


Figure 5.4.2-7. The top panel shows detection time difference (in milliseconds) of transmissions between receiver pairs at 15 m and 200 m in the vertical array over the course of the entire drift test (time across the y axis). The large green and red dots are the DTD derived from sync tags built into the receivers and correlate to the distance between those receivers, therefore

representing the possible bounds of DTD of a transmission travelling an uninterrupted straight path. T.Station (T001 – T300) represents the different depths of transmitters during the drift test, and the shaded grey bars represent the times the drift tests were occurring (white spaces between grey bars represent time between trials spent resetting the line for another drift). The bottom panel shows the DTD error based on known GPS locations of the transmitters, where 1.534 ms equates to 1 m of error.

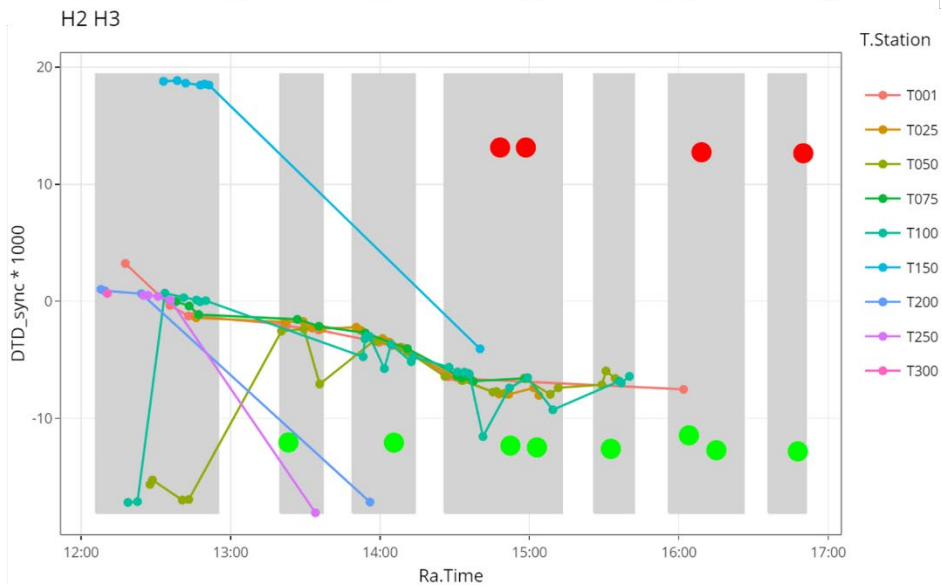
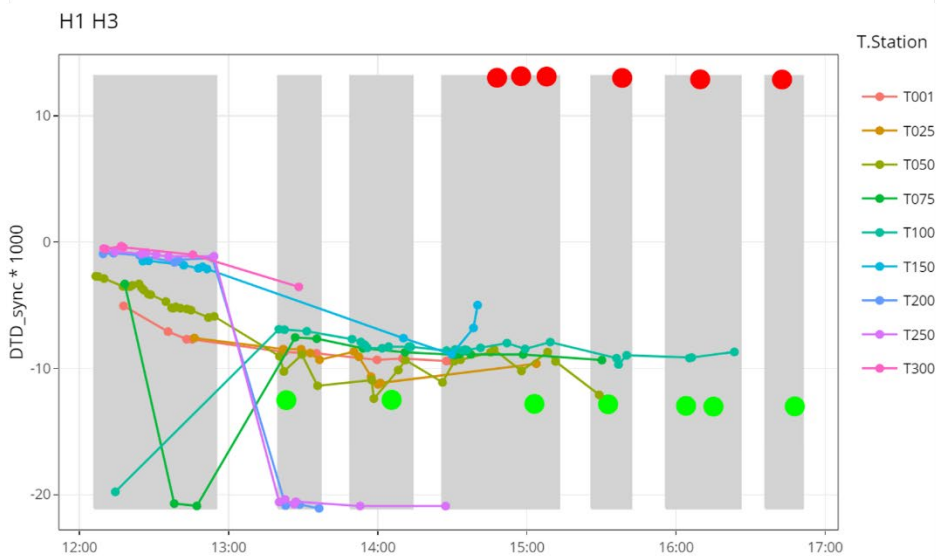
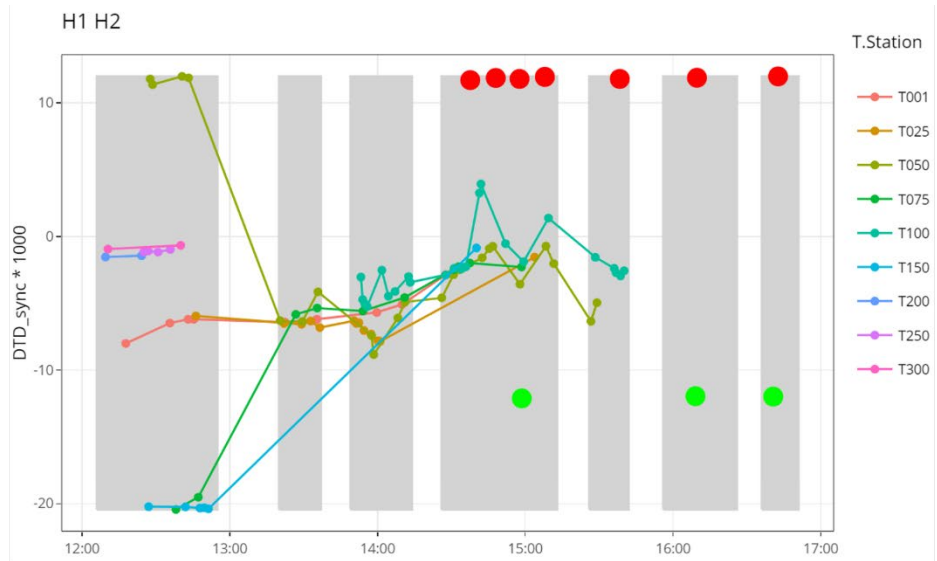


Figure 5.4.2-8. Detection time difference (in milliseconds) of a transmission between receivers H1, H2, and H3 on a horizontal plane roughly 15 m apart at 10 m depth. The large green and red dots are the DTD derived from sync tags built into the receivers and correlate to the distance between those receivers, therefore representing the possible bounds of DTD of a transmission travelling an uninterrupted straight path. T.Station (T001 – T300) represent the different depths of transmitters during the drift test, and the shaded portions of the figure represent the times the drift tests were occurring (white space between grey bars represents time between trials spent resetting the line for another drift).

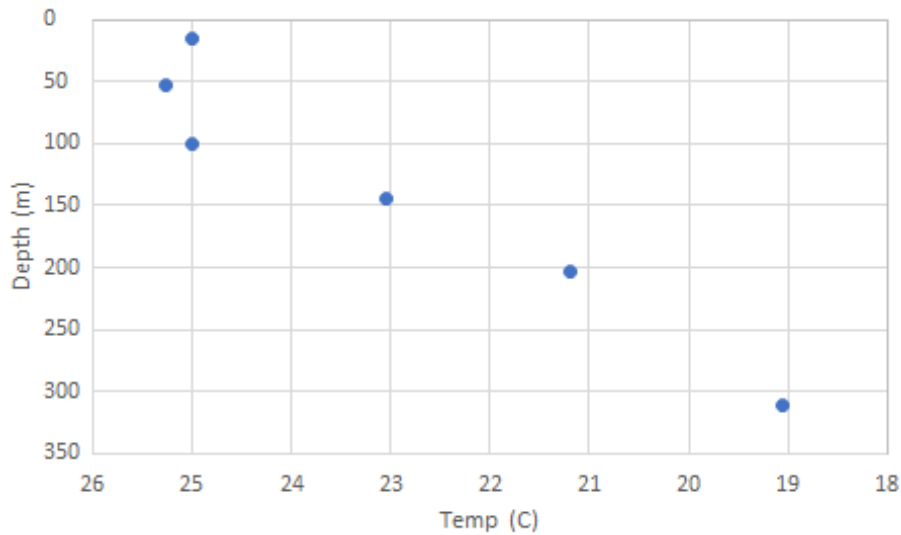


Figure 5.4.2-9. Mean water temperature through the water column at the study site measured by TDR and VR2Tx receivers during the drift tests.

### 5.4.3 Barracuda positioning

Based on the relatively low error margins around drift test-based position calculations derived from the vertical component of the array, positions of the tagged barracuda were assumed reliable with a potential  $\pm 6.5$  m average error applied to each position. Figure 5.4.3-10 shows a 40-minute-long window of detections around the array. Over the seven days of data collection, the fish's mean depth was 9.3 m (the FAD depth is 10 m) and mean distance away was 27.8 m. It made 25 excursions out of the array that lasted between one and two hours, 9

excursions of more than 2 hours, and the longest time out of the array was 10.5 hours, indicating a high degree of association with the FAD.

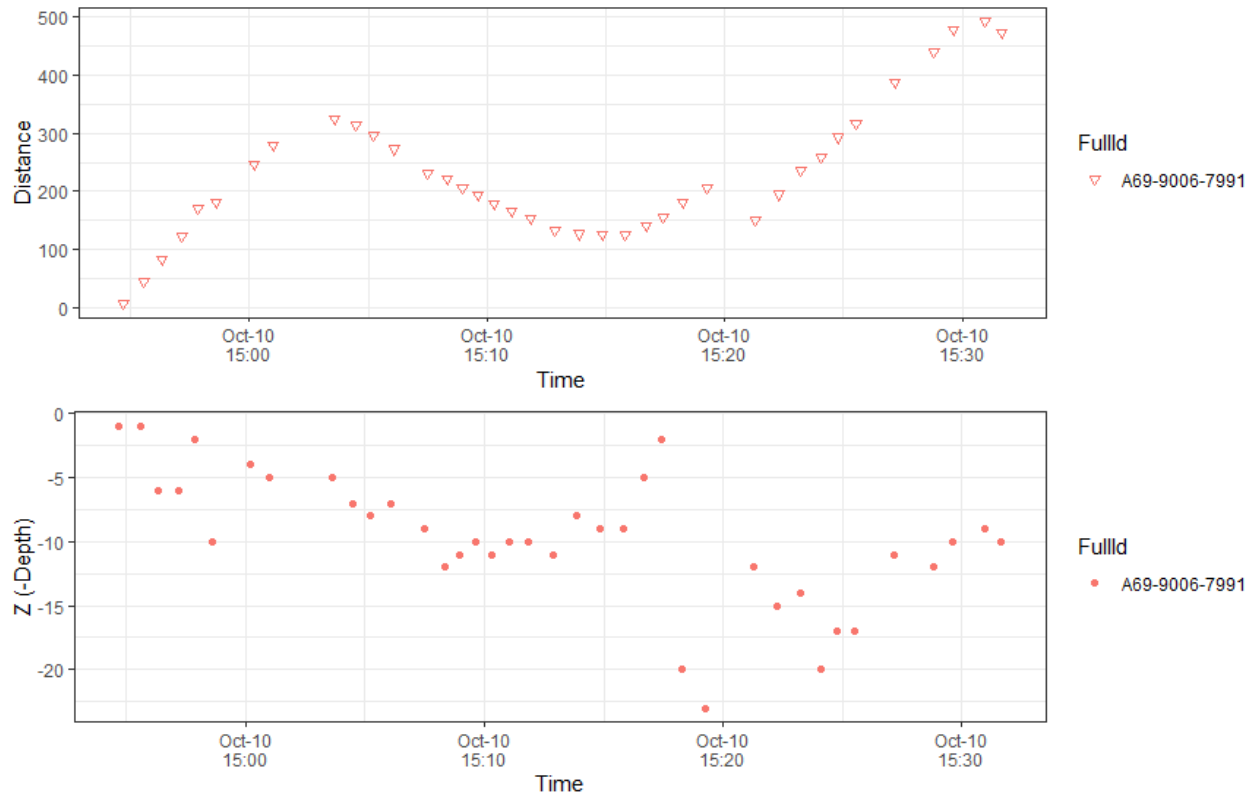


Figure 5.4.3-10. Calculated distance in meters from the array (top panel) and depth (bottom panel) of a tagged great barracuda (transmitter ID: A69-9006-7991) derived from the moored FAD-based vertical component of the array.

## 5.5 Discussion

The results from the drift tests show the potential for positioning data to be generated in open water using this VAR, however technical challenges associated with the unique receiver spacing and the habitat still remain and currently prevent certain positions from being calculated. The detectability analysis gives useful insight into the effectiveness of certain receiver-transmitter depth combinations at transmitting and receiving data, and this can inform study design in the future. Additionally, the versatility of the array components will facilitate the

investigation of animal movement around a range of types of structure that have been previously difficult to design for, eventually providing two more position metrics (distance and bearing) than have been previously possible (building on current methods which can generate residence and depth data; Forget et al., 2020).

Detection of transmissions during the drift tests was highest for shallow receiver (0 – 15 m) and shallow transmitter (0 – 100 m) combinations at 13.7% and for deep receiver (200 m) and deep transmitter (100 – 300 m) combinations at 18.7%. As these rates drop off considerably for shallow-deep combinations, this indicates a barrier between 100 m and 150 m that is impeding signal transmission. This barrier is likely due to the observed thermocline (Figure 5.4.2-9) over which water temperature drops nearly 4 C in 100 m after having stayed relatively constant at 25 C for the first 100 m. A recent study on detection efficiency in a temperate, thermally stratified lake using the same Vemco V9 transmitters as in this study showed that both detection efficiency and detection range are reduced when signals must pass through a thermocline (Kuai et al., 2021). Alternatively, transmissions produced and received beneath a thermocline can actually result in increased detection efficiency as the stratification may buffer the system from surface noise (O'Brien & Secor, 2021). As a number of epipelagic fishes that could be of research interest frequently dive into and through thermoclines to feed in the deep scattering layer (e.g.s., Braun et al., 2019; Chiang et al., 2021; Yang et al., 2019), it will be important to understand receiver placement in relation to the depth profiles of study animals to maximize detection efficiency.

Detection time difference (DTD) values that fell outside of those calculated from the internal sync tags and are therefore unreliable occurred on 5.6% of calculations between receivers in the vertical component of the array, and on 9.1% of calculations between receivers in the horizontal component of the array. These were likely due to a multipath signal, where the signal reflects off the sea surface or another boundary and arrives at the receiver later than expected, as it did not travel in a straight line (Vergeynst et al., 2020). Some multipath signals are to be expected, and these distorted signals may occur up to 5% of the time without substantially affecting the performance of one position-calculating algorithm (Vergeynst et al., 2020). However, higher occurrence can lead to unreliable position calculations and was part of the reason DTD error was not calculated for the horizontal component of the array. There are

two likely related factors that can explain the high multipath error during these trials. First, the receivers in the horizontal component were spaced 15 m apart from each other, a relatively short distance compared to standard convention of 50 – 150 m when using the Vemco Positioning System (VPS; e.g.s., Swadling, et al., 2020; Novak et al., 2020; Guzzo et al., 2018). The horizontal receiver spacing was bound by the technical challenge of creating this component of the array: a horizontally spread frame robust enough to withstand receiver weight while being light weight, portable, easy to deploy from a small boat and suspended from a single float. Further spacing was unfeasible, presenting a potential tradeoff between transmitter range and positioning error that should be evaluated carefully when designing investigations using this array. Another possible contributing factor was the receiver proximity to the sea surface, as this provides a highly reflective surface off which transmissions can bounce (Trevorrow, 1998). This factor alone would not likely cause these multipath issues, as evidenced by acceptable levels of multipath error between receiver pairings in the vertical component (that were separated by 88 – 100 m) in addition to many other studies that had receivers within similar proximity to the surface (Guzzo et al., 2018). However, the combination of receiver spacing and proximity to a reflective surface will not currently allow for accurate position calculations to occur for the horizontal component of the array.

Tracking the fine-scale movements of animals in the open-ocean continues to be challenging, however progress is being made in our ability to investigate more detailed behaviors, specifically as it pertains to animal association with structure. This array is highly prone to multipath detections that currently limit valid position calculations from being performed with the horizontal component. While the vertical component has generated acceptable DTD data resulting in a biologically plausible barracuda swimming track, the horizontal component still faces challenges that prevent accurate bearing calculations. With receiver and software improvements targeted at interpreting multipath signals more efficiently, a full array capable of calculating three-dimensional position of a transmitter in open water holds great promise for increasing our understanding of pelagic fish behavior around structure.

## 6 General Discussion

### 6.1 Ecological Insights

While the pelagic zone is by definition open water away from the shore or seafloor, structure is fairly common and extremely important in the ecology of this seemingly featureless habitat. Artificial structures in particular have become widely used tools in a range of fisheries, from commercial purse seiners targeting tunas (Miyake et al., 2010) to trolling recreational sport fishers (Merten et al., 2018). A number of likely interacting hypotheses have been presented and tested to explain the mechanisms behind fish attraction and aggregation to structure (Girard et al., 2004), but we still do not have a full picture of what drives this phenomenon and how it varies between taxonomic groups. Through the course of study on these subsurface FADs in an oligotrophic subtropical habitat, we have revealed several interesting new patterns that will help to build an understanding of the role structure plays in the ecology of pelagic species.

First, by analyzing diversity and abundance metrics, we have shown that FADs colonize over the course of a few weeks. Similar work using echosounder buoys has shown that drifting FADs also colonize in the same short timeframes (Orue et al., 2019), but that study mainly focused on commercially targeted tuna species and grouped everything else, thus lacking resolution at a species level. We have provided a finer time series for the arrival of other species that may be less important to fisheries but equally important in establishing baselines of abundance and diversity. Additionally, we have also shown that seasonality can play a strong role in the composition of a FAD assemblage. We found that many of the extraneant jack (*Carangidae*) species were more abundant in the warmer months, and unicorn filefish (*Aluterus monoceros*) and the sportfish mahi (*Coryphaena hippurus*) and wahoo (*Acanthocybium solandri*) were all more abundant in the colder months. The seasonality seen here in these migratory sportfish was expected and has been confirmed with conventional and satellite tag data showing they leave the region as temperatures increase (e.g., Merten et al., 2016), however the seasonal variation in abundance shown by filefish and jacks is less likely related to long-distance migration. Small almaco jacks (*Seriola rivoliana*) were most abundant in the summer months in our study, and a closely related congener found in the southern hemisphere has also been shown to be more abundant around moored FADs in warmer months (Dempster, 2005). However, there has yet to be research into why it is typically only small juvenile and sub-adult carangids that

associate with pelagic FADs. The most likely explanation for the seasonality is that annual waves of reproduction lead to times of abundant FAD-associating juveniles. However, the reasons as to why only this life stage aggregates around these FADs are still unknown. The most likely scenario may be that juveniles smaller than 10 cm (the low end of the size range seen in our study) are less capable of maintaining position in the water column against a current at a moored FAD, or that the predation risk is too great. *Sargassum* is a more complex drifting habitat and may provide the best refuge for post-larval jacks. When they reach a certain size, they appear to aggregate around FADs before moving to a more reef-associated coastal life as they mature. Unicorn filefish are another interesting example, as they are not known to undergo large horizontal migrations, but still show distinct seasonality, being more abundant in the winter months. Due to their body morphology and inability to maintain association with a FAD in strong currents (Dempster, 2005), it is more likely they that simply move deeper into cool water during the summer months and are therefore less likely to interact with or be surveyed at a FAD near the surface. More investigation into these two species will likely help us understand the nuances of the mechanisms behind attraction and aggregation around FADs and should be pursued in the future.

We have also provided evidence, albeit statistically weak given a low number of experimental units, that invertebrate micronekton aggregates around a moored FAD, which has not previously been shown for this group. This is interesting from the point of view of these prey species, but also of their predators, the fish that are commonly studied around FADs. For example, many invertebrates show aggregation behavior for an array of social (e.g., mating; Ritz, 1994) and feeding / protection reasons (e.g., Nowacek et al., 2011; Abe et al., 2013), but this behavior has not been documented around FADs. These pelagic invertebrates apparently perceive some benefit from close proximity to a fixed structure, and it is possible that the scent of the flora and fauna growing on the structure (biofouling) may act as an attractant. Lab studies on attraction to these chemical cues, or further investigation into potential prey items living on the FAD surface, could shed light on this new result.

These findings also make the need for dual-approach studies very clear. For example, a stomach content analysis of fish sampled close to and far away from the FAD could start to reveal connections between the presence of certain fish at a FAD and their behavior while there

(i.e., if they are there to feed on the FAD-associated invertebrates). And while our echosounder surveys yielded data that have been difficult to interpret and show a weak to no effect of distance from the FAD on biomass, we have shown the importance of a multi-method approach to answering ecological questions. Linking specific fish behaviors such as feeding to FAD residence can help us understand the mechanisms behind aggregation behavior, but also can further our understanding of whether ecological trap effects occur in different species and areas. Future investigations into these ideas should aim to ensure strong replication, a limitation in our study that used only two FADs, to understand the strength of these potential factors.

Questions still remain on why subsurface FADs appear to attract a different assemblage than surface FADs (Friedlander et al., 1994), but this provides an interesting direction forward to experimentally understanding the sensory biology of pelagic fishes. For example, multiple sources (the present study; Friedlander et al., 1994; and anecdotal evidence from the region) all seem to point to the fact that billfish are only attracted to or aggregate around surface FADs. The exact reasons are unknown, but this could be experimentally tested by deploying surface and subsurface FADs of similar design and structure into areas where billfish are known to exist. By measuring factors such as ambient noise created by the structure (which has been observed to be extremely low at our subsurface FADs) or the community of baitfish present (also observed that some species like flying fish are very locally abundant but were never seen on the 10 m deep FAD video surveys), we can fill knowledge gaps regarding how fish sense and interact with these structures. From there, there may be currently unforeseen applications that could help inform the management of FAD fisheries, such as designing FADs with or without certain attributes to decrease the probability of attracting non-target species. For example, if we find that the increased noise associated with surface FADs (compared to subsurface ones) attracts billfish, designing quieter, slightly subsurface drifting FADs may help to reduce billfish bycatch in net fisheries. In a current example, a large number of juvenile silky sharks are bycaught or entangled in Indian Ocean FADs (Filmlalter et al., 2013). Research is being conducted on biodegradable FADs to reduce environmental impacts such as entanglement and marine pollution, so we should be taking the same approach to understanding FAD design from a fish attraction perspective as well. The new telemetry array presented here will be an important tool in tracking fish behavior around experimental FADs to answer these types of questions.

## 6.2 Methodological Insights

The recent interest in outfitting FADs for data collection, or simply making use of the vast amount of data collected by fishing fleets from echosounder buoys and logbooks, has proven the need for FAD science to keep pace with the fisheries that use them. However, as with any field, it is important to understand the potential bias that comes with using fisheries-dependent data and be able to work around it when necessary. It is obviously important to work alongside these fisheries, but there are certain questions that may need separate approaches to answer. For example, there are many species that do not interact with pelagic fisheries but could be important indicators of ecosystem change. And to fully capture the breadth of species and behaviors that occur around natural and artificial structures in the open ocean, we have shown that purpose-build FADs are useful tools to facilitate conservation research. For one, it is possible to largely preclude fishing activity by using subsurface FADs, thus avoiding the removal of study species or any influences on natural behavior. It is possible that an array of subsurface FADs monitored continuously could provide additional information useful in stock assessments. However, this assumes that FAD assemblages represent a standardized measure of local fish abundance and diversity, which they may not always do as they have been shown to be species selective in some cases (Friedlander et al., 1994). Additionally, more work is needed to understand interannual site fidelity of migratory fishes with FADs, which will increase our ability to estimate abundances from long term FAD-based surveys.

Our camera surveys have also provided information that will enable the development of better study design based on specific research objectives. For example, showing seasonality of certain groups at the FADs is important to avoid surveying in certain times of the year where abundance would be expected to be low, which could lead to inaccurate conclusions on presence or abundance of certain species. Furthermore, the insights into survey methods are also important as we have shown that even a very short visual survey results in much higher abundance estimates than longer video surveys, whereas video surveys may document certain species more effectively like sharks that may be more cryptic or wary of boat noise (and circumnavigating species in general that might be frequently out of sight but still associated with the FAD). The use of 360-degree camera rigs would have eliminated some sampling bias from our study and can be

used in the future to obtain better estimations of fish abundance and diversity. Abundance can be challenging to quantify using a single camera with a limited field of view, and diversity estimates may be affected by behavioral differences between species (bold or shy behavior when approaching a novel object like a camera). This information can lead to more effective survey data that is useful in monitoring pelagic biodiversity and fish stocks.

Finally, the subsurface FAD design proposed here could also be useful for some research initiatives. The taut mooring line of our FADs fortuitously inspired the design of the vertical acoustic telemetry array and enabled its development. A vertical gear deployment is also possible through a suspended line off a drifting FAD, however, the stationary nature enabled easier access for trials longer than a few hours. If we successfully develop this array as intended, this tracking system will enable a huge leap forward in available data on structure-associated species and other investigations in blue-water animals in general, not just around FADs. We have already added one additional metric, distance away, which is arguably the most important to understand the association pattern of an animal. Previously, only presence absence-based residence information was available which limits the scope of understanding an animal's association (Filmlalter et al., 2015; Tolotti et al., 2020). Improving upon this could have implications for bycatch reduction in net fisheries, for example through targeting sets at a time when bycatch species are further away, and target species are closer. Additionally, understanding animal interactions with offshore aquaculture infrastructure, where proximity may matter in terms of disease transmission or attempted depredation, can be further explored. We aim to continue to develop the array such that bearing is also reliably calculated, which will open the door to understanding interactions between species and individuals concurrently present at a FAD. It is interesting from an ecological perspective if, for example, individuals within a species segregate based on size, which could help us determine the role the FAD plays in their social behavior. More thorough investigation into angle of approach to a FAD can also occur, which could help us understand mechanisms behind attraction. For example, if animals do not consistently arrive from the downstream direction, that could provide evidence that something other than scent (of the sessile biofouling organisms) is being used to locate and move towards a FAD. Together, the advance in tracking techniques with insights into better-tailored survey methods will hopefully lead to a continued scrutinization of these powerful fishing tools and the effects they have on the fish they attract.

### **6.3 Conclusion**

A combination of the ecological insights and methodological developments presented here will enable the continued and more efficient study of pelagic biota and its interaction with many different types of structure. From monitoring biodiversity in the largest habitable biome on Earth, to improving fine-scale tracking of individuals in the open ocean, continued study of the role of structure in the pelagic ecosystem will play a role in ensuring the effective management and stewardship of these intricate yet substantial natural resources.

## 7 References

- Abe H, Komatsu T, Natheer A, Rothausler EA, Shishido H, Yoshizawa S, Ajisaka T. 2013. Invertebrate fauna associated with floating *Sargassum horneri* (Fucales: Sargassaceae) in the East China Sea. *Species Diversity*, 18: 75-85.
- Alerstam, T., A. Hedenstrom, S. Akesson. 2003. Long-distance migration: evolution and determinants. *Oikos*, 103:247-260.
- Alevizon WS, Gorham JC, Richardson R, McCarthy SA. 1985. Use of man-made reefs to concentrate snapper (Lutjanidae) and grunts (Haemulidae) in Bahamian waters. *Bulletin of Marine Science*, 37(1): 3-10.
- Amei K, Dobashi R, Jimi N, Kitamura M, Yamaguchi A. 2021. Vertical changes in abundance, biomass and community structure of pelagic polychaetes down to 1000 m depths at Station K2 in the western subarctic Pacific Ocean covering the four seasons and day-night. *Journal of Plankton Research*, 43(3): 442-457.
- Angel MV. 1993. Biodiversity of the pelagic ocean. *Conservation Biology*, 7(4):760-772.
- Aspillaga E, Arlinghaus R, Martorell-Barceló M, Follana-Berná G, Lana A, Campos-Candela A, Alós J. 2021. Performance of a novel system for high-resolution tracking of marine fish societies. *Animal Biotelemetry*, 9(1): 1-14.
- Ballon M, Bertrand A, Lebourges-Dhaussy A, Gutierrez M, Ayon P, Grados D, Gerlotto F. 2011. Is there enough zooplankton to feed forage fish populations off Peru? An acoustic (positive) answer. *Progress in Oceanography*, 91: 360-381.
- Baske A, Gibbon J, Benn J, Nickson A. 2012. Estimating the use of drifting fish aggregation devices (FADs) around the globe. *Pew Environmental Group Discussion Paper*.
- Bates D, Machler M, Bolker B, Walker S. 2015. Fitting linear mixed-effects models using lme4. *Journal of Statistical Software*, 67(1): 1-48.
- Baum JK, Myers RA. 2004. Shifting baselines and the decline of pelagic sharks in the Gulf of Mexico. *Ecology Letters*, 7: 135-145.

- Baum JK, Myers RA, Kelhler DG, Worm B, Harley SJ, Doherty PA. 2003. Collapse and conservation of shark populations in the northwest Atlantic. *Science*, 299: 389-392.
- Bell JD, Albert J, Andrefouet S, Andrew NL, Blanc M, Bright P, Brogan D, Campbell B, Govan H, Hampton J, Hanich Q, Harley S, Jorari A, Lincoln Smith M, Pontifex S, Sharp MK, Sokimi W, Webb A. 2015. Optimising the use of near shore fish aggregating devices for food security in the Pacific Islands. *Marine Policy*, 56: 98-105.
- Benoit-Bird KJ, Lawson GL. 2016. Ecological insights from pelagic habitats acquired using active acoustic techniques. *Annual Review of Marine Science*, 8: 463-490.
- Benoit-Bird KJ, Au WWL, Wisdom DW. 2009. Nocturnal light and lunar cycle effects on diel migration of micronekton. *Limnology and Oceanography*, 54(5): 1789-1800.
- Benoit-Bird KJ, Au WWL. 2001. Target strength measurements of Hawaiian mesopelagic boundary community animals. *Journal of the Acoustic Society of America*, 110(2): 812-819.
- Block BA, Costa DP, Boehlert GW, Kochevar RE. 2003. Revealing pelagic habitat use: the tagging of Pacific pelagics program. *Oceanologica Acta*, 25: 255-266.
- Bradley D, Merrifield M, Miller KM, Lomonico S, Wilson JR, Gleason MG. 2019. Opportunities to improve fisheries management through innovative technology and advanced data systems. *Fish and Fisheries*, 20(3): 564-583.
- Braun CD, Gaube P, Sinclair-Taylor TH, Skomal GB, Thorrold SR. (2019). Mesoscale eddies release pelagic sharks from thermal constraints to foraging in the ocean twilight zone. *Proceedings of the National Academy of Science*, 116(35): 17187-17192.
- Brehmer P, Sancho G, Trygonis V, Itano D, Dalen J, Fuchs A, Faraj A, Taquet M. 2019. Towards an autonomous pelagic observatory: experiences from monitoring fish communities around drifting FADs. *Thalassas: An International Journal of Marine Sciences*, 35: 177-189.
- Brock RE. 1985. Preliminary study of the feeding habits of the pelagic fish around Hawaiian fish aggregation devices or can fish aggregation devices enhance local fisheries productivity? *Bulletin of Marine Science*, 37(1): 40-49.

- Brooks EJ, Brooks AML, Williams S, Jordan LKB, Abercrombie D, Chapman DD, Howey-Jordan LA, Grubbs RD. 2015. First description of deep-water elasmobranch assemblages in the Exuma Sound, The Bahamas. *Deep-Sea Research II*, 115: 81-91.
- Buckley TW, Miller BS. 1994. Feeding habits of yellowfin tuna associated with fish aggregation devices in American Samoa. *Bulletin of Marine Science*, 55(2-3): 445-459.
- Burgess GH, Beerkircher LR, Cailliet GM, Carlson JK, Cortés E, Goldman KJ, ... Simpfendorfer CA. 2005. Is the collapse of shark populations in the Northwest Atlantic Ocean and Gulf of Mexico real? *Fisheries*, 30(10): 19-26.
- Campbell MD, Salisbury J, Caillouet R, Driggers WB, Kilfoil J. 2018. Camera field-of-view and fish abundance estimation: A comparison of individual-based model output and empirical data. *Journal of Experimental Marine Biology and Ecology*, 501: 46-53.
- Casazza TL, Ross SW. 2008. Fishes associated with pelagic *Sargassum* and open water lacking *Sargassum* in the Gulf Stream off North Carolina. *Fisheries Bulletin*, 106: 348-363.
- Castro JJ, Santiago JA, Santana-Ortega AT. 2002. A general theory on fish aggregation to floating objects: an alternative to the meeting point hypothesis. *Reviews in Fish Biology and Fisheries*, 1: 255-277.
- Castro JJ, Santiago JA, Hernandez-Garcia V. 1999. Fish associated with fish aggregation devices off the Canary Islands (central-east Atlantic). *Scientia Marina*, 63(3-4):191-198.
- Cayré P. 1990. Behaviour of yellowfin tuna (*Thunnus albacares*) and skipjack tuna (*Katsuwonus pelamis*) around fish aggregating devices (FADs) in the Comoros Islands as determined by ultrasonic tagging. *Aquatic Living Resources*, 4: 1-12.
- Chapman L, Pasisi B, Bertram I, Beverly S, Sokimi W. 2005. Manual on fish aggregating devices (FADs): lower-cost moorings and programme management. Secretariat of the Pacific Community.
- Chapuis L, Collin SP, Yopak KE, McCauley RD, Kempster RM, Ryan LA, Schmidt C, Kerr CC, Gennari E, Egeberg CA, Hart NS. 2019. The effect of underwater sounds on shark behaviour. *Scientific Reports*, 9:6924.

- Chiang WC, Matsumoto T, Lin S-J, Chang Q-X, Musyl MK, Ho Y-S, Ohta F. 2021. Fine-scale vertical movements and behavior of immature skipjack tuna (*Katsuwonus pelamis*) off eastern Taiwan. *Journal of Marine Science and Technology*, 29(2): 207-219.
- Chouvelon T, Strady E, Harmelin-Vivien M, Radakovitch O, Brach-Papa C, Crochet S, Knoery J, Rozuel E, Thomas B, Tronczynski J, Chiffolleau J-F. 2019. Patterns of trace metal bioaccumulation and trophic transfer in a phytoplankton-zooplankton-small pelagic fish marine food web. *Marine Pollution Bulletin*, 146: 1013-1030.
- Claisse JT, Pondella DJ, Love M, Zahn LA, Williams CM, Williams JP, Bull AS. 2014. Oil platforms off California are among the most productive marine fish habitats globally. *Proceedings of the National Academy of Science*, 111(43): 15462-15467.
- Claisse JT, Clark TB, Schumacher BD, McTee SA, Bushnell ME, Callan CK, Laidley CW, Parrish JD. 2011. Conventional tagging and acoustic telemetry of a small surgeonfish, *Zebrasoma flavescens*, in a structurally complex coral reef environment. *Environmental Biology of Fishes*, 91(2): 185-201.
- Clark E, Kristof E. 1990. Deep-sea elasmobranchs observed from submersibles off Bermuda, Grand Cayman, and Freeport, Bahamas. NOAA Tech. Report NMFS 90: 269-284.
- Cole HP, Bryan GM, Gordon AL. 1970. The deep scattering layer: patterns across the Gulf Stream and the Sargasso Sea. *Proceedings of an international symposium on biological sound scattering in the ocean*. Maury Center for Ocean Science, Washington, DC, pg. 281-293.
- Cushion NE, Sullivan-Sealey K. 2008. Landings, effort and socio-economics of a small scale commercial fishery in The Bahamas. *Proceedings of the 60<sup>th</sup> Gulf and Caribbean Fisheries Institute*, Punta Cana, Dominican Republic, 162-166.
- Dagorn L, Holland KN, Filmalter J. 2010. Are drifting FADs essential for testing the ecological trap hypothesis? *Fisheries Research*, 106: 60-63.
- Dagorn L, Pincock D, Girard C, Holland K, Taquet M, Sancho G, Itano D, Aumeeruddy R. 2007. Satellite-linked acoustic receivers to observe behavior of fish in remote areas. *Aquatic Living Resources*, 20: 307-312.

- Dagorn L, Holland K, Puente E, Taquet M, Ramos A, Brault P, ... Josse E. 2006. FADIO (Fish Aggregating Devices as Instrumented Observatories of pelagic ecosystems): a European Union funded project on development of new observational instruments and the behavior of fish around drifting FADs. Western and Central Pacific Fisheries Commission, Scientific Committee Second Regular Session.
- Dagorn L, Bach P, Josse E. 2000. Movement patterns of large bigeye tuna (*Thunnus obesus*) in the open ocean, determined using ultrasonic telemetry. *Marine Biology*, 136(2): 361-371.
- Davies TK, Mees CC, Milner-Gulland EJ. 2014. The past, present and future use of drifting fish aggregating devices (FADs) in the Indian Ocean. *Marine Policy*, 45: 163-70.
- De Oliveira MR, Nobrega MF, Oliveira JEL, Chellappe S. 2017. Reproductive biology of blue runner, *Caranx crysos* (Mitchell, 1815) from the coastal waters of Rio Grande do Norte, Brazil (Southwest Atlantic Ocean). *Journal of Aquaculture and Marine Biology*, 5(5): 00136.
- De Robertis A, Higginbottom I. 2007. A post-processing technique to estimate the signal-to-noise ratio and remove echosounder background noise. *ICES Journal of Marine Science*, 64(6): 1282-1291.
- Dempster T. 2005. Temporal variability of pelagic fish assemblages around fish aggregating devices: biological and physical influences. *Journal of Fish Biology*, 66(5): 1237-1260.
- Dempster T, Kingsford MJ. 2003. Homing of pelagic fish to fish aggregation devices (FADs): the role of sensory cues. *Marine Ecology Progress Series*, 258: 213-222.
- Deudero S, Merella P, Morales-Nin B, Massuti E, Alemany F. 1999. Fish communities associated with FADs. *Scientia Marina*, 63(3-4): 199-207.
- Doray M, Josse E, Gervain P, Reynal L, Chantrel J. 2007. Joint use of echosounding, fishing, and video techniques to assess the structure of fish aggregations around moored fish aggregating devices in Martinique (Lesser Antilles). *Aquatic Living Resources*, 20: 357-366.
- Dulvy NK, Pacoureaux N, Rigby CL, Pollom RA, Jabado RW, Ebert DA, Finucci B, Pollock CM, Cheek J, Derrick DH, Herman KB, Sherman CS, VanderWright WJ, Lawson JM, Walls RHL, Carlson JK, Charvet P, Bineesh KK, Fernando D, Ralph GM, Matsushiba JH, Hilton-

- Taylor C, Fordham SJ, Simpfendorfer CA. 2021. Overfishing drives over one-third of all sharks and rays toward a global extinction crisis. *Current Biology*, 31(21): 4773-4787.
- Dulvy NK, Baum JK, Clarke S, Compagno LJV, Cortés E, Domingo A, Fordham S, Fowler S, Francis MP, Gibson C, Martínez J, Musick JA, Soldo A, Stevens JD, Valenti S. 2008. You can swim but you 'an't hide: the global status and conservation of oceanic pelagic sharks and rays. *Aquatic Conservation: Marine and Freshwater Ecosystems*, 18(5): 459-482.
- Ellis DM, DeMartini EE. 1995. Evaluation of a video camera technique for indexing abundances of juvenile pink snapper, *Pristipomoides filamentosus*, and other Hawaiian insular shelf fishes. *Fisheries Bulletin*, 93: 67-77.
- Escalle L, Gaertner D, Chavance P, Murua H, Simier M, Pascual-Alayon PJ, Menard F, Ruiz J, Abascal F, Merigot B. 2019. Catch and bycatch captured by tropical tuna purse-seine fishery in whale and whale shark associated sets: comparison with free school and FAD sets. *Biodiversity and Conservation*, 28: 467-499.
- FAO. 2022. The state of world fisheries and aquaculture 2022. Towards Blue Transformation. Rome, FAO.
- FAO 2018. The state of world fisheries and aquaculture 2018- meeting the sustainable development goals, Rome. License: CC BY-NC-SA 3.0 IGO.
- Filmalter JD, Cowley PD, Potier M, Menard F, Smale MJ, Cherel Y, Dagorn L. 2016. Feeding ecology of silky sharks *Carcharhinus falciformis* associated with floating objects in the western Indian Ocean. *Journal of Fish Biology*, 90(4): 1321-1337.
- Filmalter J, Cowley P, Forget F, Dagorn L. 2015. Fine-scale 3-dimensional movement behaviour of silky sharks *Carcharhinus falciformis* associated with fish aggregating devices (FADs). *Marine Ecology Progress Series*, 539: 207-223.
- Filmalter JD, Capello M, Deneubourg J-L, Cowley PD, Dagorn L. 2013. Looking behind the curtain: quantifying massive shark mortality in fish aggregating devices. *Frontiers in Ecology and the Environment*, 11(6): 291-296.

- Filmalter JD, Dagorn L, Cowley PD, Taquet M. 2011. First descriptions of the behavior of silky sharks, *Carcharhinus falciformis*, around drifting fish aggregating devices in the Indian Ocean. *Bulletin of Marine Science*, 87(3): 325-337.
- Forget F, Cowley PD, Capello M, Filmalter JD, Dagorn L. 2020. Drifting along in the open-ocean: The associative behaviour of oceanic triggerfish and rainbow runner with floating objects. *Marine Environmental Research*, 161: 104994.
- Forget FG, Capello M, Filmalter JD, Govinden R, Soria M, Cowley PD, Dagorn L. 2015. Behaviour and vulnerability of target and non-target species at drifting fish aggregating devices (FADs) in the tropical tuna purse seine fishery determined by acoustic telemetry. *Canadian Journal of Fisheries and Aquatic Sciences*, 72(9): 1398-1405.
- Fraiji-Fernandez N, Bouquieaux M-C, Rey A, Mendibil I, Cotano U, Irigoien X, Santos M, Rodriguez-Ezpeleta N. 2020. Marine water environmental DNA metabarcoding provides a comprehensive fish diversity assessment and reveals spatial patterns in a large oceanic area. *Ecology and Evolution*, 10: 7560-7584.
- Fraser HM, Greenstreet SPR, Piet GJ. 2007. Taking account of catchability in groundfish survey trawls: implications for estimating demersal fish biomass. *ICES Journal of Marine Science*, 64(9): 1800-1819.
- Friedlander A, Beets J, Tobias W. 1994. Effects of fish aggregating device design and location on fishing success in the U.S. Virgin Islands. *Bulletin of Marine Science*, 55(2-3): 592-601.
- Gaspar P, Georges JY, Fossette S, Lenoble A, Ferraroli S, Le Maho Y. 2006. Marine animal behaviour: neglecting ocean currents can lead us up the wrong track. *Proceedings of the Royal Society B: Biological Sciences*, 273(1602): 2697-2702.
- Gatti P, Fisher JAD, Cyr F, Galbraith PS, Robert D, Le Bris A. 2020. A review and tests of validation and sensitivity of geolocation models for marine fish tracking. *Fish and Fisheries*, 22: 1041-1066.
- Genin A. 2004. Bio-physical coupling in the formation of zooplankton and fish aggregations over abrupt topographies. *Journal of Marine Systems*, 50: 3-20.

- Gershman D, Nickson A, O'Toole M. 2015. Estimating the use of FADs around the world. Pew Environmental Group.
- Gervain P, Reynal L, Defoe J, Ishida M, Mohammed E. 2015. Manual of best practices in fisheries that use moored fish aggregating devices: FAD design, construction and deployment. CRFM Special Publication, 6(1): 1-55.
- Girard C, Benhamou S, Dagorn L. 2004. FAD: fish aggregating device or fish attracting device? A new analysis of yellowfin tuna movements around floating objects. *Animal Behaviour*, 67: 319-326.
- Glazer RA, Delgado GA, Kidney JA. 2003. Estimating queen conch (*Strombus gigas*) home ranges using acoustic telemetry: implications for the design of marine fishery reserves. *Gulf and Caribbean Research*, 14(2): 79-89.
- Gooding RM, Magnuson JJ. 1967. Ecological significance of a drifting object to pelagic fishes. *Pacific Science*, 21: 486-497.
- Goodwin JM IV, Johnson AG. 1986. Age, growth, and mortality of blue runner, *Caranx crysos*, from the Northern Gulf of Mexico. *Northeast Gulf Science*, 8:2.
- Gregory RS, Powles PM. 1985. Chronology, distribution, and sizes of larval fish sampled by light traps in macrophytic Chemung Lake. *Canadian Journal of Zoology*, 63(11).
- Grimmel HMV, Bullock RW, Dedman SL, Guttridge TL, Bond ME. 2020. Assessment of faunal communities and habitat use within a shallow water system using non-invasive BRUVs methodology. *Aquaculture and Fisheries*, 5(5): 224-233.
- Guzzo MM, Van Leeuwen TE, Hollins J, Koeck B, Newton M, Webber DM, Smith FI, Bailey DM, Killen SS. 2018. Field testing a novel high residence positioning system for monitoring the fine-scale movements of aquatic organisms. *Methods in ecology and evolution*, 9(6): 1478-1488.
- Hall M, Lennert-Cody C, Garcia M, Arenas P. 1992. Characteristics of floating objects and their attractiveness for tunas. In *Proceedings of the international workshop on the ecology and fisheries for tunas associated with floating objects* (pp. 396-446).

- Hallier J-P, Gaertner D. 2008. Drifting fish aggregation devices could act as an ecological trap for tropical tuna species. *Marine Ecology Progress Series*, 353: 255-264.
- Hampton J, Sibert JR, Kleiber P, Maunder MN, Harley SJ. 2005. Fisheries: Decline of Pacific tuna populations exaggerated? *Nature*, 434(7037): E1.
- Hastie T. 2022. GAM: Generalized Additive Models. R package version 1.20.2.  
<https://CRAN.R-project.org/package=gam>.
- Hays GC, Bailey H, Bograd SJ. 2019. Translating marine animal tracking data into conservation policy and management. *Trends in Ecology and Evolution*, 34(5): 459-473.
- Heagney EC, Lynch TP, Babcock RC, Suthers IM. 2007. Pelagic fish assemblages assessed using mid-water baited video: standardizing fish counts using bait plume size. *Marine Ecology Progress Series*, 350: 255-266.
- Hemery LG, Mackereth KF, Gunn CM, Pablo EB. 2022. Use of a 360-degree underwater camera to characterize artificial reef and fish aggregating effects around marine energy devices. *Journal of Marine Science and Engineering*, 10(555): 1-16.
- Hickford MJH, Schiel DR. 1999. Evaluation of the performance of light traps for sampling fish larvae in inshore temperate waters. *Marine Ecology Progress Series*, 186: 293-302.
- Higashi GR. 1994. Ten years of fish aggregating device (FAD) design development in Hawaii. *Bulletin of Marine Science*, 55(2-3): 651-666.
- Hussey NE, Kessel ST, Aarestrup K, Cooke SJ, Cowley PD, Fisk AT, Harcourt RG, Holland KN, Iverson SJ, Kocik JF, Flemming JEM, Whoriskey FG. 2015. Aquatic animal telemetry: a panoramic window into the underwater world. *Science*, 348(6240).
- Ignatyev SM. 1997. Pelagic fishes and their macroplankton prey: swimming speeds. *Proceedings, Forage Fishes in Marine Ecosystems*, 31-39.
- Itano D, Fukofuka S, Brogan D. 2004. The development, design and recent status of anchored and drifting FADs in the WCPO. Working Paper INF –FTWG-3, Standing Committee on Tuna and Billfish.

- Jaquemet S, Potier M, Menard F. 2011. Do drifting and anchored fish aggregating devices (FADs) similarly influence tuna feeding habits? A case study from the western Indian Ocean. *Fisheries Research*, 107: 283-290.
- Josse E, Bach P, Dagorn L. 1998. Simultaneous observations of tuna movements and their prey by sonic tracking and acoustic surveys. *Hydrobiologia*, 371: 61-69.
- Kilfoil JP, Wirsing AJ, Campbell MD, Kiszka JJ, Gastrich KR, Heithaus MR, Zhang Y, Bond ME. 2017. Baited remove underwater video surveys undercount sharks at high densities: insights from full-spherical camera technologies. *Marine Ecology Progress Series*, 585: 113-121.
- Kimura S, Nakata H, Okazaki Y. 2000. Biological production in meso-scale eddies caused by frontal disturbances of the Kuroshio Extension. *ICES Journal of Marine Science*, 57: 133-142.
- Kraus RT, Holbrook CM, Vandergoot CS, Stewart TR, Faust MD, Watkinson DA, Charles C, Pegg M, Enders EC, Krueger CC. 2018. Evaluation of acoustic telemetry grids for determining aquatic animal movement and survival. *Methods in Ecology and Evolution*, 9(6): 1489-1502.
- Kuai Y, Klinard NV, Fisk AT, Johnson TB, Halfyard EA, Webber DM, Smedbol SJ, Wells MG. 2021. Strong thermal stratification reduces detection efficiency and range of acoustic telemetry in a large freshwater lake. *Animal Biotelemetry*, 9(1): 1-13.
- Layman CA, Arrington DA, Langerhans RB, Silliman BR. 2004. Degree of fragmentation affects fish assemblage structure in Andros Island (Bahamas) estuaries. *Caribbean Journal of Science*, 40(2): 232-244.
- Lea JSE, Wetherbee BM, Queiroz N, Burnie N, Aming C, Sousa LL, Mucientes GR, Humphries NE, Harvey GM, Sims DW, Shivji MS. 2015. Repeated, long-distance migrations by a philopatric predator targeting highly contrasting ecosystems. *Scientific Reports*, 5: 11202.
- Letessier TB, Proud R, Meeuwig JJ, Cox MJ, Hosegood PJ, Brierly AS. 2022. Estimating pelagic fish biomass in a tropical seascape using echosounding and baited stereo-videography. *Ecosystems*, 25: 1400-1417.

- Lezama-Ochoa N, Murua H, Hall M, Roman M, Ruiz J, Vogel N, Caballero A, Sancristobal I. 2017. Biodiversity and habitat characteristics of the bycatch assemblages in fish aggregating devices (FADs) and school sets in the Eastern Pacific Ocean. *Frontiers in Marine Science*, 4, 256.
- Lobel PS, Robinson AR. 1986. Transport and entrapment of fish larvae by ocean mesoscale eddies and currents in Hawaiian waters. *Deep Sea Research Part A. Oceanographic Research Papers*, 33(4): 483-500.
- Løkkeborg S, Siikavuopio SI, Humborstad OB, Utne-Palm AC, Ferter K. 2014. Towards more efficient longline fisheries: fish feeding behaviour, bait characteristics and development of alternative baits. *Reviews in Fish Biology and Fisheries*, 24(4): 985-1003.
- Lopez J, Moreno G, Ibaibarriaga L, Dagorn L. 2017. Diel behavior of tuna and non-tuna species at drifting fish aggregating devices (DFADs) in the Western Indian Ocean, determined by fishers' echo-sounder buoys. *Marine Biology*, 164:44.
- Lopez J, Moreno G, Boyra G, Dagorn L. 2016. A model based on data from echosounder buoys to estimate biomass of fish species associated with fish aggregating devices. *Fishery Bulletin*, United States Department of Commerce, National Oceanic and Atmospheric Administration, National Marine Fisheries Service, 114(2): 166-178.
- Macusi EDM, Abreo NAS, Babaran RP. 2017. Local ecological knowledge (LEK) on fish behavior around anchored FADs: the case of tuna purse seine and ringnet fishers from Southern Philippines. *Frontiers in Marine Science*, 4:188.
- Madirolas A, Membiela FA, Gonzalez JD, Gabreira AG, dell'Erba M, Prario IS, Blanc S. 2016. Acoustic target strength (TS) of Argentine anchovy (*Engraulis anchoita*): the nighttime scattering layer. *ICES Journal of Marine Science*, DOI: 10.1093/icesjms/fsw185.
- Madureira L, Everson I, Murphy EJ. 1993. Interpretation of acoustic data at two frequencies to discriminate between Antarctic krill (*Euphausia superba* Dana) and other scatterers. *Journal of Plankton Research*, 15(7): 787-802.
- Marsac F, Fonteneau A, Ménard F. 2001. Drifting FADs used in tuna fisheries: an ecological trap?. *Actes de Colloques-Ifremer*, 28.

- Massé J, Uriarte A, Angelico MM, Carrera P. 2018. Pelagic survey series for sardine and anchovy in ICES subareas 8 and 9 – Towards an ecosystem approach. ICES Cooperative Research Report.
- Mathies NH, Ogburn MB, McFall G, Fangman S. 2014. Environmental interference factors affecting detection range in acoustic telemetry studies using fixed receiver arrays. *Marine Ecology Progress Series*, 495: 27-38.
- McLeod LE, Costello MJ. 2017. Light traps for sampling marine biodiversity. *Helgoland Marine Research*, 71:2.
- Menard F, Fonteneau A, Gaertner D, Nordstrom V, Stequert B, Marchal E. 2000. Exploitation of small tunas by a purse-seine fishery with fish aggregating devices and their feeding ecology in an eastern tropical Atlantic ecosystem. *ICES Journal of Marine Science*, 57: 525-530.
- Merten W, Rivera R, Appeldoorn R, Serrano K, Collazo O, Jimenez N. 2018. Use of video monitoring to quantify spatial and temporal patterns in fishing activity across sectors at moored fish aggregating devices off Puerto Rico. *Scientia Marina* 82(2).
- Merten W, Appeldoorn R, Hammond D. 2016. Movement dynamics of dolphinfish (*Coryphaena hippurus*) in the northeastern Caribbean Sea: Evidence of seasonal re-entry into domestic and international fisheries throughout the western central Atlantic. *Fisheries Research*, 175: 24-34.
- Mills D, Tilley A. 2019. Exploring options to improve livelihoods and resource management in Timor-Leste's coastal communities. Report for the Australian Centre for International Agricultural Research FR2019-46.
- Miyake MP, Guillotreau P, Sun C-H, Ishimura G. 2010. Recent developments in the tuna industry. FAO Fisheries and Aquaculture Technical Paper 543.
- Morato T, Clark MR. 2007. Seamount fishes: ecology and life histories. *Seamounts: ecology, fisheries, and conservation*. Blackwell Fisheries and Aquatic Resources Series, 12: 170-188.
- Moreno G, Boyra G, Sancristobal I, Itano D, Restrepo V. 2019. Towards acoustic discrimination of tropical tuna associated with fish aggregating devices. *PLoS ONE*, 14(6): e0216353.

- Moreno G, Jauhary R, Adam SM, Restrepo V. 2018. Moving away from synthetic materials used at FADs: evaluating biodegradable ropes degradation. *Collective Volume of Scientific Papers*, 74(5): 2192-2198.
- Moreno G, Dagorn L, Capello M, Lopez J, Filmalter J, Forget F, Sancristobal I, Holland K. 2016. Fish aggregating devices (FADs) as scientific platforms. *Fisheries Research*, 178: 122-129.
- Moyes CD, Fragoso N, Musyl MK, Brill RW. 2006. Predicting postrelease survival in large pelagic fish. *Transactions of the American Fisheries Society*, 135(5): 1389-1397.
- Nathan R, Monk C, Arlinghaus R, Adam T, Alós J, Assaf M, Baktoft H, Beardsworth CE, Bertram MG, Bijleveld AI, Brodin T, Brooks JL, Campos-Candela A, Cooke SJ, Gjelleand KØ, Gupte PR, Harel R, Hellström G, Jeltsch F, Killen SS, Klefoth T, Langrock R, Lennox RJ, Lourie E, Madden JR, Orchan Y, Pauwels IS, Říha M, Roeleke M, Schlägel U, Shohami D, Signer J, Toledo S, Vilik O, Westrelin S, Whiteside MA, Jarić I. 2022. Big-data approaches enable increased understanding of animal movement ecology. *Science*, 375: eabg1780.
- Novak AJ, Becker SL, Finn JT, Pollock CG, Hillis-Starr Z, Jordaan, A. 2020. Scale of biotelemetry data influences ecological interpretations of space and habitat use in yellowtail snapper. *Marine and Coastal Fisheries*, 12: 364-377.
- Nowacek DP, Friedlaender AS, Halpin PN, Hazen EL, Johnston DW, Read AJ, Espinasse B, Zhou M, Zhu Y. 2011. Super-aggregations of krill and humpback whales in Wilhelmina Bay, Antarctic Peninsula. *PLoS ONE*, 6(4): e19173.
- O'Brien MHP, Secor DH. 2021. Influence of thermal stratification and storms on acoustic telemetry detection efficiency: a year-long test in the US Southern Mid-Atlantic Bight. *Animal Biotelemetry*, 9(8), <http://doi.org/10.1186/s40317-021-00233-3>.
- Orue B, Lopez J, Moreno G, Santiago J, Soto M, Murua H. 2019. Aggregation process of drifting fish aggregating devices (DFADs) in the Western Indian Ocean: Who arrives first, tuna or non-tuna species? *PLoS ONE*, 14(1): e0210435.

- Oskanen J, Simpson GL, Blanchet FG, Kindt R, Legendre P, Minchin PR, O'Hara RB, Solymos P, Stevens MHH, Szoecs E, Wagner H, Barbour M, Bedward M, Bolker B, Borcard D, Carvalho G, Chirico M, De Caceres M, Durand S, Evangelista HBA, FitzJohn R, Friendly M, Furneaux B, Hannigan G, Hill MO, Lahti L, McGlenn D, Ouellette M-H, Cunha ER, Smith T, Stier A, Ter Braak CJF, Weedon J. 2022. Vegan: Community Ecology Package. R package version 2.6-2. <http://CRAN.R-project.org/package=vegan>.
- Oxenford HA, Murray PA, Luckhurst BE. 2003. The biology of wahoo (*Acanthocybium solandri*) in the western central Atlantic. *Gulf and Caribbean Research*, 15: 33-49.
- Parin NV, Fedoryako BI. 1999. Pelagic fish communities around floating objects in the ocean. *In: Scott MD, Bayliff WH, Lennert-Cody CE, Schaefer KM (eds.), Proceedings of the International Workshop on the Ecology and Fisheries for Tunas Associated with Floating Objects, February 11-13, 1992. Inter-American Tropical Tuna Commission Special Report 11, La Jolla, California, pp. 447-458.*
- Petrik CM, Stock CA, Andersen KH, van Denderen PD, Watson JR. 2020. Large pelagic fish are most sensitive to climate change despite pelagification of ocean food webs. *Frontiers in Marine Science*, 7:588482.
- Pinheiro J, Bates D, R Core Team. 2023. nlme: linear and nonlinear mixed-effects models. R package version 3.1-162, <https://CRAN.R-project.org/package=nlme>.
- Pons M, Melnychuk MC, Hilborn R. 2018. Management effectiveness of large pelagic fisheries in the high seas. *Fish and Fisheries*, 19: 260-270.
- Prince ED, Goodyear CP. 2006. Hypoxia-based habitat compression of tropical pelagic fishes. *Fisheries Oceanography*, 15(6): 451-464.
- R Core Team. 2022. R: A language and environment for statistical computing. R Foundation for Statistical Computing, Vienna, Austria. URL <http://www.R-project.org/>.
- Ringelberg J. 2009. Diel vertical migration of zooplankton in lakes and oceans: causal explanations and adaptive significances. Springer Science & Business Media, 2009.
- Ritz DA. 1994. Social aggregation in pelagic invertebrates. *Advances in Marine Biology*, 30: 155-216.

- Robert M, Dagorn L, Lopez J, Moreno G, Deneubourg J-L. 2013. Does social behavior influence the dynamics of aggregations formed by tropical tunas around floating objects? An experimental approach. *Journal of Experimental Marine Biology and Ecology*, 440: 238-243.
- Robison BH. 2009. Conservation of deep pelagic biodiversity. *Conservation Biology*, 23: 847-858.
- Rountree RA. 1989. Association of fishes with fish aggregation devices: effects of structure size on fish abundance. *Bulletin of Marine Science*, 44(2): 960-972.
- Sabarros PS, Menard F, Levenez J-J, Tew-Kai E, Ternon J-F. 2009. Mesoscale eddies influence distribution and aggregation patterns of micronekton in the Mozambique Channel. *Marine Ecology Progress Series*, 395: 101-107.
- Santana-Garcon J, Braccini M, Langlois TJ, Newman SJ, McAuley RB, Harvey ES. 2014. Calibration of pelagic stereo-BRUVs and scientific longline surveys for sampling sharks. *Methods in Ecology and Evolution*, 5: 824-833.
- Scheuerell MD, Schindler DE. 2003. Diel vertical migration by juvenile sockeye salmon: empirical evidence for the antipredation window. *Ecology*, 84(7): 1713-1720.
- Schlenker LS, Failletaz R, Stieglitz JS, Lam CH, Hoenig RH, Cox GK, Heuer RM, Pasparakis C, Benetti DD, Paris CD, Grosell M. 2021. Remote predictions of mahi-mahi (*Coryphaena hippurus*) spawning in the open ocean using summarized accelerometry data. *Frontiers in Marine Science*, 8: 626082.
- Schneider EVC, Brooks EJ, Cortina MP, Bailey DM, Killen SS, Van Leeuwen TE. 2021. Design and deployment of an affordable and long-lasting deepwater subsurface fish aggregation device. *Caribbean Naturalist*, 83: 1-16.
- Sehein T, Siuda ANS, Shank TM, Govindarajan AF. 2014. Connectivity in the slender *Sargassum* shrimp (*Latreutes fucorum*): implications for a Sargasso Sea protected area. *Journal of Plankton Research*, 36(6): 1408-1412.
- Sherman KD, Shultz AD, Dahlgren CP, Thomas C, Brooks E, Brooks A, Brumbaugh DR, Gittens L, Murchie KJ. 2018. Contemporary and emerging fisheries in The Bahamas-

- conservation and management challenges, achievements and future directions. *Fisheries Management and Ecology*, 25(5): 319-331.
- Simpfendorfer CA, Hueter RE, Bergman U, Connett SMH. 2002. Results of a fishery-independent survey for pelagic sharks in the western North Atlantic, 1977-1994. *Fisheries Research*, 55: 175-192.
- Smith NS, Zeller D. 2016. Unreported catch and tourist demand on local fisheries of small island states: the case of The Bahamas, 1950-2010. *Fisheries Bulletin*, 114(1): 117-131.
- Sogard SM, Olla BL. 1993. Effects of light, thermoclines and predator presence on vertical distribution and behavioral interactions of juvenile walleye pollock, *Theragra chalcogramma* Pallas. *Journal of Experimental Marine Biology and Ecology*, 167(2): 179-195.
- Sokimi W. 2006. Fish aggregating devices: the Okinawa/Pacific experience. *Fish. News.- South Pacific Commission*, 119, 45.
- Soria M, Dagorn L, Potin G, Freon P. 2009. First field-based experiment supporting the meeting point hypothesis for schooling in pelagic fish. *Animal Behaviour*, 78: 1441-1446.
- Stehfest KM, Dagorn L. 2010. Differences in large-scale movement between free swimming and fish aggregating device (FAD) caught tuna. *Indian Ocean Tuna Commission*.
- Stoffer D. 2019. Asts: Applied statistical time series analysis. <http://CRAN.R-project.org/package=astsa>. R package version 1.9.
- Swadling DS, Knott NA, Rees MJ, Pederson H, Adams KR, Taylor MD, Davis AR. 2020. Seagrass canopies and the performance of acoustic telemetry: implications for the interpretation of fish movements. *Animal Biotelemetry*, 8(8): DOI: <https://doi.org/10.1186/s40317-020-00197-w>.
- Taquet M, Blanc M, Dagorn L, Filmalter JD, Fonteneau A, Forget F, Gaertner JC, Galzin R, Gervain P, Goujon M, Guillotreau P, Guyader O, Hall M, Holland K, Itano D, Monteagudo JP, Morales-Nin B, Reynal L, Sharp M, Sokimi W, Tanetoa M, Yen Kai Sun S. 2011. Artisanal and industrial FADs: A question of scale. Tahiti conference reviews current FAD use and technology. *Fisheries Newsletter*, 136: 35-45.

- Taquet M, Sancho G, Dagorn L, Gaertner J-C, Itano D, Aumeeruddy R, Wendling B, Peignon C. 2007. Characterizing fish communities associated with drifting fish aggregating devices (FADs) in the Western Indian Ocean using underwater visual surveys. *Aquatic Living Resources*, 20: 331-341.
- Tilley A, Wilkinson SP, Kolding J, Lopez-Angarita J, Pereira M, Mills DJ. 2019. Nearshore fish aggregating devices show positive outcomes for sustainable fisheries development in Timor-Leste. *Frontiers in Marine Science*, 6: 487.
- Tolotti MT, Forget F, Capello M, Filmlalter JD, Hutchinson M, Itano D, Holland K, Dagorn L. 2020. Association dynamics of tuna and purse seine bycatch species with drifting fish aggregating devices (FADs) in the tropical eastern Atlantic Ocean. *Fisheries Research*, 226: 105521.
- Trevorrow MV. 1998. Boundary scattering limitations to fish detection in shallow waters. *Fisheries Research*, 35: 127-135.
- Trygonis V, Georgakarakos S, Dagorn L, Brehmer P. 2016. Spatiotemporal distribution of fish schools around drifting fish aggregating devices. *Fisheries Research*, 177: 39-49.
- Vergeynsy J, Baktoft H, Mouton A, De Mulder T, Nopens I, Pauwels I. 2020. The influence of system settings on positioning accuracy in acoustic telemetry, using the YAPS algorithm. *Animal Biotelemetry*, 8(25): 1-12.
- Verity PG, Smetacek V, Smayda TJ. 2002. Status, trends and the future of the marine pelagic ecosystem. *Environmental Conservation*, 29(2): 207-237.
- Warren JD, Stanton TK, Benfield MC, Wiebe PH, Chu D, Sutor M. 2001. *In situ* measurements of acoustic target strengths of gas-bearing siphonophores. *ICES Journal of Marine Science*, 58: 740-749.
- Watanabe C, Nishida H. 2002. Development of assessment techniques for pelagic fish stocks: applications of daily egg production method and pelagic trawl in the Northwestern Pacific Ocean. *Fisheries Science*, 68(1): 97-100.
- Watson BM, Biagi CA, Northrup SL, Ohata ML, Charles C, Blanchfield PJ, Johnston SV, Askey PJ, van Poorten BT, Devlin RH. 2019. Distinct diel and seasonal behaviours in rainbow

- trout detected by fine-scale acoustic telemetry in a lake environment. *Canadian Journal of Fisheries and Aquatic Sciences*, 76(8): 1432-1445.
- Webb TJ, Vanden Berghe E, O'Dor R. 2010. Biodiversity's big wet secret: the global distribution of marine biological records reveals chronic under-exploration of the deep pelagic ocean. *PLoS ONE*, 5(8): e10233.
- Weinz AA, Matley JK, Klinard NV, Fisk AT, Colborne SF. 2020. Identification of predation events in wild fish using novel acoustic transmitters. *Animal Biotelemetry*, 8(1): 1-14.
- Weng JS, Hung MK, Lai CC, Wu LJ, Lee MA, Liu KM. 2013. Fine-scale vertical and horizontal movements of juvenile yellowfin tuna (*Thunnus albacares*) associated with a subsurface fish aggregating device (FAD) off southwestern Taiwan. *Journal of Applied Ichthyology*, 29: 990-1000.
- Wetz JJ, Ajemian MJ, Shipley B, Stunz GW. 2020. An assessment of two visual survey methods for documenting fish community structure on artificial platform reefs in the Gulf of Mexico. *Fisheries Research*, 225: 105492.
- Wood SN. 2011. Fast stable restricted maximum likelihood and marginal estimation of semiparametric generalized linear models. *Journal of the Royal Statistical Society*, 73(1): 3-36.
- Worm B, Barbier EB, Beaumont N, Duffy JE, Folke C, Halpern BS, ... Sala E. 2006. Impacts of biodiversity loss on ocean ecosystem services. *Science*, 314(5800): 787-790.
- Worm B, Sandow M, Oschlies A, Lotze HK, Myers RA. 2005. Global patterns of predator diversity in the open oceans. *Science*, 309(5739): 1365-1369.
- Worm B, Lotze HK, Myers RA. 2003. Predator diversity hotspots in the blue ocean. *Proceedings of the National Academy of Sciences*, 100(17): 9884-9888.
- Yang S, Zhang B, Zhang H, Zhang S, Fan X, Hua C, Fan W. 2019. Bigeye tuna fishing ground in relation to thermocline in the Western and Central Pacific Ocean using Argo data. *Indian Journal of Geo Marine Sciences*, 48(04): 444-451.

## 8 Appendix

### 8.1 Section 3 (Chapter 2) Supplementary Materials

Table 8.1-1. Output statistics of a generalized additive model (GAM) with a negative binomial distribution to analyze the effects of time ('age' of FAD), season, and survey method on shark abundance. Bold text highlights significant effects.

<b>Shark Abundance</b>				
Family	Negative Binomial			
Link Function	Log			
Formula	SharkAb ~ s(Age) + factor(Season) + factor(Method)			
Parametric coefficients:	Estimate	Std. Error	z value	Pr (> z )
(Intercept)	-4.1069	0.6396	-6.421	<b>1.35e-10 ***</b>
Factor( <b>Season</b> ) <b>Warm</b>	1.1222	0.7271	1.543	0.123
Factor( <b>Method</b> ) <b>Visual</b>	-1.6589	0.6818	-2.433	<b>0.015 *</b>
Approximate significance of smooth terms:				
	edf	Ref. df	Chi. Sq	p-value
s( <b>Age</b> )	2.965	3.659	12.58	<b>0.0108 *</b>
R-sq. (adj) = 0.0325	Deviance explained = 23.4%			
-REML = 49.352	Scale est. = 1			n = 514

Table 8.1-2. Analysis of variance (ANOVA) output table for the best fitting GAM model of shark abundance (output shown in Table 8.1-1). Bold text highlights significant effects.

<b>Shark Abundance</b>				
Family	Negative Binomial			
Link Function	log			
Formula	SharkAb ~ s(Age) + factor(Season) + factor(Method)			
Parametric terms:	df	Chi sq.	p value	
Factor(Season)	1	2.382	0.123	
Factor( <b>Method</b> )	1	5.920	0.015	
Approximate significance of smooth terms:				
	edf	Ref. df	Chi.sq	p-value
s( <b>Age</b> )	2.965	3.659	12.58	<b>0.0108</b>

Table 8.1-3. Output statistics of a generalized additive model (GAM) with a Poisson distribution to analyze the effects of time ('age' of FAD), season, and survey method on total fish abundance. Bold text highlights significant effects.

<b>Total Abundance</b>				
Family	Poisson			
Link Function	log			
Formula	TotalAb ~ s(Age) + factor(Season) + factor(Method)			
Parametric coefficients:	Estimate	Std. Error	z value	Pr (> z )
(Intercept)	2.8282	0.0174	162.43	<b>&lt;2e-16 ***</b>
Factor( <b>Season</b> ) <b>Warm</b>	1.0547	0.0197	53.49	<b>&lt;2e-16 ***</b>
Factor( <b>Method</b> ) <b>Visual</b>	0.9976	0.0122	81.59	<b>&lt;2e-16 ***</b>
Approximate significance of smooth terms:				
	edf	Ref. df	Chi.sq	p-value
s( <b>Age</b> )	8.983	9	10713	<b>&lt;2e-16 ***</b>
R-sq. (adj) = 0.235	Deviance explained = 24.9%			
UBRE = 20214	Scale est. = 19794		n = 514	

Table 8.1-4. Analysis of variance (ANOVA) output table for the best fitting GAM model of total fish abundance. Bold text highlights significant effects.

<b>Total Fish Abundance</b>				
Family	Poisson			
Link Function	log			
Formula	TotalAb ~ s(Age) + factor(Season) + factor(Method)			
Parametric terms:	df	Chi sq.	p value	
Factor( <b>Season</b> )	1	2862	<b>&lt;2e-16</b>	
Factor( <b>Method</b> )	1	6657	<b>&lt;2e-16</b>	
Approximate significance of smooth terms:				
	edf	Ref. df	Chi.sq	p-value
s( <b>Age</b> )	8.983	9.000	10713	<b>&lt;2e-16</b>

Table 8.1-5. Output statistics of a generalized additive model (GAM) with a Gaussian distribution to analyze the effects of time ('age' of FAD), season, and survey method on Shannon's diversity. Bold text highlights significant effects.

<b>Diversity</b>				
Family	Gaussian			
Link Function	Identity			
Formula	Diversity ~ s(Age) + factor(Season) + factor(Method)			
Parametric coefficients:	Estimate	Std. Error	t value	Pr (> t )
(Intercept)	0.3857	0.0363	10.61	<b>&lt;2e-16 ***</b>
Factor( <b>Season</b> ) <b>Warm</b>	0.1999	0.0512	3.91	<b>&lt;0.001 ***</b>
Factor(Method)Visual	0.0181	0.0305	0.59	0.55
Approximate significance of smooth terms:				
	edf	Ref. df	F	p-value
s( <b>Age</b> )	8.448	8.922	8.687	<b>&lt;2e-16 ***</b>
R-sq. (adj) = 0.28	Deviance explained = 29.5%			
GCV = 0.1085	Scale est. = 0.1061			n = 514

Table 8.1-6. Analysis of variance (ANOVA) output table for the best fitting GAM model of Shannon's diversity. Bold text highlights significant effects.

<b>Shannon's Diversity</b>				
Family	Gaussian			
Link Function	identity			
Formula	Shannon ~ s(Age) + factor(Season) + factor(Method) + factor(Location)			
Parametric terms:	df	F	p value	
Factor(Method)	1	0.352	0.5532	
Factor( <b>Season</b> )	1	15.269	<b>0.0001</b>	
Factor(Location)	1	0.029	0.8653	
Approximate significance of smooth terms:				
	edf	Ref. df	F	p-value
s( <b>Age</b> )	8.445	8.921	8.965	<b>&lt;2e-16</b>

Table 8.1-7. Output statistics of generalized additive models (GAMs) with Poisson distributions to analyze the effects of time ('age' of FAD), season, and survey method on the abundance of seven individual species (Bar jacks *Caranx ruber*, almaco jacks *Seriola rivoliana*, scad *Decapterus sp.*, *Clupeidae*, unicorn filefish *Aluterus monoceros*, wahoo *Acanthocybium solandri*, and mahi *Coryphaena hippurus*). Bold text highlights significant effects.

<b>Bar Jack Abundance</b>				
Family	Poisson			
Link Function	log			
Formula	BarJackAb ~ s(Age) + factor(Season) + factor(Method)			
Parametric coefficients:	Estimate	Std. Error	z value	Pr (> z )
(Intercept)	-27.4935	0.9898	-27.78	<b>&lt;2e-16 ***</b>
Factor( <b>Season</b> ) <b>Warm</b>	4.3126	0.1392	30.98	<b>&lt;2e-16 ***</b>
Factor( <b>Method</b> ) <b>Visual</b>	1.0713	0.0203	52.85	<b>&lt;2e-16 ***</b>
Approximate significance of smooth terms:				
	edf	Ref. df	Chi.sq	p-value
s( <b>Age</b> )	8.993	9	4208	<b>&lt;2e-16 ***</b>
R-sq. (adj) = 0.298	Deviance explained = 55.6%			
UBRE = 55.995	Scale est. = 1		n = 514	
<b>Almaco Jack Abundance</b>				
Family	Poisson			
Link Function	log			
Formula	AlmacoJackAb ~ s(Age) + factor(Season) + factor(Method)			
Parametric coefficients:	Estimate	Std. Error	z value	Pr (> z )
(Intercept)	-2.0207	0.6889	-2.934	<b>&lt;0.01 **</b>
Factor( <b>Season</b> ) <b>Warm</b>	0.2386	0.1132	2.108	<b>0.035 *</b>
Factor( <b>Method</b> ) <b>Visual</b>	0.347	0.079	4.391	<b>&lt;0.001 ***</b>
Approximate significance of smooth terms:				
	edf	Ref. df	Chi.sq	p-value
s( <b>Age</b> )	7.747	8.083	662.6	<b>&lt;2e-16 ***</b>
R-sq. (adj) = 0.274	Deviance explained = 42.9%			
UBRE = 2.8755	Scale est. = 1		n = 514	
<b>Scad Abundance</b>				
Family	Poisson			
Link Function	log			
Formula	ScadAb ~ s(Age) + factor(Season) + factor(Method)			

Parametric coefficients:	Estimate	Std. Error	z value	Pr (> z )
(Intercept)	-19.8919	3.5811	-5.555	<0.001 ***
Factor( <b>Season</b> ) <b>Warm</b>	1.2201	0.0967	12.61	<2e-16 ***
Factor( <b>Method</b> ) <b>Visual</b>	0.6729	0.0285	23.64	<2e-16 ***
Approximate significance of smooth terms:				
	edf	Ref. df	Chi.sq	p-value
s( <b>Age</b> )	8.969	8.999	4109	<2e-16 ***
R-sq. (adj) = 0.247	Deviance explained = 51.1%			
UBRE = 32.263	Scale est. = 1		n = 514	
<b>Clupeid Abundance</b>				
Family	Poisson			
Link Function	log			
Formula	ClupeidAb ~ s(Age) + factor(Season) + factor(Method)			
Parametric coefficients:	Estimate	Std. Error	z value	Pr (> z )
(Intercept)	-1.499e4	5.364e5	-0.028	0.978
Factor( <b>Season</b> ) <b>Warm</b>	0.684	0.3246	2.114	<b>0.035 *</b>
Factor( <b>Method</b> ) <b>Visual</b>	0.3217	5.364e5	0.000	1.000
Approximate significance of smooth terms:				
	edf	Ref. df	Chi.sq	p-value
s( <b>Age</b> )	5.477	5.742	198.6	<2e-16 ***
R-sq. (adj) = 0.273	Deviance explained = 70.9%			
UBRE = 0.40863	Scale est. = 1		n = 514	
<b>Unicorn Filefish Abundance</b>				
Family	Poisson			
Link Function	log			
Formula	UnicornFilefishAb ~ s(Age) + factor(Season) + factor(Method)			
Parametric coefficients:	Estimate	Std. Error	z value	Pr (> z )
(Intercept)	-0.9558	0.2242	-4.263	<0.001 ***
Factor( <b>Season</b> ) <b>Warm</b>	-2.6941	0.2105	-12.799	<2e-16 ***
Factor( <b>Method</b> ) <b>Visual</b>	0.4708	0.0518	9.097	<2e-16 ***
Approximate significance of smooth terms:				
	edf	Ref. df	Chi.sq	p-value
s( <b>Age</b> )	8.84	8.99	1878	<2e-16 ***
R-sq. (adj) = 0.108	Deviance explained = 51.1%			
UBRE = 12.582	Scale est. = 1		n = 514	
<b>Wahoo Abundance</b>				

Family	Poisson			
Link Function	log			
Formula	WahooAb ~ s(Age) + factor(Season) + factor(Method)			
Parametric coefficients:	Estimate	Std. Error	z value	Pr (> z )
(Intercept)	-2.5134	0.4723	-5.322	<b>&lt;0.001</b> ***
Factor( <b>Season</b> ) <b>Warm</b>	-2.5061	0.8702	-2.88	<b>&lt;0.01</b> **
Factor( <b>Method</b> ) <b>Visual</b>	-0.8333	0.4433	-1.88	0.0601
Approximate significance of smooth terms:				
	edf	Ref. df	Chi.sq	p-value
s( <b>Age</b> )	5.729	6.803	16.28	<b>0.0199</b> *
R-sq. (adj) = 0.066	Deviance explained = 27.5%			
UBRE = -0.7347	Scale est. = 1	n = 514		
<b>Mahi Abundance</b>				
Family	Poisson			
Link Function	log			
Formula	MahiAb ~ s(Age) + factor(Season) + factor(Method)			
Parametric coefficients:	Estimate	Std. Error	z value	Pr (> z )
(Intercept)	-3.8757	0.7915	-4.896	<b>&lt;0.001</b> ***
Factor( <b>Season</b> ) <b>Warm</b>	-1.3502	0.204	-6.617	<b>&lt;0.001</b> ***
Factor( <b>Method</b> ) <b>Visual</b>	0.9214	0.1765	5.22	<b>&lt;0.001</b> ***
Approximate significance of smooth terms:				
	edf	Ref. df	Chi.sq	p-value
s( <b>Age</b> )	7.735	8.264	169.4	<b>&lt;2e-16</b> ***
R-sq. (adj) = 0.0611	Deviance explained = 33.8%			
UBRE = 1.0467	Scale est. = 1	n = 514		

Table 8.1-8. Analysis of variance (ANOVA) output table for the best fitting GAM model of abundance of seven individual species (Bar jacks *Caranx ruber*, almaco jacks *Seriola rivoliana*, scad *Decapterus sp.*, *Clupeidae*, unicorn filefish *Aluterus monoceros*, wahoo *Acanthocybium solandri*, and mahi *Coryphaena hippurus*). Bold text highlights significant effects.

<b>Bar Jack Abundance</b>			
Family	Gaussian		
Link Function	identity		
Formula	BarJack ~ s(Age) + factor(Season) + factor(Method)		
Parametric terms:	df	F	p value

Factor( <b>Season</b> )	1	16.02	<b>7.2e-5</b>
Factor( <b>Method</b> )	1	16.12	<b>6.83e-5</b>

Approximate significance of smooth terms:

	edf	Ref. df	F	p-value
s( <b>Age</b> )	7.519	8.491	4.864	<b>6.78e-6</b>

#### Almaco Jack Abundance

Family	Gaussian
Link Function	identity
Formula	AlmacoJack ~ s(Age) + factor(Season) + factor(Method)

Parametric terms:	df	F	p value
Factor(Season)	1	0.032	0.857
Factor(Method)	1	1.648	0.2

Approximate significance of smooth terms:

	edf	Ref. df	F	p-value
s( <b>Age</b> )	8.063	8.785	13.15	<b>&lt;2e-16</b>

#### Scad Abundance

Family	Gaussian
Link Function	identity
Formula	Scad ~ s(Age) + factor(Season) + factor(Method)

Parametric terms:	df	F	p value
Factor(Season)	1	0.945	0.3315
Factor( <b>Method</b> )	1	4.065	<b>0.0443</b>

Approximate significance of smooth terms:

	edf	Ref. df	F	p-value
s( <b>Age</b> )	8.424	8.916	9.205	<b>&lt;2e-16</b>

#### Clupeid Abundance

Family	Gaussian
Link Function	identity
Formula	Clupeid ~ s(Age) + factor(Season) + factor(Method)

Parametric terms:	df	F	p value
Factor(Season)	1	1.352	0.246
Factor(Method)	1	1.510	0.220

Approximate significance of smooth terms:

	edf	Ref. df	F	p-value
s(Age)	3.034	3.775	1.209	0.33

#### Unicorn Filefish Abundance

Family	Gaussian			
Link Function	identity			
Formula	Filefish ~ s(Age) + factor(Season) + factor(Method)			
Parametric terms:	df	F	p value	
Factor(Season)	1	1.601	0.206	
Factor(Method)	1	0.382	0.537	
Approximate significance of smooth terms:				
	edf	Ref. df	F	p-value
s(Age)	8.273	8.868	4.311	<b>2.46e-5</b>
<b>Wahoo Abundance</b>				
Family	Gaussian			
Link Function	identity			
Formula	Wahoo ~ s(Age) + factor(Season) + factor(Method)			
Parametric terms:	df	F	p value	
Factor( <b>Season</b> )	1	6.404	<b>0.0117</b>	
Factor(Method)	1	1.925	0.1659	
Approximate significance of smooth terms:				
	edf	Ref. df	F	p-value
s(Age)	1	1	1.649	0.2
<b>Mahi Abundance</b>				
Family	Gaussian			
Link Function	identity			
Formula	Mahi ~ s(Age) + factor(Season) + factor(Method)			
Parametric terms:	df	F	p value	
Factor(Season)	1	2.722	0.0996	
Factor(Method)	1	1.331	0.2492	
Approximate significance of smooth terms:				
	edf	Ref. df	F	p-value
s(Age)	6.503	7.688	2.625	<b>0.00731</b>

## 8.2 Section 4 (Chapter 3) Supplementary Materials

Table 8.2-1. Output statistics of a linear model (LM) to analyze the effects of distance away from FAD, lunar illumination, deployment time, depth, and the interactions between illumination and

depth, and distance away and depth, on light trap log(CPUE) of all organisms at the North FAD. Significant terms are bolded.

<b>lm(formula = log(CPUE) ~ Distance*Depth + DeploymentTime + Illumination * Depth)</b>					
Residuals:					
	Min	1Q	Median	3Q	Max
	-1.7059	-0.4355	-0.0665	0.4867	2.287
Coefficients:					
	Estimate	Std. Error	t value	Pr (> t )	
(Intercept)	1.149e5	6.959e4	1.651	0.104	
<b>Distance Away</b>	-9.221e-4	4.499e-4	-2.05	<b>0.0449 *</b>	
<b>Illumination</b>	-0.93	0.454	-2.048	<b>0.0451 *</b>	
<b>Depth</b>	-1.643e-3	6.877e-4	-2.389	<b>0.0202 *</b>	
DeploymentTime	5.202e-5	3.15e-5	1.651	0.104	
DistAway:Depth	7.459e-7	1.291e-6	0.578	0.5656	
Illumination:Depth	9.464e-4	1.382e-3	0.685	0.496	
Significance codes:	0 '***'	0.001 '**'	0.01 '*'	0.05 '.'	0.1 ' ' 1
Residual standard error: 0.7411 on 58 degrees of freedom					
Multiple R-squared: 0.2903, Adjusted R-squared: 0.2169					
F-statistic: 3.955 on 6 and 58 DF, p-value: 0.002209					

Table 8.2-2. Analysis of variance (ANOVA) output table for the linear model (LM) to analyze the effects of distance away from FAD, lunar illumination, deployment time, depth, and the interactions between illumination and depth, and distance away and depth, on light trap log(CPUE) of all organisms at the North FAD. Significant terms are bolded.

	Df	Sum Sq	Mean Sq	F value	Pr (>F)
DistanceAway	1	5.180	5.1799	9.4308	<b>0.0032 **</b>
Depth	1	3.555	3.555	6.4724	<b>0.0136 *</b>
DepTime	1	0.406	0.4061	0.7394	0.3934
Illumination	1	2.937	2.9365	5.3464	<b>0.0243 *</b>
DistAway:Depth	1	0.698	0.6977	1.2703	0.2644
Depth:Illum	1	0.258	0.2576	0.469	0.4962
Residuals	58	31.857	0.5493		

---

Signif. codes: 0 ‘\*\*\*’ 0.001 ‘\*\*’ 0.01 ‘\*’ 0.05 ‘.’ 0.1 ‘ ’

---

Table 8.2-3. Output statistics of a linear model (LM) to analyze the effects of distance away from FAD, lunar illumination, deployment time, depth, and the interactions between illumination and depth, and distance away and depth, on log(CPUE) of polychaetes at the North FAD.

---

**lm(formula = log(CPUEPoly) ~ Distance\*Depth + DeploymentTime + Illumination \* Depth)**

---

Residuals:

	Min	1Q	Median	3Q	Max
	-1.3395	-0.5205	-0.1314	0.4429	2.6406

---

Coefficients:

	Estimate	Std. Error	t value	Pr (> t )
(Intercept)	1.123e5	7.832e4	1.433	0.1571
<b>Distance Away</b>	<b>-1.078e-3</b>	<b>5.064e-4</b>	<b>-2.129</b>	<b>0.0375 *</b>
Illumination	-0.5738	0.511	-1.123	0.2661
Depth	-1.374e-3	7.741e-4	-1.775	0.0811
DeploymentTime	5.082e-5	3.546e-5	1.433	0.1571
DistAway:Depth	1.701e-6	1.453e-6	1.171	0.2464
Illumination:Depth	3.413e-4	1.556e-3	0.219	0.8271

---

Significance codes: 0 ‘\*\*\*’ 0.001 ‘\*\*’ 0.01 ‘\*’ 0.05 ‘.’ 0.1 ‘ ’ 1

---

Residual standard error: 0.8342 on 58 degrees of freedom  
Multiple R-squared: 0.157, Adjusted R-squared: 0.0698  
F-statistic: 1.8 on 6 and 58 DF, p-value: 0.1151

---

Table 8.2-4. Analysis of variance (ANOVA) output table for the linear model (LM) to analyze the effects of distance away from FAD, lunar illumination, deployment time, depth, and the interactions between illumination and depth, and distance away and depth, on log(CPUE) of polychaetes at the North FAD.

---

	Df	Sum Sq	Mean Sq	F value	Pr (>F)
DistanceAway	1	2.696	2.6959	3.8742	0.0538 .
Depth	1	1.16	1.1597	1.6666	0.2018
DepTime	1	0.674	0.6737	0.9682	0.3292
Illumination	1	1.316	1.3162	1.8915	0.1743

---

DistAway:Depth	1	1.635	1.6354	2.3502	0.1307
Depth:Illum	1	0.033	0.0335	0.0481	0.8271
Residuals	58	40.360	0.6959		
Signif. codes:	0 '***'	0.001 '**'	0.01 '*'	0.05 '.'	0.1 ' '

Table 8.2-5. Output statistics of a linear model (LM) to analyze the effects of distance away from FAD, lunar illumination, deployment time, depth, and the interaction between illumination and depth on the log of total length of light trapped individuals at the North FAD.

lm(formula = log(TotalLength) ~ Distance + DeploymentTime + Illumination * Depth)					
Residuals:					
	Min	1Q	Median	3Q	Max
	-2.838	-0.309	0.0704	0.380	1.615
Coefficients:					
	Estimate	Std. Error	t value	Pr (> t )	
<b>(Intercept)</b>	-1.937e4	7.204e3	-2.689	<b>0.0074</b> **	
<b>Distance Away</b>	-1.594e-4	7.144e-5	-2.231	<b>0.0261</b> *	
Illumination	-1.581e-1	1.392e-1	-1.136	0.2566	
<b>Depth</b>	3.363e-4	1.582e-4	2.126	<b>0.034</b> *	
<b>DeploymentTime</b>	-8.771e-6	3.216e-6	-2.69	<b>0.0074</b> **	
Illumination:Depth	-7.826e-5	4.098e-4	-0.191	0.849	
Significance codes:	0 '***'	0.001 '**'	0.01 '*'	0.05 '.'	0.1 ' ' 1
Residual standard error: 0.5776 on 541 degrees of freedom					
Multiple R-squared: 0.05799, Adjusted R-squared: 0.04928					
F-statistic: 6.66 on 5 and 541 DF, p-value: 4.936e-6					

Table 8.2-6. Analysis of variance (ANOVA) output table for the linear model (LM) to analyze the effects of distance away from FAD, lunar illumination, deployment time, depth, and the interaction between illumination and depth on the log of total length of light trapped individuals at the North FAD.

	Df	Sum Sq	Mean Sq	F value	Pr (>F)
DistanceAway	1	4.233	4.2334	12.6906	<b>0.0004</b> ***
Illumination	1	1.138	1.1378	3.4107	0.0653

Depth	1	3.321	180.73	6.0059	<b>0.0146 *</b>
DepTime	1	162.0	162.01	5.3839	<b>0.0207 *</b>
Illum:Depth	1	44.0	44.03	1.4633	0.2269
Residuals	541	16279.4	30.09		
Signif. codes:	0 '***'	0.001 '**'	0.01 '*'	0.05 '.'	0.1 ' '

Table 8.2-7. Output statistics of a linear model (LM) to analyze the effects of distance away from FAD, lunar illumination, deployment time, depth, and the interaction between illumination and depth on the diversity (at order level) of light trapped individuals at the North FAD.

<b>lm(formula = DiversityOrders ~ Distance + DeploymentTime + Illumination * Depth)</b>					
Residuals:					
	Min	1Q	Median	3Q	Max
	-1.2414	-0.597	-0.0821	0.3514	1.7627
Coefficients:					
	Estimate	Std. Error	t value	Pr (> t )	
(Intercept)	9.705e4	7.218e4	1.345	0.184	
Distance Away	-2.37e-4	3.159e-4	-0.75	0.456	
Illumination	-0.5255	0.438	-1.2	0.235	
Depth	1.397e-4	6.513e-4	0.215	0.831	
DeploymentTime	4.393e-5	3.268e-5	1.345	0.184	
Illumination:Depth	-8.681e-4	1.207e-3	-0.719	0.475	
Significance codes:	0 '***'	0.001 '**'	0.01 '*'	0.05 '.'	0.1 ' ' 1
Residual standard error: 0.7697 on 59 degrees of freedom					
Multiple R-squared: 0.1504, Adjusted R-squared: 0.0785					
F-statistic: 2.09 on 5 and 59 DF, p-value: 0.0794					

Table 8.2-8. Analysis of variance (ANOVA) output table for the linear model (LM) to analyze the effects of distance away from FAD, lunar illumination, deployment time, depth, and the interaction between illumination and depth on the diversity (at order level) of light trapped individuals at the North FAD.

	Df	Sum Sq	Mean Sq	F value	Pr (>F)
DistanceAway	1	1.315	1.3151	2.22	0.1416

Illumination	1	3.057	3.0573	5.1612	<b>0.0268 *</b>
Depth	1	0.236	0.236	0.3983	0.5304
DepTime	1	1.274	1.2745	2.1515	0.1477
Illum:Depth	1	0.306	0.3062	0.517	0.475
Residuals	59	34.949	0.59236		
Signif. codes:	0	****	0.001 ***	0.01 **	0.05 ‘.’ 0.1 ‘ ’

Table 8.2-9. Output statistics of a linear mixed effects model (LME) to analyze the effects of distance away from FAD, lunar illumination, temperature, location (North FAD or South FAD), and period (day or night) on logNASC in the ‘weak scatterer’ category (between -50 dB and -85 dB S<sub>v</sub>). Significant terms are bolded.

<b>logNASC of Weak Scatterers</b>						
Linear mixed-effects model fit by REML						
	AIC	BIC	logLik			
	646.5224	695.8749	-315.2612			
Random effects:						
Formula: ~1   SiteIndex						
	(Intercept)	Residual				
StdDev:	0.283	0.249				
Fixed effects: logNASC ~ Distance + Temp + Illumination + Location + Period						
	Value	Std. Error	DF	t-value	p-value	
<b>(Intercept)</b>	<b>-1.198</b>	<b>0.237</b>	<b>3441</b>	<b>-5.057</b>	<b>0.000</b>	
Distance Away	0.000	0.000	3441	0.262	0.793	
<b>Temperature</b>	<b>0.125</b>	<b>0.009</b>	<b>3441</b>	<b>14.58</b>	<b>0.000</b>	
<b>Illumination</b>	<b>-0.292</b>	<b>0.019</b>	<b>3441</b>	<b>-15.424</b>	<b>0.000</b>	
<b>LocationSouth</b>	<b>0.058</b>	<b>0.012</b>	<b>3441</b>	<b>4.826</b>	<b>0.000</b>	
<b>PeriodNight</b>	<b>0.094</b>	<b>0.013</b>	<b>3441</b>	<b>7.421</b>	<b>0.000</b>	
Correlation:	(Intr)	DstAwy	Temp	Illum	LocSouth	
DistAway	-0.033					
Temperature	-0.990	0.003				
Illumination	-0.254	0.003	0.219			
LocationSouth	-0.715	-0.017	0.707	<b>0.203</b>		
PeriodNight	-0.053	-0.008	0.045	<b>-0.330</b>	0.034	
Standardized Within-	Min	Q1		Med	Q3	Max

Group Residuals:	-5.180	-0.716	0.032	0.634	3.715
Number of Observations: 3536		Number of Groups: 90			

Table 8.2-10. Analysis of variance (ANOVA) output table for the linear mixed effects model (LME) to analyze the effects of distance away from FAD, lunar illumination, temperature, location (North FAD or South FAD), and period (day or night) on logNASC in the ‘weak scatterer’ category (between -50 dB and -85 dB Sv). Significant terms are bolded.

	numDF	denDF	F-value	p-value
(Intercept)	1	3441	4519.426	< 0.0001
DistanceAway	1	3441	0.011	0.9172
Temperature	1	3441	311.167	< 0.0001
Illumination	1	3441	230.573	< 0.0001
Location	1	3441	20.917	< 0.0001
Period	1	3441	55.077	< 0.0001

Table 8.2-11. Output statistics of a generalized linear mixed effects model (GLM) to analyze the effects of distance away from FAD, period (day or night), temperature, location (North FAD or South FAD), and lunar illumination on the presence of strong scatterers (binomial NASC > -50 dB Sv). Significant effects are bolded.

<b>Binomial NASC South FAD</b>					
Generalized linear mixed model fit by maximum likelihood (Laplace Approximation)					
Family: Binomial					
Formula: binomialNASC ~ Distance + Period + Temperature + Location + Lunar Illumination + (1   Index)					
	AIC	BIC	logLik	deviance	df.resid
	1974.9	2018.1	-980.4	1960.9	3529
Scaled	Min	1Q	Median	3Q	Max
Residuals:	-0.8706	-0.333	-0.2123	-0.182	7.4574
Random effects:					
	Groups	Name	Variance	Std. Dev.	
	Index	(Intercept)	0.4441	0.6664	

Number of obs: 3536, groups: Index, 24

---

Fixed effects:

	Estimate	Std. Error	z value	Pr (> z )
<b>(Intercept)</b>	<b>-10.51</b>	<b>4.434</b>	<b>-2.37</b>	<b>0.0178 *</b>
Distance	2.18e-4	2.1e-4	1.039	0.299
Away				
<b>PeriodNight</b>	<b>1.019</b>	<b>-0.3137</b>	<b>3.248</b>	<b>0.0012 **</b>
Temperature	0.2763	0.1582	1.746	0.0807
LocationSouth	-0.196	0.361	-0.543	0.5871
Illumination	0.0812	0.4936	0.164	0.8694

---

Significance 0 '\*\*\*' 0.001 '\*\*' 0.01 '\*' 0.05 '.' 0.1 ' ' 1

codes:

---

Correlation of Fixed Effects:

	(Intr)	DistAway	PrdNight	Temp	LocSouth
DistAway	-0.025				
PeriodNight	-0.008	0.000			
Temperature	-0.997	0.001	-0.023		
LocSouth	-0.527	-0.007	0.019	0.5	
Illumination	-0.479	0.002	-0.105	0.435	0.19

---

Optimizer (Nelder\_Mead) convergence code: 0 (OK)

---

Table 8.2-12. Analysis of variance (ANOVA) output table for the generalized linear mixed effects model (GLM) to analyze the effects of distance away from FAD, period (day or night), temperature, location (North FAD or South FAD), and lunar illumination on the presence of strong scatterers (binomial NASC > -50 dB S<sub>v</sub>). Significant terms are bolded.

---

Analysis of Variance Table

---

	npar	Sum Sq	Mean Sq	F value
DistanceAway	1	1.0187	1.0187	1.0187
Period	1	10.9044	10.9044	10.9044
Temperature	1	5.9026	5.9026	5.9026
Location	1	0.3429	0.3429	0.3429
Illumination	1	0.0270	0.0270	0.0270

---